

Photosynthesis in a tropical montane rainforest of Southeast Asia:
field measurements and model analysis

Dissertation

zur Erlangung des akademischen Grades Doctor of Philosophy (PhD)
der Fakultät für Forstwissenschaften und Waldökologie
der Georg-August-Universität Göttingen

vorgelegt von

Md. Golam Rakkibu
geboren in Natore, Bangladesh

Göttingen, 2008

1. Gutachter: Prof. Dr. Andreas Ibrom
2. Gutachter: prof. Dr. Rudolf Mitlöhner

Tag der mündlichen Prüfung: 23.05.2008

Summary

Tropical rain forests occupy about 12% of the terrestrial surface and are assumed to contain as much as 55% of the carbon stored in the world as terrestrial biomass. Of the three major blocks (South and Central American, African and Asian) of tropical rain forests in the world, the Asian block (centered on southeast Asia) is the least studied in terms of ecosystem functioning and of regulating the global climate through carbon and water cycles. Models of photosynthesis have been widely used for such characterization of plants and forests. The biochemically based leaf photosynthesis model of Farquhar et al. (1980) was parameterized for selected tree species of the tropical montane rainforest at central Sulawesi, Indonesia, to characterize the photosynthetic capacities and their regulations. The three key parameters of the photosynthesis model, the maximum carboxylation rate of Rubisco (V_{cmax}), the maximum electron transport capacity (J_{max}) and the dark respiration rate (R_{d}) were estimated from the relationships of leaf photosynthesis (A) to intercellular carbon-dioxide concentration (C_i), irradiance (Q) and leaf temperature.

The field study was conducted in 2005 within the interdisciplinary research project “*Stability of Rainforest Margins in Indonesia (STORMA)*” in the Lore Lindu National Park in Central Sulawesi, Indonesia. The objectives of the study were (i) to estimate the photosynthetic capacity and dark respiration (parameter values for V_{cmax} , J_{max} and R_{d}) of major tree species, (ii) to quantify the variability in these parameters, (iii) to determine the sources of variability, (iv) to scale photosynthetic capacity and respiration from leaf level to canopy level and (v) to simulate gross primary productivity and foliage respiration of the forest, with a canopy photosynthesis model, and to compare the results of the model with the results of measurements. Data on photosynthetic capacity, respiration and leaf biochemical and morphological properties were collected around the meteorological tower built by STORMA.

Photosynthetic capacity of the sampled tree species in general was found to be high, suggesting that the trees in that forest are strong assimilators. $V_{\text{cmax}25}$ values, i.e. V_{cmax} values at 25 °C, ranged between 20.0 and 61.0 $\mu\text{mol m}^{-2} \text{s}^{-1}$, and $J_{\text{max}25}$ values ranged between 47.0 and 107.0 $\mu\text{mol m}^{-2} \text{s}^{-1}$. Foliage dark respiration (R_{d}) values were generally low and $R_{\text{d}25}$ ranged between 0.77 and 1.30 $\mu\text{mol m}^{-2} \text{s}^{-1}$. Variations in the temperature dependence, that is activation and deactivation energies, of V_{cmax} , J_{max} and R_{d} among species was much less compared to the variations in the values of $V_{\text{cmax}25}$, $J_{\text{max}25}$ and $R_{\text{d}25}$. Measured similarity in the temperature dependence implies similarity in the physiological processes among leaves and species of the investigated

forest. The sources of variation in photosynthetic capacity (V_{cmax} and J_{max}) and respiration (R_d) among leaves and species could be well described by leaf chemical (nitrogen and phosphorus per unit area) and physical (leaf mass per unit area) properties. Leaf nitrogen concentration (N_a , g m^{-2}) described the variation of photosynthesis parameters best and overall there was a strong and significant linear relationship (P , ranging from 0.05 to 0.001 among species) between physiological model parameters and leaf nitrogen. Despite the species differences in photosynthetic capacities and respiration, it was possible to upscale leaf level measurements to canopy level. It was also possible to simulate the canopy photosynthesis with considerable agreement to the results of measured turbulent CO_2 flux. Physiological parameters for a canopy photosynthesis model were derived by up-scaling leaf level parameters with N_a and temperature dependencies of photosynthesis and respiration.

A one-dimensional forest canopy was generated from the measured forest structure data to represent the investigated forest. The canopy photosynthesis model MAESTRA was used to simulate the carbon-dioxide exchange for the months of May, June and July, with the estimated parameters and measured meteorological data. Model outputs were sensitive to parameters related to crown structure and physiology. Simulated gross primary productivity (P_g) and canopy foliage respiration (R_f) rates were $7.15 \text{ g (C) m}^{-2} \text{ day}^{-1}$ and $3.18 \text{ g (C) m}^{-2} \text{ day}^{-1}$ respectively, in yearly terms that would be $2608 \text{ g (C) m}^{-2} \text{ year}^{-1}$ and $1161 \text{ g (C) m}^{-2} \text{ year}^{-1}$ respectively. The simulated P_g was only 4.0% less compared to the estimated value from turbulent flux measurements. P_g of the investigated forest was expected to be driven only by absorbed photosynthetically active radiation (Q_{abs}), making a constant light use efficiency (E_{GPP}). But that was not the case in the model investigations. It was influenced by vapour pressure saturation deficit (D) and E_{GPP} of the investigated canopy was not constant. P_g was found to be saturated at higher light intensities, not only at half hourly time scales but also in both daily and monthly time scales. P_g saturation level of light (Q_{sat}) was decreasing under high D . This saturation of simulated primary productivity is also seen in data of light response curves from eddy covariance flux measurements. These findings are important when developing models for CO_2 fixation in tropical montane rain forests. Further studies are needed in this diverse forest to be able to explain seasonal variations in the P_g saturation level that are not connected to variations in D .

Zusammenfassung

Tropische Regenwälder nehmen etwa 12 % der Landoberfläche ein und man nimmt an, dass sie bis zu 55 % des Kohlenstoffs enthalten, der auf der Erde als terrestrische Biomasse gespeichert ist. Von den drei Hauptblöcken (Süd- und Zentralamerika, Afrika und Asien) der tropischen Regenwälder der Welt ist der asiatische (mit seinem Zentrum in Südostasien) am wenigsten untersucht bezüglich seiner globalen Klimaregulation durch die Kohlenstoff- und Wasserkreisläufe. Photosynthesemodelle wurden häufig benutzt für eine derartige Charakterisierung von Pflanzen und Wäldern. Das biochemische Blatt-Photosynthesemodell von Farquhar et al. (1980) wurde hier parametrisiert für ausgewählte Baumarten des tropischen Bergregenwaldes in Zentralsulawesi, Indonesien, um die Photosyntheseleistung und ihre Regulation zu charakterisieren. Die drei Schlüsselparameter des Photosynthesemodells, nämlich die maximale Carboxylation Rate von Rubisco (V_{cmax}), die maximale Elektronentransportkapazität (J_{max}) und die Dunkelatmungsrate (R_{d}) wurden dabei geschätzt aus dem Zusammenhang der Blattphotosynthese (A) mit der interzellularen Kohlendioxid-Konzentration (C_i), der solaren Einstrahlung (Q) und der Blatttemperatur.

Die Feldmessungen wurden im Jahr 2005 durchgeführt im Rahmen des interdisziplinären Forschungsprojekts „*Stability of Rainforest Margins in Indonesia* (STORMA)“ im Lore Lindu Nationalpark in Zentralsulawesi, Indonesien. Die Ziele der Untersuchung waren (1) die Photosyntheseleistung und die Dunkelatmung (d. h. Parameterwerte für V_{cmax}) der Hauptbaumarten zu schätzen, (2) die Variabilität dieser Parameter zu quantifizieren, (3) die Ursachen der Variabilität zu bestimmen, (4) die Photosyntheseleistung und Atmung von der Blatt- auf die Bestandesebene zu transformieren und (5) die Bruttoprimärproduktion und Blattatmung des Waldes mit einem Bestandes-Photosynthese-Modell zu simulieren und diese Ergebnisse mit vorliegenden Messungen zu vergleichen. Die Daten zur Photosyntheseleistung, zur Atmung sowie zu den biochemischen und morphologischen Eigenschaften wurden erhoben im Bereich des meteorologischen Messturms, der im Rahmen des STORMA-Projektes errichtet wurde.

Die Photosyntheseleistung der ausgewählten Baumarten war generell hoch, was darauf hinweist, dass die Bäume dieser Wälder effizient assimilieren. Die $V_{\text{cmax}25}$ -Werte, d. h. bei 25 °C Lufttemperatur, lagen zwischen 20.0 und 61.0 $\mu\text{mol m}^{-2} \text{s}^{-1}$, während die $J_{\text{max}25}$ -Werte von 47.0 – 107.0 $\mu\text{mol m}^{-2} \text{s}^{-1}$ reichten. Die Blattdunkelatmung (R_{d}) war allgemein niedrig und $R_{\text{d}25}$ lag zwischen 0.77 und 1.30 $\mu\text{mol m}^{-2} \text{s}^{-1}$. Die Variation in der Temperaturabhängigkeit von V_{cmax} , J_{max} und R_{d} unter den Arten war viel geringer als die Variation der Werte von V_{cmax} , J_{max} und R_{d} . Die gemessene Ähnlichkeit in der Temperaturabhängigkeit impliziert ähnliche physiologische Prozesse unter den Blättern und Arten des untersuchten Waldes. Die Variationsursachen in der Photosyntheseleistung (V_{cmax}

und J_{\max}) und Atmung (R_d) unter den Blättern und Arten konnten sehr gut erklärt werden mit chemischen (Stickstoff- und Phosphorgehalt pro Blattfläche) und physikalischen (Blattmasse pro Blattfläche) Eigenschaften der Blätter. Dabei erklärte die Blattstickstoffkonzentration (N_a , g m^{-2}) die Variation der Photosyntheseparameter am besten. Insgesamt gab es eine enge und signifikante lineare Beziehung zwischen physiologischen Modellparametern und Blattstickstoffgehalt. Trotz der artspezifischen Unterschiede in der Photosyntheseleistung und Atmung war es möglich, die Messungen auf Blattebene auf die Bestandesebene zu transformieren. Ebenso konnte die Bestandesphotosyntheseleistung simuliert werden und die Ergebnisse stimmten überraschend gut mit Messungen des turbulenten Flusses überein. Die physiologischen Parameter für das Bestandesphotosynthesemodell wurden dabei abgeleitet, indem die Blattparameter mit N_a und ihr Temperatureinfluss auf die Photosynthese und Atmung transformiert wurden.

Zur Charakterisierung des untersuchten Waldes wurde aus den gemessenen Strukturdaten ein eindimensionaler Bestand konstruiert. An diesem wurde das Photosynthesemodell MAESTRA angewandt, um für die Monate Mai, Juni und Juli den Kohlenstoffdioxidaustausch mit den geschätzten Modellparametern und meteorologischen Messdaten zu simulieren. Die Modellergebnisse erwiesen sich als empfindlich gegenüber Parametern der Kronenstruktur und Baumphysiologie. Für die Bruttoprimärproduktion (P_g) und die Bestandes-Blattatmung (R_f) ergaben sich Raten von $7.15 \text{ g (C) pro m}^{-2} \text{ Tag}^{-1}$ und $3.18 \text{ pro m}^{-2} \text{ Tag}^{-1}$; im Jahr ergibt das 2608 g (C) bzw. $1161 \text{ g (C) m}^{-2}$. Dieser für P_g ermittelte Wert lag nur um 4.0 % unter dem aus turbulenten Flussmessungen abgeleiteten Wert. Für P_g wurde hier angenommen, dass sie nur durch die absorbierte photosynthetisch aktive Strahlung (Q_{abs}) bestimmt wird, was zu einer konstanten (E_{GPP}) führt. Dies war aber nicht der Fall bei den Modellanalysen. P_g wurde beeinflusst durch das Wasserdampfsättigungsdefizit (D) und E_{GPP} war nicht konstant. Bei höherer Lichtintensität erwies sich P_g als gesättigt, und das nicht nur bei halbstündiger, sondern auch bei täglicher und monatlicher Zeitskala. Der P_g -Sättigungspunkt des Lichts (Q_{sat}) nahm dabei mit höherem D ab. Diese Sättigung der modellierten Primärproduktion wurde auch beobachtet bei Lichtantwortkurven mit Daten von Eddy-Kovarianz-Flussmessungen. Diese Ergebnisse sind wichtig für die Entwicklung von Modellen zur CO_2 -Aufnahme von montanen tropischen Regenwäldern. Weitere Untersuchungen sind in diesen diversen Wäldern nötig, um die saisonale Variation des P_g -Sättigungspunktes zu erklären, die nicht mit Variationen im Sättigungsdefizit D korreliert.

Table of Contents

Summary	
Table of Contents	I
List of Tables	III
List of Figures	V
1 Chapter- I: General introduction of the thesis	1
1.1 Background and rationale of the present study.....	1
1.2 Materials and methods.....	5
1.2.1 Study site.....	5
1.2.2 Topography and climate.....	6
1.2.3 Forest structure and vegetation.....	7
1.3 Field measurements of leaf gas exchange.....	7
1.3.1 Steady-state gas exchange measurements and parameter estimation	7
1.3.2 $A-Q$ response curve measurements.....	10
1.3.3 $A-C_i$ response curve measurements.....	10
1.3.4 Respiration (R_d) measurements.....	11
1.4 Analysis of leaf chemical and physical properties.....	11
1.5 Description of the leaf photosynthesis models.....	12
1.6 Calculation of photosynthetic parameters.....	15
1.7 Reference.....	17
2 Chapter- II: Photosynthetic and respiration parameters and their temperature dependence in tropical montane rainforests of Central Sulawesi, Indonesia	20
2.1 Abstract.....	20
2.2 Introduction.....	21
2.3 Materials and methods.....	23
2.3.1 Model overview.....	23
2.3.2 Study site.....	24
2.3.3 Data analysis.....	25
2.4 Results and discussions.....	25
2.4.1 Quantum yield (α) and theta (θ) values of light response curves.....	25
2.4.2 Temperature dependence of V_{cmax}	27
2.4.3 Temperature dependence of J_{max}	32
2.4.4 Interrelationship between J_{max} and V_{cmax}	36
2.4.5 Temperature dependence of R_d	39
2.5 Conclusions.....	42
2.6 Reference:.....	42
3 Chapter- III: Scaling of photosynthesis and respiration in a montane rainforest with leaf properties and temperature dependencies	45
3.1 Abstract.....	45
3.2 Introduction.....	45
3.3 Materials and methods.....	48
3.3.1 Models used.....	48
3.3.2 Data analysis.....	50

3.4	Results and discussions.....	50
3.4.1	Species wise relationships between V_{cmax} and leaf biochemical and morphological properties	50
3.4.2	Species wise relationships between J_{max} and leaf biochemical and morphological properties	52
3.4.3	Species wise relationships between R_{d} and leaf biochemical and morphological properties	54
3.4.4	Overall relationships between photosynthetic capacities and leaf biochemical and morphological properties within the crown.....	56
3.4.5	Interrelationship among leaf chemical and physical properties.....	57
3.4.6	Species wise photosynthetic model parameters and their temperature responses when scaled with leaf properties	59
3.4.7	Canopy photosynthesis model parameters and their temperature responses when scaled with leaf properties	63
3.5	Conclusions.....	69
3.6	Reference:	70
4	Chapter- IV: Simulation of CO₂ exchange of a tropical montane rain forest canopy of Central Sulawesi, Indonesia.	73
4.1	Abstract.....	73
4.2	Introduction.....	73
4.3	Material and methods.....	74
4.3.1	Forest site topography, climate and vegetation.....	74
4.3.2	Parameterisation of the forest canopy model MAESTRA.....	75
4.3.3	Climate.....	75
4.3.4	Tree dimensions and canopy structure.....	75
4.3.5	Photosynthetic responses to PAR and temperature	77
4.3.6	Stomatal conductance	77
4.3.7	Simulations	78
4.3.8	Sensitivity analysis.....	78
4.4	Results and discussions.....	80
4.4.1	Crown structure of the simulated forest.....	80
4.4.2	Sensitivity analyses.....	81
4.4.2.1	<i>Gross canopy photosynthesis and PAR absorption to leaf area distribution.....</i>	<i>81</i>
4.4.2.2	<i>Sensitivity of gross primary productivity to the physiological parameters related to light and temperature responses</i>	<i>82</i>
4.4.2.3	<i>Sensitivity of gross primary productivity to the parameters related to leaf nitrogen content.....</i>	<i>83</i>
4.4.2.4	<i>Sensitivity of gross primary productivity to the parameters related to leaf stomatal conductance</i>	<i>84</i>
4.4.2.5	<i>Influence of number of vertical layers in the canopy on simulated outputs</i>	<i>85</i>
4.5	Simulated versus observed CO ₂ uptake	86
4.5.1	Comparisons of gross primary productivity	86
4.5.2	Simulated budget of gross primary productivity and foliage respiration	88
4.5.3	Comparisons of canopy photosynthetic light response.....	89
4.6	Conclusion	90
4.7	References.....	91

5	Chapter- V: Photosynthetic light use efficiency of a tropical montane rain forest canopy of Central Sulawesi, Indonesia.....	92
5.1	Abstract.....	92
5.2	Introduction.....	92
5.3	Materials and methods.....	93
5.3.1	Simulation of gross primary productivity (P_g) of the investigated canopy.....	93
5.3.2	Simulation of PAR absorption by the canopy.....	93
5.3.3	PAR response of gross canopy photosynthesis.....	94
5.4	Results and discussions.....	94
5.4.1	PAR response of gross canopy photosynthesis.....	94
5.4.2	PAR use efficiency of gross canopy photosynthesis (E_{GPP}).....	98
5.5	Conclusion.....	101
5.6	Reference.....	102
	Acknowledgements.....	103
	Declaration of Honor.....	104
	Eidesstattliche Erklärung.....	104
	Curriculum vitae.....	105

List of Tables

Table 1.1.	Carbon fixed by the Earth's vegetations, as Net Primary Productivity (NPP) and the possible sink strength. The total carbon pool includes vegetation and soil organic matter.....	2
Table 1.2.	Photosynthesis primary model parameters and their temperature dependence used to estimate V_{cmax} from $A-C_i$ curves and J_{max} from $A-C_i$ and $A-Q$ curves. The RUBISCO parameters K_c , K_o and T^* are appropriate to an infinite internal conductance to CO_2 diffusion.....	14
Table 2.1.	Light limited apparent quantum yields ($\mu\text{mol } CO_2 \text{ mol}^{-1}$ incident photon) of CO_2 exchange. Results are fitted values of 20 – 25 data sets from 8-10 leaves of each species. Overall, data pooled from five species. Values in parentheses are r^2 of linear regressions. Significance of the Parameter values were $P < 0.05$ (*), $P < 0.01$ (**), $P < 0.001$ (***).....	26
Table 2.2.	Light limited true quantum yields ($\mu\text{mol e}^- \text{ mol}^{-1}$ absorbed PAR) of CO_2 exchange. Results are fitted values of 20 – 25 data sets from 8-10 leaves of each species. Overall, data pooled from five species. Values in the parentheses are r^2 of linear regressions. Significance of the Parameter values were $P < 0.05$ (*), $P < 0.01$ (**), $P < 0.001$ (***).....	26
Table 2.3.	Curvature of light response curve (theta, θ). Values in the parentheses are standard deviations. Overall, data pooled from five species.....	27
Table 2.4.	Values (\pm SE when statistical analysis was possible) of the parameters describing temperature responses of leaf photosynthetic capacity of five tree species from tropical montane rain forests, Sulawesi, Indonesia: maximal rate of carboxylation at 25 °C (V_{cmax25}), maximal rate of electron flow at 25°C (J_{max25}), dark respiration at 25°C (R_{d25}), activation energy (E_a), deactivation energy (E_d) and temperature coefficient for dark respiration (Q_{10}). Significance of the Parameter values were $P < 0.05$ (*), $P < 0.01$ (**), $P < 0.001$ (***).....	30
Table 3.1.	Linear regression results for V_{cmax25} ($\mu\text{mol m}^{-2} \text{ s}^{-1}$) versus N_a (g m^{-2}), M_a (g m^{-2}) and P_a (mg m^{-2}). Significance of the slopes and non-zero intercepts were $P < 0.05$ (*),	

$P < 0.01$ (**) and $P < 0.001$ (***) Abbreviations: Cb (<i>C. buruana</i>), Gd (<i>G. dulcis</i>), Lh (<i>L. havilandii</i>), Pc (<i>P. coccinea</i>) and Va (<i>V. arborea</i>).....	51
Table 3.2. Multiple linear regression results for $V_{\text{cmax}25}$ ($\mu\text{mol m}^{-2} \text{s}^{-1}$) versus N_a (g m^{-2}) and P_a (mg m^{-2}) combined together. Significance of the slopes and non-zero intercepts were $P < 0.05$ (*), $P < 0.01$ (**) and $P < 0.001$ (***).....	52
Table 3.3. Linear regression results for $J_{\text{max}25}$ ($\mu\text{mol m}^{-2} \text{s}^{-1}$) versus N_a (g m^{-2}), M_a (g m^{-2}) and P_a (mg m^{-2}). Significance of the slopes and non-zero intercepts were $P < 0.05$ (*), $P < 0.01$ (**) and $P < 0.001$ (***) Abbreviations: Cb (<i>C. buruana</i>), Gd (<i>G. dulcis</i>), Lh (<i>L. havilandii</i>), Pc (<i>P. coccinea</i>) and Va (<i>V. arborea</i>).....	53
Table 3.4. Multiple linear regression results for $J_{\text{max}25}$ ($\mu\text{mol m}^{-2} \text{s}^{-1}$) versus N_a (g m^{-2}) and P_a (mg m^{-2}) combined together. Significance of the slopes and non-zero intercepts were $P < 0.05$ (*), $P < 0.01$ (**) and $P < 0.001$ (***).....	54
Table 3.5. Linear regression results for $R_{\text{d}25}$ ($\mu\text{mol m}^{-2} \text{s}^{-1}$) versus N_a (g m^{-2}), M_a (g m^{-2}) and P_a (mg m^{-2}). Significance of the slopes and non-zero intercepts were $P < 0.05$ (*), $P < 0.01$ (**) and $P < 0.001$ (***) Abbreviations: Cb (<i>C. buruana</i>), Gd (<i>G. dulcis</i>), Lh (<i>L. havilandii</i>), Pc (<i>P. coccinea</i>) and Va (<i>V. arborea</i>).....	56
Table 3.6. Species wise and over all mean values for leaf traits of sample trees.....	58
Table 3.7. Species wise photosynthetic parameter values as functions of leaf nitrogen per unit area (N_a , g m^{-2}) at the reference leaf temperature of 25 °C: a and b are proportionality coefficients (slope and intercept respectively) of regressions between V_{cmax} , J_{max} and R_d and the scaling parameter N_a activation energy (E_a), deactivation energy (E_d) and temperature coefficient for dark respiration (Q_{10}). Significance of the Parameter values were $P < 0.05$ (*), $P < 0.01$ (**), $P < 0.001$ (***).....	61
Table 3.8. Species wise photosynthetic parameter values as functions of leaf mass per unit area (M_a , g m^{-2}) at the reference leaf temperature of 25 °C: a and b are slope and intercept respectively of linear regressions, activation energy (E_a), deactivation energy (E_d) and temperature coefficient for dark respiration (Q_{10}).....	62
Table 3.9. Species wise photosynthetic parameter values as functions of leaf phosphorus per unit area (P_a , g m^{-2}) at the reference leaf temperature of 25 °C: a and b are slope and intercept respectively of linear regressions, activation energy (E_a), deactivation energy (E_d) and temperature coefficient for dark respiration (Q_{10}).....	62
Table 3.10. Canopy photosynthesis model parameters at 25 °C leaf temperature when scaled with N_a (g m^{-2}): a and b are slope and intercept respectively of regressions between V_{cmax} , J_{max} and R_d and the scaling parameter, activation energy (E_a), deactivation energy (E_d) and temperature coefficient for dark respiration (Q_{10}). Significance of the parameter values were $P < 0.05$ (*), $P < 0.01$ (**), $P < 0.001$ (***) Canopy: (data from all five species), Sun Crown: (data from Lh and Va situated at the forest edge), Shade Crown: (data from Cb, Gd and Pc situated inside forest canopy).....	64
Table 3.11. Canopy photosynthesis model parameters at 25 °C leaf temperature when scaled with M_a (g m^{-2}): a and b are slope and intercept respectively of regressions between V_{cmax} , J_{max} and R_d and the scaling parameter, activation energy (E_a), deactivation energy (E_d) and temperature coefficient for dark respiration (Q_{10}).....	65
Table 3.12. Canopy photosynthesis model parameters at 25 °C leaf temperature when scaled with P_a (g m^{-2}): a and b are slope and intercept respectively of regressions between V_{cmax} , J_{max} and R_d and the scaling parameter (P_a , g m^{-2}), activation energy (E_a), deactivation energy (E_d) and temperature coefficient for dark respiration (Q_{10}).....	65
Table 4.1. Parameter values of normalized β -functions of vertical leaf area density distributions used in the simulation. (Calculated from Grote 2007).....	78
Table 4.2. Physiological and biophysical parameter values used in the simulation.....	79

Table 4.3. Sensitivity of gross photosynthesis rates (P_g) and photosynthetically active radiation absorption rates (Q_{abs}) to two different leaf area distributions in the simulation. Abbreviations: UD stands for uniform; and 1D for one dimensional vertical leaf area density distribution.....	82
Table 4.4. Simulated daily average gross photosynthesis (P_g) and foliage respiration (R_f) from monthly and periodic data and extrapolation to yearly values from the averages. Values in the parentheses are standard deviations.....	89
Table 5.1. Regression results between simulated canopy gross photosynthesis (P_g) and absorbed PAR (Q_{abs}). The parameters α , θ and P_{max} are the initial slope, a curvature parameter and the saturated photosynthesis rate respectively. Index 'c' stands for combined Q -response model. Parameters a and b are empirical parameters for the vapour pressure saturation deficit (D) dependency of P_{max_0} , i.e. the Q saturated canopy photosynthesis rate at $D = 0$ Pa. R^2 is the relative proportion of the variability of simulated P_g rates that can be explained by model predictions.....	98

List of Figures

Figure 1.1. Sulawesi in the Indonesian archipelago east of the Wallace line. The location of the study site Bariri on the fringe of the Lore Lindu National Park is indicated south of Palu in Central Sulawesi.....	5
Figure 1.2. Meteorological tower for flux measurements.....	6
Figure 1.3. Leaf chamber of photosynthetic gas analyzing apparatus Licor 6400.....	8
Figure 1.4. Sample (J - Q) response curve of electron transport rate to photosynthetically active radiation. Stars are measured values and the fitted line is the predicted values of the model.....	10
Figure 1.5. Sample (A - C_i) response curve of carboxylation velocity to inter cellular CO_2 concentrations. Stars are measured values and the fitted model in the lower part (continuous line) is for V_{cmax} and the fitted model in the upper part (dotted line) is for J_{max}	11
Figure 2.1. Relationship between theta (θ) and specific leaf area (SLA).....	27
Figure 2.2. Species wise average values for the maximum RUBISCO carboxylation rate at 25 °C leaf temperature and their standard deviations.....	30
Figure 2.3. Species wise average values for activation energies of V_{cmax} and their standard deviations.....	31
Figure 2.4. Relationship between simulated values of V_{cmax} and leaf temperatures (°C). Open symbols for sun crown and solid symbols for shade crown.....	31
Figure 2.5. Responses of V_{cmax} to leaf temperatures. Simulated values are normalized to 1 at 25 °C.....	32
Figure 2.6. Species wise average values for the maximum rate of electron transport at 25 °C leaf temperature and their standard deviations.....	34
Figure 2.7. Species wise average values for activation energies of J_{max} and their standard deviations.....	35
Figure 2.8. Relationships between simulated values for J_{max} and leaf temperature (°C). Open symbols for sun crown and solid symbols for shade crown.....	35
Figure 2.9. Responses of J_{max} to leaf temperatures. Simulated values are normalized to 1 at 25 °C.....	36
Figure 2.10. Relationship between J_{max} and V_{cmax} at 25 °C leaf temperature.....	37

Figure 2.11. Relationship between V_{cmax} and J_{max} (J_{max} calculated from A/Q response curves) at different leaf temperatures ranging between 18 °C to 30 °C.	38
Figure 2.12. Relationship between leaf temperatures and the ratios of maximum rate of electron transport to maximum rate of rubisco carboxylation. The relationship among species looks very similar, so a single line was fitted to the pooled data.	38
Figure 2.13. Species wise average values for the dark respiration at the reference leaf temperature of 25 °C and their standard deviations.....	40
Figure 2.14. Species wise average values for the temperature of dark respiration (Q_{10}) and their standard deviations.	40
Figure 2.15. Relationships between simulated dark respirations and leaf temperatures.	41
Figure 2.16. Responses of dark respiration to leaf temperatures. Simulated values are normalized to 1 at 25 °C.	41
Figure 3.1. Relationships for five tree species between V_{cmax} at 25° C leaf temperature and (a) leaf nitrogen per unit area, (b) leaf mass per unit area and (c) leaf phosphorus per unit area	51
Figure 3.2. Relationships for five tree species between J_{max} at 25 °C leaf temperature and (a) leaf nitrogen per unit area, (b) leaf mass per unit area and (c) leaf phosphorus per unit area	53
Figure 3.3. Relationships for five tree species between R_d at 25 °C leaf temperature and (a) leaf nitrogen per unit area, (b) leaf mass per unit area and (c) leaf phosphorus per unit area	55
Figure 3.4. Relationships of V_{cmax} , J_{max} and R_d to leaf nitrogen per unit area (g m^{-2}) when data from five species were pooled together.	57
Figure 3.5. Relationships of leaf nitrogen per unit area, $N_a \text{ g m}^{-2}$, with (a) leaf phosphorus per unit area (b) leaf mass per unit area and (c) relationship of P_a with M_a . Data from all the five species polled together.....	59
Figure 3.6. Plots of measured versus modeled V_{cmax} with N_a as scaling parameter. (a): Results of canopy model, Slope- 1.01, r^2 - 0.5 (b): Results of sun crown model, Slope- 1.02, r^2 - 0.68 (c): Results of shade crown model, Slope- 1.0, r^2 - 0.62	67
Figure 3.7. Plots of measured versus modeled J_{max} with N_a as scaling parameter. (a): Results of canopy model, Slope- 0.99, r^2 - 0.34 (b): Results of sun crown model, Slope- 0.96, r^2 - 0.52 (c): Results of shade crown model, Slope- 1.02, r^2 - 0.37	68
Figure 3.8. Plots of measured versus modeled R_d with N_a as scaling parameter. (a): Results of canopy model, Slope- 1.0, r^2 - 0.63 (b): Results of sun crown model, Slope- 1.0, r^2 - 0.66 (c): Results of shade crown model, Slope- 1.01, r^2 - 0.66	69
Figure 4.1. Vertical distribution of leaf area density of the investigated forest canopy. The integral of leaf area density equals to leaf area index (6.7) of the forest canopy.	76
Figure 4.2. Measured (curved line) and predicted (smooth line) leaf area density with the calculated beta distribution coefficients.	81
Figure 4.3. Relative sensitivity of gross primary productivity (P_g) to the physiological parameters related to light and temperature responses. Parameter values have been changed from the estimated reference (0%) to higher and lower values in steps of 15%.....	83
Figure 4.4. Relative sensitivity of gross primary productivity (P_g) to the physiological parameters related to leaf nitrogen content. Parameter values have been changed from the estimated reference (0%) to higher and lower values in steps of 15%.....	84
Figure 4.5. Relative sensitivity of gross primary productivity (P_g) to the physiological parameters related to leaf stomatal conductance. Parameter values have been changed from the estimated reference (0%) to higher and lower values in steps of 15%.....	85

- Figure 4.6. Relationships between simulated and observed gross photosynthetic rates (P_g) of the investigated forest. (a) scatter diagram of observed versus simulated P_g , regression line and parameter (solid) and 1:1 line (dashed). (b) Diurnal course of simulated P_g (solid) line and observed P_g (dots) averaged over the period of May, June and July 2004.....87
- Figure 4.7. Half hourly average of air vapour pressure saturation deficit (D) for the month of May, June and July 2004.....88
- Figure 4.8. Responses of canopy photosynthesis (P_g) to photosynthetically active radiation (PAR). The arrow indicates saturation of simulated P_g . Open circles are simulated values and small dots are measured values from turbulent flux. Abbreviation: $Q =$ PAR photon flux.....90
- Figure 5.1. (a) Simulated half-hourly canopy gross primary production rates (P_g) versus simulated Q_{abs} for the period of May to July 2004. Broken curves are predicted P_g at a vapour pressure saturation deficit (D) = 0 Pa (upper curve) and $D = 2000$ Pa (lower curve). The solid line shows predicted P_g without any D dependency. 5.1. (b) shows the reducing effect of increasing D on saturated P_g (according to Equation 5.3) and 5.1. (c) shows the effect of increasing D on saturating Q_{abs} (Q_{sat}) according to Equation 5.4. The parameter values of the regression models are listed in Table 5.1.....96
- Figure 5.2. Sensitivity of P_g to D_0 at three different values of maximum stomatal conductance.97
- Figure 5.3. Simulated daily (a) and monthly (c) averaged daily gross primary productivity (P_g) versus simulated daily absorbed PAR (Q_{abs}) and the respective PAR-use efficiencies for P_g (E_{GPP}) (2 b and 2 d).100
- Figure 5.4. Average diurnal courses of absorbed PAR (Q_{abs}), water vapour pressure saturation deficits (D), gross primary production rates (P_g) and PAR use efficiencies of P_g (E_{GPP}).101

1 Chapter- I: General introduction of the thesis

1.1 Background and rationale of the present study

Tropical rain forests exist in a broad band across the Earth's warm, moist equatorial regions between 23.5° S and 23.5° N. They are characterized by their very diverse structure (exceeding 30m in height), a wide range of life forms (including many trees with buttresses, thick stemmed climbers, and herbaceous epiphytes), and a large number of tree species (30-300 woody species per hectare) (Grace et al. 2001). They are among the most important biomes in terms of annual carbon (C) turnover and evapotranspiration. Although tropical rain forests extend over only about eight percent of the global land surface (Whittaker & Likens 1973), they contain about 40% of the biomass (Skole & Tucker 1993) and account for about 50% of the annual net primary production of the terrestrial part of biosphere (Williams et al. 1998; Grace et al. 2001) and contribute approximately 30% of net terrestrial photosynthesis (Field et al. 1998). Recent indications are that these ecosystems may also be a significant net sink for C (Williams et al. 1998). As they are a major component of the global carbon cycle, any change in its ecosystem functioning will be important.

Net primary productivity (NPP) of forest is on the increase because of fertilization by CO₂ and deposition of active nitrogen, but heterotrophic respiration which is related to temperature and therefore is also increasing, does not keep pace with NPP due to the residence time of carbon in the vegetation and soil. Model-based estimates of the global terrestrial carbon sink data suggest that the sinks are predominantly in forests and savannas, which amounts 2-3 Gt C year⁻¹ (Grace 2004). A model of the global carbon fluxes (NEE) to terrestrial vegetation developed by Lloyd (1999) is considered a more realistic one, which explicitly considers both the effect of elevated CO₂ and nitrogen deposition on photosynthesis and respiration as a function of temperature. The model suggested a strong C sink in the tropical regions and a weaker sink in North America and Europe. Possible net primary productivity and carbon sink strengths of different biomes are given in Table 1.1.

Table 1.1. Carbon fixed by the Earth's vegetations, as Net Primary Productivity (NPP) and the possible sink strength. The total carbon pool includes vegetation and soil organic matter.

Biome	NPP (t C ha ⁻¹ year ⁻¹)	Area (million km ²)	Total carbon pool (Gt C)	Total NPP (Gt C year ⁻¹)	Estimated total sink (Gt C year ⁻¹)	Average sink per ha (t C ha ⁻¹ year ⁻¹)
Tropical forests	12.5	17.5	553	21.9	0.66	0.37
Temperate forests	7.7	10.4	292	8.1	0.35	0.34
Boreal forests	1.9	13.7	395	2.6	0.47	0.34
Arctic tundra	0.9	5.6	117	0.5	0.14	0.02
Mediterranean shrublands	5.0	2.8	88	1.4	0.21	0.75
Crops	3.1	13.5	15	4.1	0.20	0.15
Tropical savanna and grasslands	5.4	27.6	326	14.9	0.39	0.14
Temperate grasslands	3.7	15	182	5.6	0.21	0.14
Deserts	1.2	27.7	169	3.5	0.20	0.07
Ice		15.3				
Total		149.3		62.6	2.85	

Source: Grace 2004

A substantial amount of carbon is transferred from the terrestrial reservoir to the atmosphere as a result of deforestation. Worldwide, tropical rain forest is being converted to agriculture or being degraded at slightly less than 1% per year (FAO, 1997). The carbon dioxide emitted during this land conversion in the tropics accounts for almost all of the estimated 1.6 – 2.4 Gt of carbon that is transferred globally from vegetation to atmosphere each year as a result of change in land use (Fearnside, 2000). Despite the importance of tropical rain forests as a store of carbon, their role in the carbon cycle is not well understood because they are extensive, variable, and generally more difficult to study than other vegetation types.

Past studies, such as the Anglo-Brazilian Amazonian Climate Observation Study (ABRACOS) at the ecosystem-atmosphere level (Gash et al. 1996), have described the major environmental controls on tropical canopy gas and energy exchange. These controls are physical (e.g. temperature, irradiance, soil moisture), biochemical (e.g. photosynthetic capacity, enzyme reaction rates) and biological (e.g. leaf area, stomatal opening). But quantifying the interactions between these controls, and the links between carbon and energy exchange necessitates the use of mathematical models based on a mechanistic understanding of the coupled mechanisms of photosynthesis and transpiration. Once these models have been parameterized from leaf-level data, they can be tested against independent whole

canopy process measurements. Once validated, the models can be used to generate regional and long-term predictions of gas exchange (Williams et al. 1998).

Models of canopy gas exchange provide a theoretical framework for thorough analysis and interpretation of the scaling of physiological processes, enabling physiologists to extend their work to larger scales. They also fit the requirements of assessing effects of climate change on vegetation. Process-based models of forest canopy carbon uptake predict fluxes from individual leaves and canopies, and have been extended to provide estimates of carbon uptake at national and global scales (e.g., Whitehead et al. 2001). Fundamental to such models is the scaling of leaf photosynthesis to canopies by considering interception of solar radiation and leaf photosynthetic capacity (Leuning et al. 1995; Jarvis 1995). The net carbon gain of a tree canopy is the balance between carbon assimilated through photosynthesis and carbon lost through respiration. The within-canopy distribution of photosynthetic capacity is related to the distribution of leaf nitrogen, which can determine canopy-level carbon assimilation because of the nitrogen-rich photosynthetic enzyme Rubisco (ribulose-1,5-bisphosphate carboxylase/oxygenase) and electron-transport capacity. Photosynthesis of a canopy element depends, *inter alia*, on the biochemical capacity for photosynthesis of that element, its temperature, its carbon dioxide at the sites of carboxylation, and its absorbed irradiance (De Pury & Farquhar 1997).

During the last decade, process-based simulation models have been increasingly used to deepen the understanding of tree growth and development. Of the processes controlling tree growth and yield represented in these models, photosynthetic capacities are always of prime importance, because they determine (along with foliage distribution) potential tree carbon gains. Furthermore, environmental variables largely control actual photosynthetic rates. Thus, developing a process-based model of tree growth for a given species calls for reliable and comprehensive information on functional relationships between leaf CO₂ assimilation and plant and environmental variables (Roux et al. 1999).

Farquhar et al. (1980) model of photosynthesis was used to parameterize the photosynthetic characteristics in tropical montane rainforest trees of Central Sulawesi, Indonesia. Despite the increased use of this model for describing the daily and seasonal gain of carbon through CO₂ assimilation, it is increasingly being realized that parameterizing this rather complex model for leaves of a single species only, let alone for the many species that make up an ecosystem, is not straightforward. An important

question to address, therefore, prior to implementation of this or any other process oriented model for describing CO₂ assimilation is to what extent species differ in their gas-exchange characteristics.

Within the context of Farquhar et al. model these characteristics include the activity of ribulose 1,5-bisphosphate carboxylase-oxygenase, the rate of ribulose 1,5-bisphosphate regeneration via electron transport, and the rate of triose phosphate utilization. If the range of these estimates between species is small then the choice of appropriate parameter estimates for one or many species may be of only minor concern. If, however, considerable differences exist between species for these estimates then care must be taken to understand how species, or groups of species, differ in this regard.

Grace (2004) listed the contributions of the terrestrial biomes to the global terrestrial carbon sink, and he showed that not only the stocks and primary production are largest in the tropical forest biomes but also the CO₂ sink strength is largest compared to other biomes. Despite the above mentioned importance of the tropics, related studies are biased towards North America and Europe. Few available studies in the tropics are almost entirely from South American low-lying forests such as Amazonian rain forests. As far as tropical montane rain forest is concerned there is almost no such study so far. Considering the contribution of tropical forest biomes, it is of great importance to characterize tropical montane forests in this regard.

The overall goal of this study is to characterize the photosynthetic capacities of the tropical montane rainforests, in particular of Central Sulawesi, Indonesia. To accomplish this goal, this thesis first gives the general description of the study site, methods of field study, photosynthesis models and their parameterisation. Next, it describes species parameter values and to what extent they differ in their gas-exchange capacities and their temperature dependence. Third, it describes the sources of variability in photosynthetic capacities within leaves of individual tree species and among species and the possibility of explaining these variations by means of scaling parameters. Fourth, it describes physiological parameters for canopy photosynthesis model. Finally, it describes simulations of forest canopy photosynthesis model MAESTRA to estimate productivity of the investigated forest and use it to explain the light response of canopy photosynthesis. This thesis is structured with the concept of a cumulative thesis. It tries to write individual chapters as independent as possible from each other with the intension of publishing them separately.

1.2 Materials and methods

1.2.1 Study site

The study was carried out in a tropical montane natural rain forest in Central Sulawesi, Indonesia during February to August 2005. Sulawesi is with ~175000 km² the largest island of the Wallacea, a biogeographical region east of the Wallace line which separates especially the fauna of Sulawesi from the Asian continent to the west (Wallace 1869). While dominating the Wallacea region, Sulawesi is the third largest island in the Indonesian archipelago (Figure 1.1). With the establishment of the Lore Lindu National Park in 1993, an area of 2290 km² of Central Sulawesi, just south of its district capital Palu, is designated to the protection of the high biodiversity and endemism found in this region where Asian and Austronesian species merge. Stretching from about 1000 m to the peaks of Mt. Nokilalaki at 2355 m asl, this park harbors a variety of natural vegetation types.

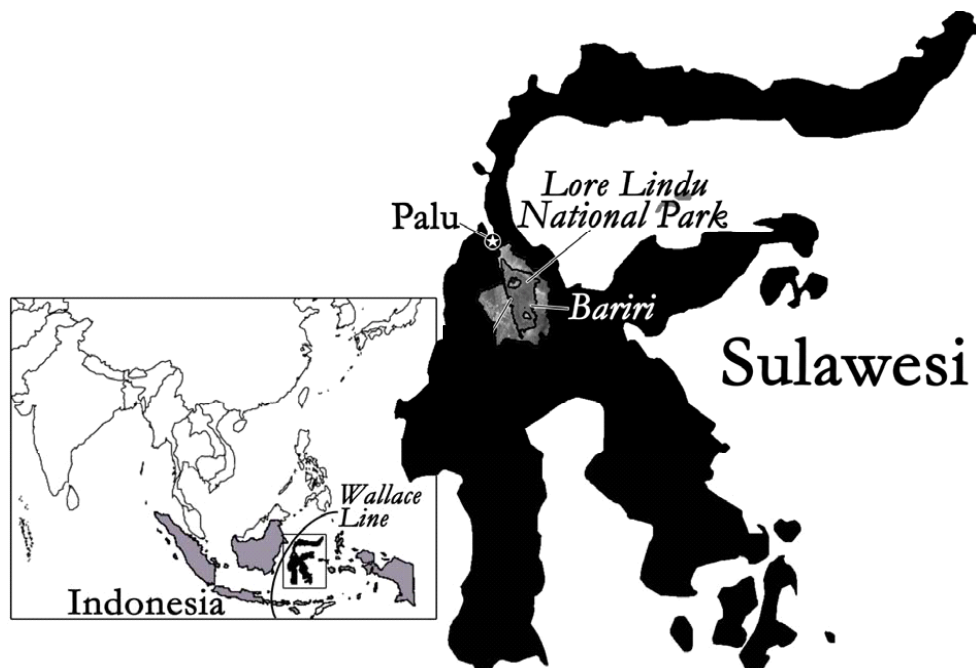


Figure 1.1. Sulawesi in the Indonesian archipelago east of the Wallace line. The location of the study site Bariri on the fringe of the Lore Lindu National Park is indicated south of Palu in Central Sulawesi.

The study site lies in the Besoa region, in the eastern part ($1^{\circ} 39.476'S$ $120^{\circ} 10.409'E$) of the Lore Lindu National Park, at an altitude of 1416 m, about 12 km northwest from the village of Bariri. As no settlements exist in the vicinity of the site,

it can be reached by vehicle only under favorable road conditions or else on foot accompanied by buffalo-drawn carriages. The special feature of this site is a 72 m high meteorological scaffolding tower (Figure 1.2), erected in the middle of a stretch of natural forest.



Figure 1.2. Meteorological tower for flux measurements

1.2.2 Topography and climate

The study site is situated on a level plateau, defined by a steep drop within ~300 m to the north, west and south. The forest floor shows a mildly undulating micro-relief of ~1 m difference, apparently created by pits of constantly falling trees and mounds of their slowly decomposing fragments. The study area has a humid tropical climate with almost no seasonal changes in temperature, and with small seasonal changes in rainfall without a pronounced dry season. Mean annual precipitation and mean annual temperature at the study site during October 2003 to February 2005 was 1700 mm yr⁻¹ and 19.6°C respectively (Ibrom et al. 2007). However, at night it becomes considerably cooler and enhanced nocturnal cooling results in substantial amounts of dew fall and fog, particularly in the early morning hours. Seasonality is

normally affected by the course of the Inter Tropical Convergence Zone. However the climate of Indonesia is also affected by occasionally occurring ENSO events, leading to strong anomalies in rainfall (Gunawan et al. 2003).

1.2.3 Forest structure and vegetation

The natural forest in Bariri is rich in rattan (*Calamus* spp.) and in epiphytic plants. The understorey contains a sparse layer of young trees. With an estimated number of 100 tree species per hectare, the forest is highly diverse (Kessler et al. 2005). According to a recent inventory the dominant tree species with 12% of all individuals with diameter at breast height (dbh) ≥ 7 cm is *Castanopsis acuminatissima* of the most abundant family Fagaceae (18%), which is followed in abundance by Myrtaceae (13%), Elaeocarpaceae (7%), and Monimiaceae (7%) Grote (2006). The forest is a closed stand with a stem density of 557 ha⁻¹ (dbh ≥ 10 cm). Additionally there were 10-fold larger number of seedlings and saplings with dbh < 10 cm. The wood basal area per hectare was 53 m². Average height of trees with dbh ≥ 10 cm was 24 m with a range from 12 m to 36 m. Leaf area index (LAI) determined with hemispherical photography after correction for leaf clumping effects was estimated to 6.7. The forest shows no signs of major anthropogenic impact.

1.3 Field measurements of leaf gas exchange

1.3.1 Steady-state gas exchange measurements and parameter estimation

Steady-state leaf gas exchange rates were measured with a portable photosynthesis apparatus LI-6400, Li-Cor, Inc., Lincoln, USA, (Figure 1.3) which was equipped with CO₂ and H₂O infra-red gas analyzers and an integrated blue-red light source mounted at the top of the leaf chamber that allowed control of environmental variables within the leaf chamber. Leaf temperature was measured using a calibrated leaf-chamber thermocouple. Fully expanded and apparently non-senescent leaves were measured while they were attached to the trees. This was necessary because measuring leaves on cut branches from top of the canopy did not work. Stomatal conductance started to decrease soon after the branch was cut. There is evidence that the fractional allocation of nitrogen to Rubisco and chlorophyll can decrease with leaf age and this decrease correlated with a down-regulation in

photosynthesis, V_{cmax} and J_{max} (Grassi et al. 2005, Rey and Jarvis 1998). A reduction in V_{cmax} with leaf age explained by corresponding changes in leaf nitrogen was also reported by Field (1983), Field and Mooney (1983) and Karlsson (1994).

Five most frequent tree species that were accessible from the tower were selected for measurements. One tree namely *Castanopsis buruana* (CB) could be reached at 20m height inside the canopy from the meteorological scaffolding tower erected by STORMA. Two other tree species namely *Garcinia dulcis* (GD) and *Phaleria coccinea* (PC) were selected from the shade crown. These three species (CB, GD and PC) situated inside the forest canopy are considered as shade crown. The other two species *Lithocarpus havilandii* (LH) and *Vernonia arborea* (VA) which could only be measured at the forest edge and facing the open field and therefore have been considered as sun crown. For every species ten leaves were measured for the relationships between intercellular CO_2 concentrations and carbon assimilation rate ($A-C_i$) curves, between photosynthetic photon flux (Q) and carbon assimilation rate ($A-Q$) curves and for their dark respiration (R_d) at three different leaf temperatures of 20 °C, 25 °C and 30 °C.



Figure 1.3. Leaf chamber of photosynthetic gas analyzing apparatus Licor 6400

Before placing leaves into the leaf chamber the LI-6400 was prepared for about half an hour to make the IRGAs ready and stable. Both analyzers were calibrated

regularly with CO₂ and H₂O free air and known standards. Once the IRGAs were operational (warmed up) the leaf chamber conditions (light, air flow, CO₂ concentration and leaf temperature) were set and then clamped onto the leaf. Before starting measurements the leaf was allowed to be adjusted to the initial chamber conditions until stability was achieved. Criteria for stability of the steady state measurement conditions within the leaf chamber were set to overall coefficient of variation CV < 1% for CO₂, H₂O and air flow in the sample cell. After placing the leaf into the chamber, considerable time was given for the acclimation of the leaf to the initial cuvette conditions. During the course of measurements of each response curve, enough time was given for every change in cuvette conditions before logging the data in order to attain the criteria for stability that was set before hand.

Our objective was to maintain stable conditions (leaf chamber micro-climate) throughout one full response curve of both $A-C_i$ and $A-Q$ measurements. Accordingly leaf temperature was set fixed to a desired value for any response curve. During the course of measurements at every step of changes in chamber CO₂ concentrations (C_a) for $A-C_i$ response curve and changes in photosynthetic photon flux (Q) for $A-Q$ response curve the leaf was allowed to be acclimated to the changed chamber conditions to attain stability criteria. During the course of response curve run, with the increase of ambient air temperature in case of $A-C_i$ and additionally with the change of PAR inside the chamber for $A-Q$ response, the block of leaf chamber and chamber air and ultimately leaf temperature was influenced and deviated from the set fixed value. The machine tried to attain the set fixed leaf temperature by cooling or warming chamber block and consequently chamber air. This phenomenon was very difficult to handle in the tropical forest conditions, where ambient air temperature changed fast over a large magnitude and it took considerable time to attain the set stability before the data could be logged in each steps of response curve. Many times it was beyond the capacity of the machine to attain stability and then IRGAs were no more ready and were malfunctioning and had to abandon the whole run. Because of this problem it was not possible measuring response curve beyond the range of 18 – 30 °C leaf temperature. The minimum and maximum waiting times for attaining stability before the observation was logged were 180 seconds and 600 seconds respectively. The responses of photosynthesis (A $\mu\text{mol m}^{-2} \text{s}^{-1}$) to Q ($\mu\text{mol m}^{-2} \text{s}^{-1}$) and to the inferred CO₂ concentration within the intercellular air space (C_i $\mu\text{mol mol}^{-1}$) were recorded. Before each observation was logged, the sample and reference IRGAs

were matched. Gas exchange parameters were calculated using the equations of von Caemmerer & Farquhar (1981).

1.3.2 A - Q response curve measurements

To determine the relationship between Q and carbon assimilation rate A , leaves were first subject to a low CO_2 concentrations to open up stomata. Then at saturating CO_2 concentration of $1000 \mu\text{mol mol}^{-1}$ steady state values of A were measured at 14 decreasing steps of photon flux densities, i.e. in an order of 1500, 1400, 1200, 1000, 800, 600, 400, 200, 100, 60, 40, 10, 5, 0 $\mu\text{mol m}^{-2} \text{s}^{-1}$. A full response curve took about one hour to run (Figure 1.4).

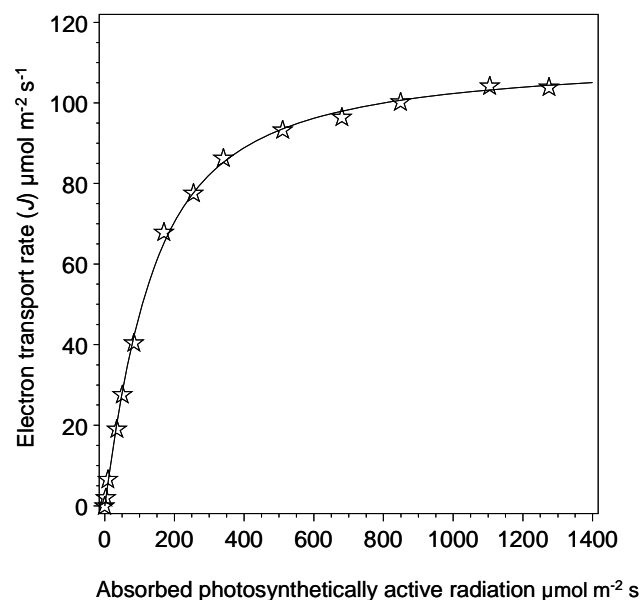


Figure 1.4. Sample (J - Q) response curve of electron transport rate to photosynthetically active radiation. Stars are measured values and the fitted line is the predicted values of the model.

1.3.3 A - C_i response curve measurements

To determine the relationship between intercellular CO_2 concentration (C_i) and carbon assimilation rate A , leaves were subject to a constant predetermined saturating Q of $1500 \mu\text{mol m}^{-2} \text{s}^{-1}$. Then the CO_2 concentration in the leaf chamber (C_a) was changed stepwise starting from about ambient concentration ($400 \mu\text{mol mol}^{-1}$) down to $50 \mu\text{mol mol}^{-1}$, and further after returning to ambient concentrations, up to a saturating CO_2 concentration at $1200 \mu\text{mol mol}^{-1}$ in an order of 400, 250, 200, 150,

100, 50, 400, 600, 800, 900, 1000, 1100, 1200 $\mu\text{mol mol}^{-1}$ in thirteen steps. A full response curve took about one hour to be run (Figure 1.5).

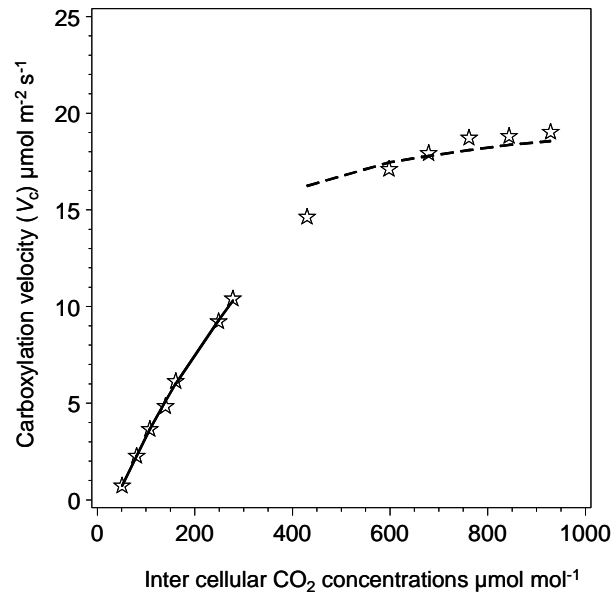


Figure 1.5. Sample ($A-C_i$) response curve of carboxylation velocity to inter cellular CO_2 concentrations. Stars are measured values and the fitted model in the lower part (continuous line) is for V_{cmax} and the fitted model in the upper part (dotted line) is for J_{max} .

1.3.4 Respiration (R_d) measurements

Dark respiration was measured at about ambient CO_2 concentration (400 $\mu\text{mol mol}^{-1}$) to minimise effect of small leaks, with no light in the leaf chamber. Observations were recorded every five seconds for five minutes and IRGAs were matched every after 15 recordings. The efflux rate of CO_2 from the leaves was assumed to represent the rate of leaf respiration.

1.4 Analysis of leaf chemical and physical properties

The shape of a fresh leaf was transferred to a sheet of white paper soon after detaching from tree. The area of each leaf was determined with an optical area meter using those paper sheets. The leaf was oven dried at 70°C for 72 hours or longer until constant mass. Specific leaf area (A_m , $\text{cm}^2 \text{g}^{-1}$) was calculated from leaf mass determined by an electric precision balance and leaf area. Leaf total nitrogen (N) concentration (i.e., on a dry mass basis) and carbon concentration of each leaf were

determined using Vario EL, (Elementar, Germany) and leaf total phosphorus (P) concentration was determined using ICP-OES (Optima 2000 DV, Perkin Elmer) in the STORMA laboratory, University of Tadulako, Palu, Indonesia. Mass-based leaf N and P concentrations were converted to area-based leaf nitrogen (N_a , g m^{-2}) and area based leaf phosphorus (P_a , g m^{-2}) concentrations by multiplying by the leaf area: mass ratio (i.e., specific leaf area).

1.5 Description of the leaf photosynthesis models

The rate of photosynthesis in a leaf is determined by the rates of carboxylation and regeneration of ribulose-1,5-bisphosphate (RuBP) catalyzed by the enzyme RUBISCO (ribulose-1,5-bisphosphate carboxylase-oxygenase). The net leaf photosynthesis (A_n) is limited by the minimum of these two limiting processes (Farquhar et al., 1980, von Caemmerer and Farquhar 1981):

$$A_n = \min(A_c, A_j) - R_d \quad (1.1)$$

A_c is the rate of photosynthesis when Rubisco activity is limiting and A_j is the rate when ribulose-1,5-bisphosphate (RuBP)-regeneration is limiting. R_d is the rate of mitochondrial respiration.

Rubisco-limited photosynthesis is given by:

$$A_c = \frac{V_{c\max}(C_i - \Gamma^*)}{\left[C_i + K_c \left(1 + \frac{O_i}{K_o} \right) \right]} \quad (1.2)$$

Where $V_{c\max}$ is the maximum rate of Rubisco-catalyzed RuBP carboxylation (i.e, rubisco activity) when CO_2 is at limiting and RuBP is at saturating concentrations, C_i and O_i are the intercellular concentrations of CO_2 and O_2 , respectively, K_c and K_o , the Michaelis-Menten coefficients of Rubisco activity for CO_2 and O_2 , respectively, and Γ^* is the CO_2 compensation point (the value of C_i at which net CO_2 uptake is zero due to photo respiration) in the absence of mitochondrial respiration. This formulation of the model assumes that the cell-wall

conductance, the conductance between intercellular space and the site of carboxylation, is negligible.

The rate of photosynthesis when RuBP regeneration is limiting is given by:

$$A_j = \left(\frac{J}{4}\right) \frac{(C_i - \Gamma^*)}{(C_i + 2\Gamma^*)} \quad (1.3)$$

Where J is the rate of electron transport, which is related to absorbed photosynthetically active photon flux density (Q_{abs}) by the following equation (de Pury and Farquhar 1997, Medlyn et al. 2002):

$$\theta J^2 - (\alpha Q_{\text{abs}} + J_{\text{max}})J + \alpha Q_{\text{abs}}J_{\text{max}} = 0$$

or

$$J = \frac{\alpha Q_{\text{abs}} + J_{\text{max}} - \sqrt{(\alpha Q_{\text{abs}} + J_{\text{max}})^2 - 4\theta\alpha Q_{\text{abs}}J_{\text{max}}}}{2\theta} \quad (1.4)$$

Where J_{max} is the potential rate of electron transport when Q_{abs} is saturating, θ determines the curvature of the light response curve, α is the quantum yield of electron transport and Q_{abs} is the absorbed Q by the photosystem II ($Q_{\text{abs}} = Q(1 - \text{reflectivity} - \text{transmissivity})$).

The key parameters of the model, which vary among species, are J_{max} , V_{cmax} and R_d . These parameters are temperature dependent and this dependence might vary among species. In addition, it is known that the parameters K_c , K_o and Γ^* also vary with temperature. But these parameters, by contrast, are thought to be intrinsic properties of the Rubisco enzyme and are generally assumed constant among C_3 species (Dungan et al. 2003), thereby reducing the number of parameters to be fitted. On this basis, literature values (Table 1.2) were used to describe their temperature response when estimating photosynthetic parameters at each leaf temperature. The parameters K_c , K_o and Γ^* have alternative formulations which could influence estimates of key parameters. It is found that the parameter J_{max} is only slightly sensitive to the formulation of either K_m or Γ^* but the parameter V_{cmax} is highly

sensitive to K_m . The ratio of $J_{\max} : V_{\text{cmax}}$ is thus also highly sensitive to the formulation of K_m (Medlyn et al. 2002).

Temperature dependence of Γ^* is given by:

$$\Gamma^* = 36.9 + 1.88 * (T-25) + 0.036 * (T-25)^2 \quad (1.5)$$

Where T is leaf temperature in °C (von Caemmerer et al. 1994).

Table 1.2. Photosynthesis primary model parameters and their temperature dependence used to estimate V_{cmax} from A - C_i curves and J_{\max} from A - C_i and A - Q curves. The RUBISCO parameters K_c , K_o and Γ^* assume an infinite internal conductance to CO_2 diffusion.

Parameters	Values	Unites
K_c (Michaelis-Menten coefficient of Rubisco for CO_2)	^a 404	$\mu\text{mol mol}^{-1}$
K_o (Michaelis-Menten coefficient of Rubisco for O_2)	^a 248000	$\mu\text{mol mol}^{-1}$
$K_c E_a$ (Activation energy for K_c)	^b 59400	J mol^{-1}
$K_o E_a$ (Activation energy for K_o)	^b 36000	J mol^{-1}
Γ^* (CO_2 compensation point in the absence of mitochondrial respiration at 25 °C leaf temperature)	^a 36.9	$\mu\text{mol mol}^{-1}$
$\Gamma^* E_a$ (Activation energy for Γ^*)	^d 29000	J mol^{-1}
O_i (Oxygen partial pressure)	205000	$\mu\text{mol mol}^{-1}$

^a von Caemmerer et al. (1994); ^b Badger & Collatz (1977); ^d Jordan & Ogren (1984)

The temperature dependence of V_{cmax} was modeled using the following Arrhenius function:

$$V_{\text{cmax}}(T_{\text{leaf}}) = V_{\text{cmax}25} \exp\left[\frac{E_a(T_k - 298\text{K})}{298RT_k}\right] \quad (1.6)$$

Where $V_{\text{cmax}25}$ is the value of V_{cmax} at 25 °C or 298 K reference leaf temperature, E_a is the activation energy (describes the exponential rate of rise of the function) of V_{cmax} , R is the universal gas constant ($8.314 \text{ J mol}^{-1}\text{K}^{-1}$), T_{leaf} is the leaf temperature in °C and T_k is leaf temperature in K.

The temperature response of J_{\max} was fitted using a peaked function, which is essentially the Arrhenius equation modified by a term that describes how conformational changes in the enzyme at higher temperature start to negate the on-going benefits that would otherwise come from further increase in temperature.

$$J_{\max}(T_k) = J_{\max 25} \exp\left[\frac{E_a(T_k - 298K)}{298RT_k}\right] \frac{1 + \exp\left(\frac{298\Delta S - E_d}{298R}\right)}{1 + \exp\left(\frac{T_k\Delta S - E_d}{T_k R}\right)} \quad (1.7)$$

Where $J_{\max}(25)$ is the value of J_{\max} at 25 °C or 298 K reference temperature, E_a is the activation energy of J_{\max} , R is the universal gas constant (8.314 J mol⁻¹ K⁻¹), T_k is leaf temperature in K, E_d is the deactivation energy (determines the rate of decrease of the function above the optimum) of J_{\max} and ΔS is known as an entropy term (700 J mol⁻¹ K⁻¹).

Temperature response of R_d was fitted using the following model:

$$R_d = R_{ref} Q_{10}^{\frac{(T_{leaf} - T_{ref})}{10}} \quad (1.8)$$

Where R_{ref} is respiration at reference leaf temperature in °C, Q_{10} is the relative increase in reaction rate at which R_d increases with an increase in temperature of 10 °C, T_{leaf} is the leaf temperature in °C and T_{ref} is reference leaf temperature.

1.6 Calculation of photosynthetic parameters

Photosynthetic parameters were estimated by fitting the model equations described above of Farquhar et al. (1980) to the measurements of leaf gas exchange by nonlinear regression. Fitting the model involved an optimization procedure in which the parameters were adjusted to minimize the sums of squares of the residuals between observed and modeled photosynthesis over the range of C_i and Q_{abs} . In the model of Farquhar et al. (1980), photosynthesis is limited by either the maximum rate of Rubisco carboxylation (V_{cmax}) or the maximum rate of electron transport (J_{\max}), parameters that indicate internal biological limitations on photosynthetic capacity.

Both the $A-Q$ and $A-C_i$ data sets (i.e., all measurements made for each leaf and at each temperature) were used to estimate J_{\max} and the data sets of $A-C_i$ and R_d (respiration measurements) were used to estimate V_{\max} and R_d respectively. Average values for dark respiration (R_d) at any leaf temperature were calculated directly from the respiration measurements at zero light with CO_2 concentrations similar to that one in the ambient air. Parameters V_{\max} were determined from AC_i curves when C_i (intercellular CO_2 concentration) $\leq 301 \mu\text{mol mol}^{-1}$. Values of Rubisco parameters such as K_c , (Michaelis-Menten coefficient of Rubisco for CO_2), K_o (Michaelis-Menten coefficient of Rubisco for O_2) and Γ^* (CO_2 compensation point in the absence of mitochondrial respiration) and their temperature dependence were taken from the literature as they are shown in the Table 1.2.

Light response curve parameters were estimated by fitting $A-Q$ data to a non-rectangular hyperbola (Equation 1.4). Apparent quantum yield (initial slope of the A/Q response curve) was obtained by fitting linear regression of data points on the initial light limited part (A values at $Q < 60 \mu\text{mol m}^{-2} \text{s}^{-1}$) of the light response curve. The apparent quantum yield of photosynthesis (α) is a measure of photosynthetic efficiency expressed in moles of photons per mole of CO_2 fixed or O_2 evolved. In order to estimate the maximum true quantum yield and the convexity (θ) of the $A-Q$ response curve, A was converted to J using the Equation 1.3. True quantum yield was obtained by linear regression between J and absorbed PAR (J values at $Q < 60 \mu\text{mol m}^{-2} \text{s}^{-1}$). The curvature of the J/Q response curve, theta (θ), was fitted by least-squares using Equation 1.4 to the data sets of $A-Q$ responses. The parameter J_{\max} was determined from both $A-C_i$ and $A-Q$ curves when $C_i \geq 400 \mu\text{mol mol}^{-1}$ to avoid data when photosynthesis was limited by carboxylation. Overall average values for true quantum yield and theta were estimated from data sets of five investigated species pooled together. These overall values were used for successive fittings to derive further parameter values and for the simulation of canopy photosynthesis model MAESTRA. The value for photosynthetically active radiation (PAR) absorptance of sample leaves (Q_{abs}) was taken as 0.87 (87% of incident PAR) from literature (e.g. Souza and Valio 2003; Singaas et al. 2001; Lee et al. 1990; Lee 1987). The values of J_{\max} and V_{\max} were obtained by fitting equations 1.1, 1.2, 1.3 and 1.4 to respective $A-C_i$ and $A-Q$ curves using a nonlinear regression routine with Gauss algorithm in SAS (SAS Institute Inc. 2004, Cary, NC, USA) with values of R_d determined from corresponding respiration measurements. Temperature response parameters were

obtained by fitting equations 1.6, 1.7 and 1.8 to response curves of V_{cmax} , J_{max} and R_{d} respectively, to leaf temperature. Relationships of V_{cmax} , J_{max} and R_{d} with leaf nitrogen per unit area (N_{a}), leaf mass per unit area (L_{a}) and leaf phosphorus per unit area (P_{a}) were investigated and compared among species.

1.7 Reference

- Bernacchi, C.J., Singaas, E.L., Pimentel, C., Portis, A.R. Jr. and Long, S.P. (2001) Improved temperature response functions for models of Rubisco-limited photosynthesis. *Plant, Cell and Environment* **24**, 355-361.
- De Pury, D.G.G. and Farquhar, G.D. (1997) Simple scaling of photosynthesis from leaves to canopies without the errors of big-leaf models. *Plant Cell and Environment* **20**, 537-557.
- Dungan, R.J., Whitehead, D. and Duncan, R.P. (2003) Seasonal and temperature dependence of photosynthesis and respiration for two co-occurring broad-leaved tree species with contrasting leaf phenology. *Tree Physiology* **23**, 561-568.
- FAO (1997) State of the World's Forests 1997. FAO, Rome, Italy.
- Farquhar, G.D., Caemmerer, S. Von and Berry, J.A. (1980) A biochemical model of photosynthetic CO_2 assimilation in leaves of C_3 species. *Planta* **149**, 78-90
- Fearnside, P.M. (2000) Global warming and tropical land-use change: greenhouse gas emissions from biomass burning, decomposition and soils in forest conversion, shifting cultivation and secondary vegetation. *Climate Change* **46**, 115-158.
- Field, C. (1983) Allocating leaf nitrogen for the maximization of carbon gain: Leaf age as a control on the allocation programme. *Oecologia* **56**, 341-347.
- Field, C. and Mooney, H.A. (1983) Leaf age and seasonal effects on light, water and nitrogen use efficiency in a California shrub. *Oecologia* **56**, 348-355.
- Field, C.B., Behrenfeld, M. J., Randerson, J.T. and Falkowski, P. (1998) Primary production of the biosphere: integrating terrestrial and oceanic components. *Science* **281**, 237-240.
- Gash, J.H.C., Nobre, C.A., Roberts, J.M. and Victoria, R.L. (1996) *Amazonian deforestation and climate*. John Wiley & Sons, Chichester, 611 p.
- Grace, J. (2004) Understanding and managing the global carbon cycle. British Ecological Society, *Journal of Ecology* **92**, 189-2002.
- Grace, J., Lloyd, J., McIntyre, J., Miranda, A.C., Meir, P., Miranda, H.S., Nobre, C., Moncrieff, J., Massheder, J., Malhi, Y., Wright, I., and Gash, J., (1995b) Carbon dioxide uptake by an undisturbed tropical rain forest in south-west Amazonia, 1992-93. *Science* **270**, 778-780.
- Grace, J., Malhi Y., Higuchi N., and Meir P. (2001) Productivity of tropical rain forests. In *Terrestrial Global Productivity* (eds J. Roy, B. Saugier and H.A. Mooney). Academic Press, 525 B Street, Suite 1900, San Diego, California.
- Grassi, G., Vicinelli, E., Ponti, F., Cantoni, L. and Magnani, F. (2005) Seasonal and interannual variability of photosynthetic capacity in relation to leaf nitrogen in a deciduous plantation in northern Italy. *Tree Physiology* **25**, 349-360.
- Grote, S. (2006) Struktur eines submontanen tropischen natürlichen Regenwaldes bei Bariri auf der indonesischen Insel Sulawesi. Masterarbeit, Institut für Bioklimatologie, Georg August Universität Göttingen.

- Gunawan, D., Gravenhorst, G. and Jacob, D., (2003) Rainfall variability studies in South Sulawesi, using Regional Climate Model, REMO. *J. Met. Geo.* **4(5)**, 65-70.
- Harley, P.C., Tenhunen, J.D. and Lange, O.L. (1986) Use of an analytical model to study limitation on net photosynthesis in *Arbutus unedo* under field conditions. *Oecologia* **70**, 393-401.
- Ibrom, A., Oltchev, A., June, T., Ross, T., Kreilein, H., Falk, U., Merklein, J., Twele, A., Rakkibu, G., Grote, S., Rauf, A., and Gravenhorst, G. (2007) Effects of land-use change on matter and energy exchange between ecosystems in the rain forest margin and the atmosphere. In: Tschardtke, T., Leuschner, C., Zeller, M., Guhardja, E. and Bidin, A. (eds), *The stability of tropical rain forest margins, linking ecological, economic and social constraints of land use and conservation*, Springer Berlin 2007, pp 463-492.
- Jarvis, P.G. (1995) Scaling process and problems. *Plant, Cell and Environment* **18**, 1079-1089.
- Karlsson, P.S. (1994) The significance of internal nutrient cycling in branches for growth and reproduction of *Rhododendron lapponicum*. *Oikos* **70**, 191-200.
- Lee, D.W. (1987) The spectral distribution of radiation in two neotropical rainforests. *Biotropica* **19(2)**, 161-166.
- Lee, D.W., Bone, R.A., Tarsis, S.L. and Storch, D. (1990) Correlates of leaf optical properties in tropical forest sun and extreme-shade plants. *American Journal of Botany* **77(3)**, 370-380.
- Leuning, R., Kelliher, F.M., de Pury, D.G. and Schulze, E.D. (1995) Leaf nitrogen, photosynthesis, conductance, and transpiration: scaling from leaves to canopies. *Plant, Cell and Environment* **18**, 1183-1200.
- Lloyd, J. (1999) The CO₂ dependence of photosynthesis, plant growth responses to elevated CO₂ concentrations and their interactions with soil nutrient status. II. Temperate and boreal forest productivity and the combined effects of increasing CO₂ concentrations and increased nitrogen deposition at a global scale. *Functional Ecology*, **13**, 439-459.
- Medlyn, B.E., Dreyer, E., Ellsworth, D., Forstreuter, M., Harley, P.C., Kirschbaum, M.U.F., Leroux, X., Montpied, P., Strassmeyer, J., Walcroft, A., Wang, K. and Loustau, D. (2002) Temperature response of parameters of a biochemically based model of photosynthesis. II. A review of experimental data. *Plant, Cell and Environment* **25**, 1167-1179.
- Rey, A. and Jarvis, P.G. (1998) Long-term photosynthetic acclimation to increased atmospheric CO₂ concentration in young birch (*Betula pendula*) trees. *Tree physiology* **18**, 441-450.
- Roux, X.L., Grand, S., Dreyer, E. and Daudet, F.A. (1999) Parameterization and testing of a biochemically based photosynthesis model for walnut (*Juglans regia*) trees and seedlings. *Tree Physiology* **19**, 481-492.
- SAS Institute Inc. (2004) SAS 9.1.3 Help and Documentation, Cary, NC, USA
- Skole, D. and Tucker, C., (1993) Tropical deforestation and habitat fragmentation in the amazon: satellite data from 1978 to 1988. *Science* **260**, 1905-1910.
- Souza, R.P. and Valio, I.F.M. (2003) Leaf optical properties as affected by shade in saplings of six tropical tree species differing in successional status. *Brazilian Journal of Plant Physiology* **15(1)**, 49-54.
- Tschardtke, T., Leuschner, C., Zeller, M., Guhardja, E. and Bidin, A. (eds) (2007) *Stability of Tropical Rainforest Margins, linking ecological, economic and social constraints of land use and conservation*, Springer Berlin 2007, pp 515.

- von Caemmerer, S. & Farquhar, G.D. (1981) Some relationships between the biochemistry of photosynthesis and the gas exchange of leaves. *Planta* **153**, 367-387.
- von Caemmerer, S., Evans, J.R., Hudson, G.S. and Andrews, T.J. (1994) The kinetics of Rubisco inferred from measurements of photosynthesis in leaves of transgenic tobacco with reduced Rubisco content. *Planta* 195, 33-47.
- Wallace, A.R. . (1869) The Malay Archipelago. Paperback edition Periplus Ltd., 515 pp.
- Whitehead, D., Leathwick, J.R. and Walcroft, A.S. (2001) Modeling annual carbon uptake for the indigenous forest of New Zealand. *For. Sci.* 47, 9-20.
- Whittaker, R.H. and Likens, G.E. (1973) Carbon in the biota. In *Carbon and the Biosphere* (eds G.M. Woodwell & E.V.Pecan), pp.281-302. National Technical Information Service, Washington D.C.
- Williams, M., Malhi, Y., Nobre, A.D., Rastetter, E.B., Grace, J. and Pereira, M.G.P. (1998) Seasonal variation in net carbon exchange and evapotranspiration in a Brazilian rain forest: a modeling analysis. *Plant, Cell and Environment* **21**, 953-968.

2 Chapter- II: Photosynthetic and respiration parameters and their temperature dependence in tropical montane rainforests of Central Sulawesi, Indonesia.

2.1 Abstract

Photosynthetic capacities such as maximum carboxylation rate of enzyme RUBISCO (V_{cmax}), the potential rate of electron transport (J_{max}) and the dark respiration (R_{d}) are known to be temperature dependent. The temperature dependence of C_3 photosynthesis is again known to vary with growth environment and species. In an attempt to quantify the variability and temperature dependencies of these photosynthetic and respiration capacities of a tropical montane rainforest trees in Central Sulawesi, Indonesia, a commonly used biochemically based photosynthesis model of Farquhar, von Caemmerer & Berry (1980) was parameterized with values from gas exchange studies on leaves of five major tree species.

There were variations in the values of V_{cmax} , J_{max} and R_{d} at 25 °C leaf temperature among leaves of trees and species. The J_{max} and V_{cmax} values were strongly correlated with an average $J_{\text{max}}: V_{\text{cmax}}$ ratio of 2.0. The $J_{\text{max}}: V_{\text{cmax}}$ ratio increased with an increase in measurement temperature at lower level from 15 °C up to 25 °C leaf temperature and the ratio declined strongly at higher leaf temperature beyond 25 °C. Two species *L. havilandii* and *V. arborea* had higher values of V_{cmax} (61.4 and 46.0 $\mu\text{mol m}^{-2} \text{s}^{-1}$ respectively) and J_{max} (107.2 and 90.6 $\mu\text{mol m}^{-2} \text{s}^{-1}$ respectively), but had lower $J_{\text{max}}: V_{\text{cmax}}$ ratios (1.8 and 1.9 respectively). Three other species *C. buruana*, *G. dulcis* and *P. coccinea* had lower values of V_{cmax} (33.0, 20.4 and 31.0 $\mu\text{mol m}^{-2} \text{s}^{-1}$ respectively) and J_{max} (61.2, 46.9 and 68.3 $\mu\text{mol m}^{-2} \text{s}^{-1}$ respectively), but had higher $J_{\text{max}}: V_{\text{cmax}}$ ratios (2.3 and 2.2 respectively) except species *C. buruana*.

Activation energies (E_{a}) for V_{cmax} were similar in four species except *G. dulcis* (32.5 KJ mol^{-1}) which had lower E_{a} than the average of the other four species. E_{a} ranged between 40.0 KJ mol^{-1} and 51.0 KJ mol^{-1} with an average value of 43.0 KJ mol^{-1} . On the other hand variations in E_{a} of J_{max} was relatively higher and it ranged between 129.0 KJ mol^{-1} and 178.0 KJ mol^{-1} and averaged to 160.8 KJ mol^{-1} . Energies of deactivation (E_{d}) for J_{max} were very similar among all the investigated species and ranged from 205.8 KJ mol^{-1} to 208.7 KJ mol^{-1} with an average value of 207.4 kJ mol^{-1} .

Deactivation energy for V_{cmax} was not applicable to our data sets, i.e. in the observed temperature range from 20 °C to 30 °C.

Dark respiration (R_d) at 25 °C leaf temperature was also very similar among species except in one species (*G. dulcis*), which had a lower ($0.77 \mu\text{mol m}^{-2} \text{s}^{-1}$) value compared to other species. R_{d25} for the other four species ranged between 1.0 and $1.3 \mu\text{mol m}^{-2} \text{s}^{-1}$, with an average value of $1.12 \mu\text{mol m}^{-2} \text{s}^{-1}$. Dark respiration increased with leaf temperature. Q_{10} of R_d ranged from 1.5 to 2.0 among the five species with an average value of 1.8. The results suggest that both growth environment and species can influence the photosynthetic response to temperature of tropical montane rain forest trees.

2.2 Introduction

Rates of photosynthesis and respiration depend strongly on leaf temperature (Dungan et al. 2003). Rates generally increase exponentially with temperature, although it has been shown that photosynthetic parameters can reach an optimum, beyond which further increase in temperature yield decreased rates (e.g., Walcroft et al. 1997). Quantifying the response of individual species is important for comparing species responses to environmental conditions. With the predicted greenhouse-induced rise in global surface temperature the effects of increasing temperature on plant growth and ecosystem function have become a major area of concern (Gunderson, Norby & Wullschleger 2000). Temperature effects on individual plant processes have been extensively studied. The results of these individual-process studies may be integrated using process based computer models to predict effects of increasing temperature on overall forest ecosystem function (Grant & Nalder 2000; Medlyn et al., 2002). For most of such models, photosynthesis is the driving process, being the mechanism by which plants take up carbon and thus a key determinant of the rate of plant growth. Photosynthetic response to temperature is therefore an important part of the models (Medlyn et al., 2002).

Biochemically based models of C_3 photosynthesis at the leaf level, which have their origins in the seminal work of Farquhar et al., (1980) are now widely used to simulate photosynthesis at the canopy level (De Pury and Farquhar 1997), to compare photosynthetic performance among species and to predict photosynthetic acclimation to high CO_2 concentrations and growth irradiance (Erwin et al., 2001). The key

parameters of these photosynthesis models are the maximum rate of carboxylation (V_{cmax}), the light (=RuBP) saturated rate of electron transport (J_{max}), and mitochondrial respiration due to phosphorylative oxidation (i.e. dark respiration; R_d). These parameters are strongly influenced by (i) leaf morphological, such as leaf mass per unit area and biochemical characteristics including the total amount of nitrogen per unit leaf area, and the fraction of nitrogen invested in the different photosynthetic functions, and (ii) leaf temperature (Dreyer et al., 2001).

The model of Farquhar et al., (1980) can accurately describe leaf level photosynthesis, provided values of eight parameters of the model are known. There is considerable variation between and within species in the two key parameters V_{cmax} and J_{max} , although some of this variation may be ascribed to differences in leaf nitrogen concentration (Leuning, Cromer & Rance 1991; Harley et al. 1992; Kellomäki & Wang 1997). Another important aspect of these two parameters is, that they are temperature dependent and the dependence varies significantly between and within species (Leuning 2002). Many of the current models use the biochemically based photosynthesis model of Farquhar, von Caemmerer & Berry (1980), a mechanistic model that can realistically describe the photosynthetic responses to environmental variables. However, this model is not straightforward to parameterize, and there have been very few studies that have fully parameterized the temperature responses of the model (Leuning 1997; Dreyer 2001).

All published carbon gain models use a temperature response function (Harley and Tenhunen 1991, Leuning 1997). However, only a few studies have produced data sets for the temperature dependencies of V_{cmax} and J_{max} for trees (Falge et al. 1996, Walcroft et al. 1997, Niinemets et al. 1999a, Ibrom et al. 2006). To date, though a limited number of studies examining temperature response in the context of Farquhar model has been conducted (Leuning 1997), the majority of them are on temperate forests and only a few on low land tropical rain forests. There has been almost none such studies on tropical montane rain forests, especially in South-East Asian forests, despite the immense importance of tropical rain forests in terms of annual carbon (C) turnover and evapotranspiration (Williams et al. 1998). Thus the aim of this study was to assess the parameter values and their temperature dependency of the key parameters (V_{cmax} , J_{max} and R_d) of Farquhar et al. (1980) model of photosynthesis for five tree species of the tropical montane rain forest trees of Central Sulawesi,

Indonesia: *C. buruana* (CB), *G. dulcis* (GD), *L. havilandii* (LH), *P. coccinea* (PC) and *V. arborea* (VA).

2.3 Materials and methods

2.3.1 Model overview

The rate of photosynthesis in a leaf is determined by the rates of carboxylation and regeneration of ribulose-1,5-bisphosphate (RuBP) catalyzed by the enzyme RUBISCO (ribulose-1,5-bisphosphate carboxylase-oxygenase) (Farquhar et al., 1980, von Caemmerer and Farquhar 1981). The rate of photosynthesis is limited by the smaller of these two rates. Parameters for the model describing this relationship are V_{cmax} , the maximum rate of RUBISCO-catalyzed RuBP carboxylation when CO_2 is at limiting concentrations; J_{max} , the rate of electron transport where irradiance (Q) is saturating (=RuBP is limiting); R_d , the rate of dark respiration (i.e., respiration due to processes other than photosynthesis). Leaf gas exchange data were fitted to the Farquhar et al (1980) model, giving responses of the model parameters J_{max} , V_{cmax} and R_d to leaf temperatures. The temperature response of V_{cmax} was fitted using an Arrhenius equation:

$$V_{cmax}(T_{leaf}) = V_{cmax25} \exp\left[\frac{E_a(T_{leaf} - 25)}{298RT_k}\right] \quad (2.1)$$

Where V_{cmax25} is the value of V_{cmax} at 25 °C or 298 K reference leaf temperature, E_a is the activation energy (describes the exponential rate of rise of the function below optimum) of V_{cmax} , R is the universal gas constant ($8.314 \text{ J mol}^{-1}\text{K}^{-1}$), T_{leaf} is the leaf temperature in °C and T_k is leaf temperature in K.

The temperature response of J_{max} was fitted using a peaked function, which is essentially the Arrhenius equation modified by a term that describes how conformational changes in the enzyme at higher temperature starts to negate the on-going benefits that would otherwise come from further increase in temperature.

$$J_{\max}(T_k) = J_{\max 25} \exp\left[\frac{E_a(T_k - 298)}{298RT_k}\right] \frac{1 + \exp\left(\frac{298\Delta S - E_d}{298R}\right)}{1 + \exp\left(\frac{T_k\Delta S - E_d}{T_k R}\right)} \quad (2.2)$$

Where $J_{\max}(25)$ is the value of J_{\max} at 25 °C or 298 K reference temperature, E_a is the activation energy of J_{\max} , R is the universal gas constant (8.314 J mol⁻¹ K⁻¹), T_k is leaf temperature in K, E_d is the deactivation energy (describes the rate of decrease of the function above the optimum) of J_{\max} and ΔS is known as an entropy term (700 J mol⁻¹ K⁻¹).

Temperature response of R_d was fitted using the following model:

$$R_d = R_{d25} Q_{10}^{\frac{(T_{\text{leaf}} - 25)}{10}} \quad (2.3)$$

Where R_{ref} is respiration at reference leaf temperature (°C), Q_{10} is the relative increase in reaction rate at which R_d increases with an increase in temperature of 10 °C, T_{leaf} is the leaf temperature in °C and T_{ref} is reference leaf temperature.

2.3.2 Study site

The study was carried out in a tropical natural rain forest in Central Sulawesi, Indonesia during February to August 2005. The study site is a part of the Lore Lindu National Park in the Besoa region near the village Bariri (1° 39.476'S 120° 10.409'E) at an altitude of 1416 m. The study area has a humid tropical climate with almost no seasonal changes in temperature but with small seasonal changes in rainfall without a pronounced dry season. Mean annual precipitation and mean annual temperature at the study site during October 2003 to February 2005 was 1700 mm yr⁻¹ and 19.1°C respectively (Ibrom et al. 2007). Seasonality is normally affected by the course of the Inter Tropical Convergence Zone. However the climate of Indonesia is also affected by occasionally occurring ENSO events, leading to strong anomalies in rainfall (Gunawan et al. 2003).

2.3.3 Data analysis

Photosynthetic parameters were estimated by fitting the model equations of Farquhar et al. (1980) to the measurements of leaf gas exchange, described in the previous chapter, by nonlinear least square regressions. Temperature response parameters were obtained by fitting equations 1, 2 and 3 to response curves of V_{cmax} , J_{max} and R_{d} respectively, to leaf temperature response data using SAS.

2.4 Results and discussions

2.4.1 Quantum yield (α) and theta (θ) values of light response curves

Values for apparent quantum yield (initial slope of the A/Q response curve) are presented in Table 2.1. Values ranged between 0.046 and 0.07 mol CO₂ mol⁻¹ photon among the five investigated species and the pooled value was 0.055 (mol CO₂ mol⁻¹ photon). These values were similar to that reported by Zhang et al. (2006) for tropical wet forest (0.07) and rainforest (0.049) and also similar to that reported in Singaas (2001). On the contrary, the present estimated α values were larger compared to the values 0.033 and 0.031 mol CO₂ mol⁻¹ photon reported for Central Amazonian forest understorey trees (Marengo and Vieira 2005) and for dipterocarp seedlings of Sabah, Malaysia (Barker et al. 1997), respectively. The maximum true quantum yields, when electron transport rate (J) was fitted against absorbed PAR, are given in Table 2.2. It ranged between 0.247 and 0.367 mol e⁻ mol⁻¹ absorbed PAR among the five investigated species. The overall value was 0.29 mol e⁻ mol⁻¹, when data from five species pooled together.

Table 2.1. Light limited apparent quantum yields (mol CO₂ mol⁻¹ incident photon) of CO₂ exchange. Results are fitted values of 20 – 25 data sets from 8-10 leaves of each species. Overall, data pooled from five species. Values in parentheses are r² of linear regressions. Significance of the Parameter values were P<0.05 (*), P<0.01 (**), P<0.001 (***).

Species	α - (T _{leaf} 20-30 °C)	α - (T _{leaf} <26 °C)	α - (T _{leaf} ≥26 °C)
<i>C. buruana</i>	0.046 ± 0.003*** (0.76)	0.046	0.046
<i>G. dulcis</i>	0.046 ± 0.002*** (0.74)	0.053	0.039
<i>L. havilandii</i>	0.057 ± 0.003*** (0.78)	0.058	0.056
<i>P. coccinea</i>	0.056 ± 0.003*** (0.76)	0.065	0.047
<i>V. arborea</i>	0.070 ± 0.003*** (0.81)	0.074	0.065
Overall	0.055 ± 0.001*** (0.74)	0.059	0.050

Table 2.2. Light limited true quantum yields (mol e- mol⁻¹ absorbed PAR) of CO₂ exchange. Results are fitted values of 20 – 25 data sets from 8-10 leaves of each species. Overall, data pooled from five species. Values in the parentheses are r² of linear regressions. Significance of the Parameter values were P<0.05 (*), P<0.01 (**), P<0.001 (***).

Species	α - (T _{leaf} 20-30 °C)	α - (T _{leaf} <26 °C)	α - (T _{leaf} ≥26 °C)
<i>C. buruana</i>	0.248 ± 0.018*** (0.74)	0.242	0.254
<i>G. dulcis</i>	0.247 ± 0.013*** (0.76)	0.274	0.223
<i>L. havilandii</i>	0.307 ± 0.016*** (0.79)	0.309	0.306
<i>P. coccinea</i>	0.296 ± 0.017*** (0.77)	0.336	0.260
<i>V. arborea</i>	0.367 ± 0.018*** (0.82)	0.384	0.352
Overall	0.292 ± 0.008*** (0.75)	0.311	0.277

The curvatures of the J/Q response curve, theta (θ), are presented in Table 2.3. Average values for θ ranged from 0.49 to 0.88 among species and the overall average value for five species pooled together was 0.7. In general theta values of the investigated species seems to be relatively low. This low theta value would influence the electron transport rate and, therefore, would increase the fitted J_{\max} values. According to June (2005), variation in θ among leaves or among species could be

related to the leaf thickness. She suggested that in the case of a bifacial leaf measured with light given only to the upper surface, the upper and lower parts of the leaf would reach saturation at different light intensities causing the light response curve to bend more slowly and saturating in a lower value of the curvature factor. Accordingly, theta values should be decreasing with the decrease of specific leaf area (A_m , $\text{cm}^2 \text{g}^{-1}$). This relationship of species average values is shown in Figure 2.1. The result supports the above statement but the relationship is not very strong among the investigated species.

Table 2.3. Curvature of light response curve (theta, θ). Values in the parentheses are standard deviations. Overall, data pooled from five species.

Species	<i>C. buruana</i>	<i>G. dulcis</i>	<i>L. havilandii</i>	<i>P. coccinea</i>	<i>V. arborea</i>	Overall
Theta	0.49 (0.25)	0.72 (0.15)	0.85 (0.117)	0.62 (0.25)	0.88 (0.12)	0.7 (0.17)

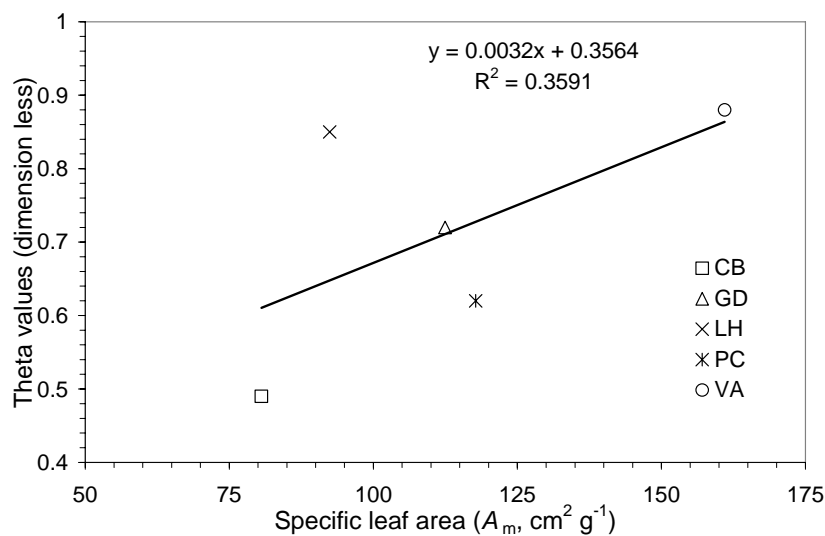


Figure 2.1. Relationship between theta (θ) and specific leaf area (SLA).

2.4.2 Temperature dependence of V_{cmax}

Fitted parameters of the temperature response of V_{cmax} , J_{max} and R_d are given in Table 2.4. Values of V_{cmax} , J_{max} and R_d at the reference temperature of 25 °C differed considerably among species and within leaves of an individual species. Variation in maximum carboxylation rate at 25 °C leaf temperature (V_{cmax25}) and variation in

activation energies for V_{cmax} (E_{av}) within and among species are shown in Figures 2.2 and 2.3 respectively. In general variation in V_{cmax25} was higher compared to the variation in E_{av} indicating similarity in the physiological processes among species. Species averages of V_{cmax25} had large standard deviations (Figure 2.2) indicating large variations in photosynthetic RUBISCO capacity among leaves of a single species at any given leaf temperature. This variation in V_{cmax25} could arise from the variations in chemical and morphological properties among leaves which will be described in the next chapter. Because of this variations values for r^2 of the overall temperature response fitting of photosynthetic capacities have become low in Table 2.4. The temperature dependence of the predicted values of V_{cmax} is shown in Figures 2.4 and 2.5. Generally the V_{cmax} increased steadily with increasing temperature, and within the range of measured leaf temperatures (18 °C to 30°C) there was no sign of reaching optimum level.

The values of V_{cmax25} , the maximum rate of Rubisco activity at 25 °C leaf temperature, varied across species by a factor of three. It ranged between $20.4 \pm 1.5 \mu\text{mol m}^{-2} \text{s}^{-1}$ to $61.4 \pm 6.6 \mu\text{mol m}^{-2} \text{s}^{-1}$. A great proportion of the variations among and within species could be described by the variations in leaf nitrogen content. The two species (*L. havilandii* and *V. arborea*) which could be measured at the forest edge and could therefore be classified as sun crown had much higher V_{cmax25} values of 61.4 and $46.4 \mu\text{mol m}^{-2} \text{s}^{-1}$ respectively. Whereas the other leaves measured at the tree species *C. buruana*, *G. dulcis* and *P. coccinea* were situated inside the forest canopy and considered as shade crown had lower values of 33.0, 20.4 and $31.0 \mu\text{mol m}^{-2} \text{s}^{-1}$ respectively. Note that all rates are expressed on one-sided leaf area basis.

The values for V_{cmax} of the present study species falls within the ranges of values from other studies of the tropical rain forest species. Meir et al. (2002) reported a range of $20 \sim 40 \mu\text{mol m}^{-2} \text{s}^{-1}$ for a tropical rain forest site, 60 km north of Manaus in Central Amazonia, Brazil. Compared to this range, our values for V_{cmax} coincides with the lower limit but exceeds the upper limit by $20 \mu\text{mol m}^{-2} \text{s}^{-1}$. In another retrospective analysis of $A-C_i$ curves of individual leaves, Wullschleger (1993) calculated a mean value of V_{cmax} for tropical forest species of $51.0 \mu\text{mol m}^{-2} \text{s}^{-1}$. This mean value was based on a reported range of $9.0 - 126.0 \mu\text{mol m}^{-2} \text{s}^{-1}$ which is a much wider range compared to ours. Also, the mean value of V_{cmax} ($38.0 \mu\text{mol m}^{-2} \text{s}^{-1}$) of

the present study is considerably lower than that of Wullschleger (1993). This lower photosynthetic capacity can be attributed to the low nitrogen concentration (1.49 g m^{-2}) in the leaves of montane rain forest trees of Sulawesi, Indonesia compared to the central Amazonian (2.66 g m^{-2}) rain forest trees (Carswell et al. 2000; Meir et al. 2002).

Variation in activation energy for V_{cmax} is low among species and the rate of carboxylation increased with the increase in leaf temperature. The activation energy (E_a) for V_{cmax} of four species was in the range of $40.0 - 51.0 \text{ kJ mol}^{-1}$ and averaged to 45.2 kJ mol^{-1} , implying a similarity in the temperature responses of V_{cmax} across species. The other species, *G. dulcis*, had a value of E_a (32.5 kJ mol^{-1}) considerably lower than the above mentioned range. This low value of E_a could be the intrinsic property of this species. This species differs considerably from others in leaf nitrogen content (1.18 g m^{-2} , species average) per unit area compared to the average (1.56 g m^{-2}) of the other four species. The variability in the temperature response of V_{cmax} is illustrated in Figure 2.5, which shows the temperature responses normalized to 1 at 25°C . The average value (43.0 kJ mol^{-1}) and the range ($32.5 - 51.2 \text{ kJ mol}^{-1}$) of E_a for V_{cmax} of the present sample tree species could not be compared as there was no available data from similar forest type. But these values were somewhat similar (e.g. Medlyn et al. 2002) and in other cases they were a little lower (e.g. Dreyer et al. 2001; Medlyn et al. 2002; Leuning 2002) compared to European forest tree species.

Table 2.4. Values (\pm SE when statistical analysis was possible) of the parameters describing temperature responses of leaf photosynthetic capacity of five tree species from tropical montane rain forests, Sulawesi, Indonesia: maximal rate of carboxylation at 25 °C ($V_{\text{cmax}25}$), maximal rate of electron flow at 25°C ($J_{\text{max}25}$), dark respiration at 25°C ($R_{\text{d}25}$), activation energy (E_a), deactivation energy (E_d) and temperature coefficient for dark respiration (Q_{10}). Significance of the Parameter values were $P<0.05$ (*), $P<0.01$ (**), $P<0.001$ (***)

	<i>C. buruana</i>	<i>G. dulcis</i>	<i>L. havilandii</i>	<i>P. coccinea</i>	<i>V. arborea</i>
Values for V_{cmax}					
$V_{\text{cmax}25}$ ($\mu\text{mol m}^{-2} \text{s}^{-1}$)	33.0 \pm 3.8***	20.4 \pm 1.5***	61.4 \pm 6.6***	31.0 \pm 2.7***	46.0 \pm 4.0***
E_a (kJ mol $^{-1}$)	39.4 \pm 17.0*	32.5 \pm 14.6*	48.4 \pm 21.4*	41.9 \pm 18.0*	51.2 \pm 16.9**
r^2	0.2	0.23	0.21	0.2	0.3
Values for J_{max}					
$J_{\text{max}25}$ ($\mu\text{mol m}^{-2} \text{s}^{-1}$)	61.2 \pm 2.6***	47.0 \pm 1.6***	107.2 \pm 5.4***	68.3 \pm 4.3***	90.6 \pm 4.0***
E_a (kJ mol $^{-1}$)	128.6 \pm 9.3***	171.5 \pm 7.7***	178 \pm 10.3***	155.5 \pm 14***	170.0 \pm 9.2***
E_d (kJ mol $^{-1}$)	208.715	205.754	207.445	207.522	207.789
r^2	0.15	0.1	0.22	0.08	0.2
Values for R_d					
$R_{\text{d}25}$ ($\mu\text{mol m}^{-2} \text{s}^{-1}$)	1.06 \pm 0.05***	0.77 \pm 0.03***	1.3 \pm 0.06***	1.0 \pm 0.04***	1.12 \pm 0.06***
Q_{10}	1.62 \pm 0.2***	1.5 \pm 0.2***	2.0 \pm 0.3***	2.1 \pm 0.2***	1.97 \pm 0.3***
R^2	0.43	0.27	0.53	0.68	0.44

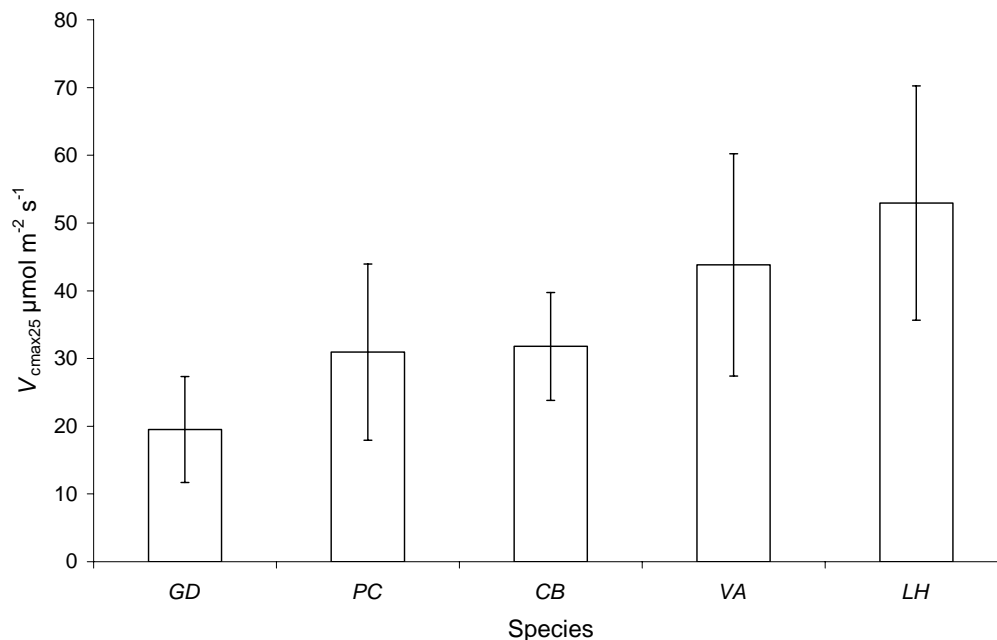


Figure 2.2. Species wise average values for the maximum RUBISCO carboxylation rate at 25 °C leaf temperature and their standard deviations.

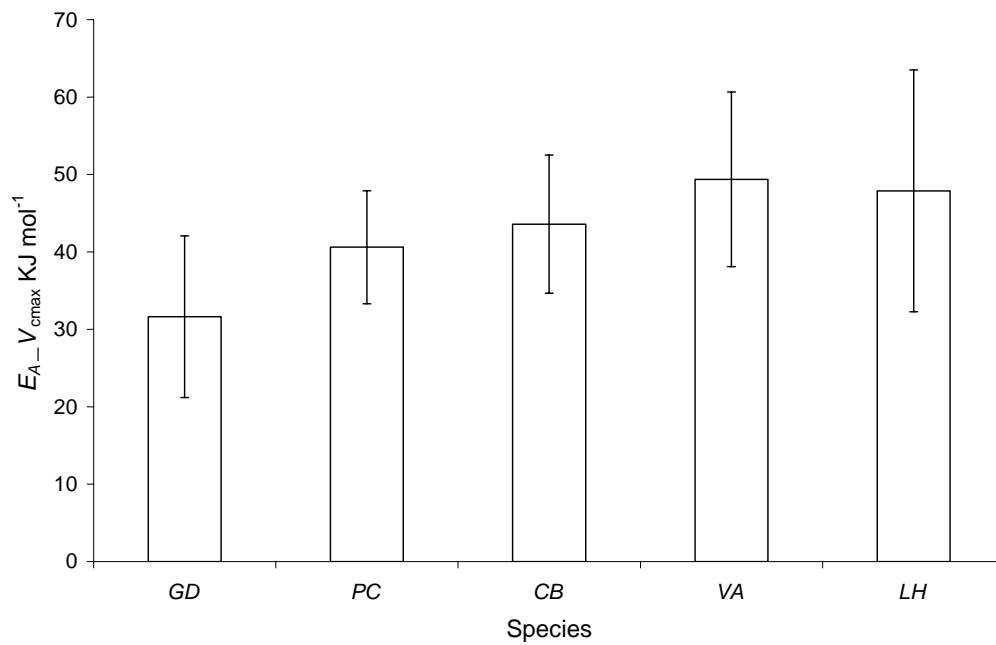


Figure 2.3. Species wise average values for activation energies of V_{cmax} and their standard deviations.

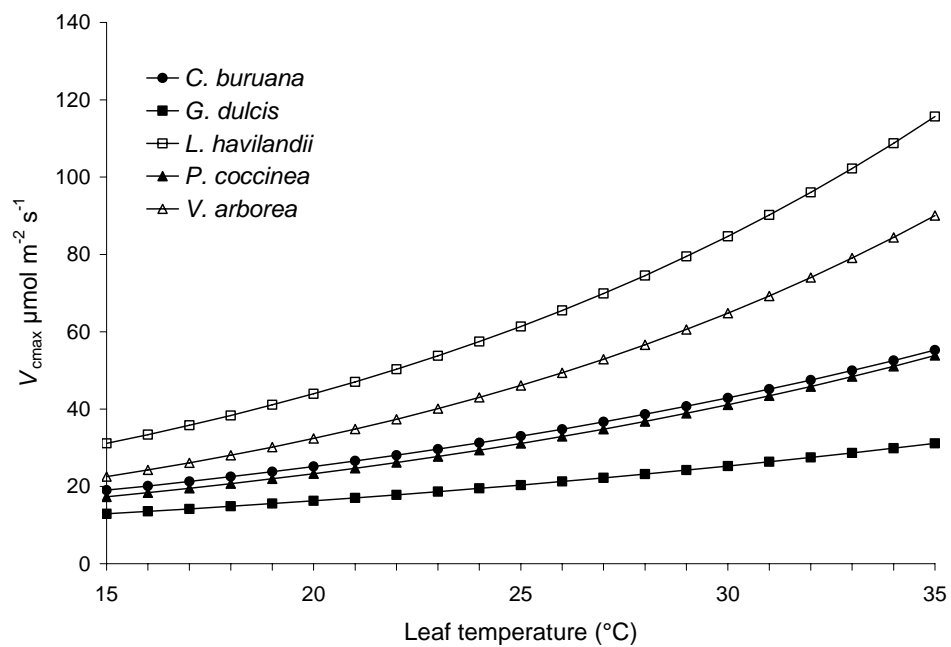


Figure 2.4. Relationship between simulated values of V_{cmax} and leaf temperatures ($^{\circ}\text{C}$). Open symbols for sun crown and solid symbols for shade crown.

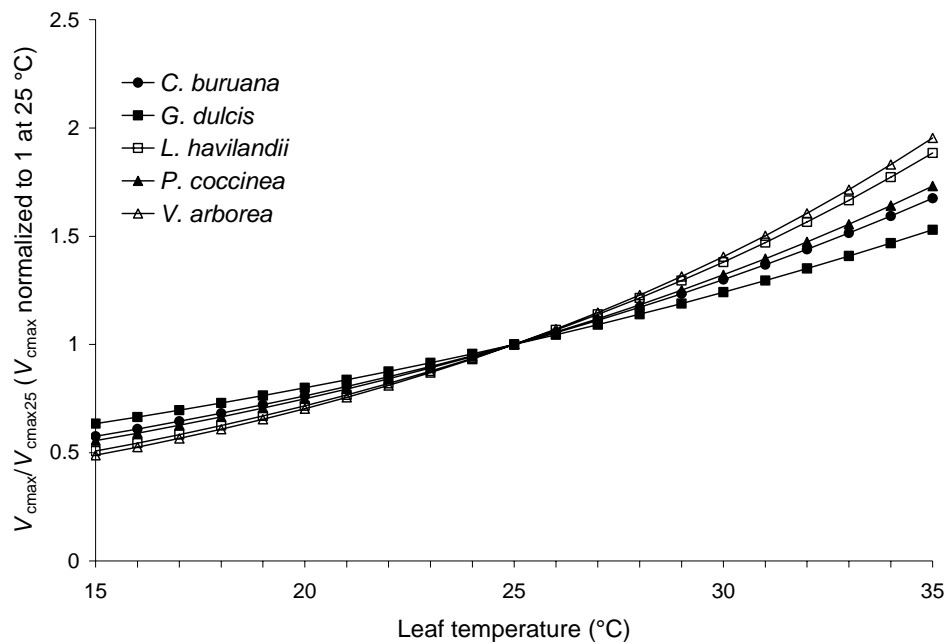


Figure 2.5. Responses of V_{cmax} to leaf temperatures. Simulated values are normalized to 1 at 25 °C.

2.4.3 Temperature dependence of J_{max}

Temperature dependence of the maximum electron transport rate (E_{aj}) and parameter values for the maximum electron transport rate at the reference leaf temperature of 25 °C (J_{max25}) varied considerably across and within species. Variation in J_{max25} and variation in E_{aj} within and across species are presented in Figures 2.6 and 2.7 respectively. Like with V_{cmax} variation in $E_{A_}J_{max}$ within and among species was much less than that of the variation in J_{max25} indicating a similar physiological process in electron transport within leaves of a species and across species. Though temperature dependence was similar (Figure 2.7) but the parameter values at reference temperature (J_{max25}) varied largely among and within species standard deviations in Figure 2.6. This variation could be caused by the variation in leaf properties (i.e., N_a and L_a) among and within species, which resulted in low r^2 values (Table 2.4) for overall temperature response fitting of the maximum electron transport rate. The sources of variation in J_{max} will be discussed in the next chapter.

Compared to the maximum carboxylation rate (V_{cmax}), the maximum electron transport rate (J_{max}) showed a smaller increase with increasing temperature. The temperature dependence of the predicted values of J_{max} is shown in Figures 2.8 and 2.9. Generally J_{max} increased with increasing leaf temperature, reached a maximum and then declined with further increase in temperature. Optimum temperatures for J_{max} of the two species considered as sun crown (*L. havilandii* and *V. arborea*) were 31 °C and 29 °C respectively with corresponding J_{max} values of 127.9 and 102.0 $\mu\text{mol m}^{-2} \text{s}^{-1}$. The other three understorey species considered as shade crown had a same lower optimum temperature of 27 °C. The corresponding optimum J_{max} values for *PC*, *CB* and *GD* were 70.9, 62.9 and 47.5 $\mu\text{mol m}^{-2} \text{s}^{-1}$ respectively. Beyond optimum all five species showed gradual decrease in the electron transport rate although these temperatures have not been measured. It is thus hypothetical i.e. found by increase of the regression model.

The values of $J_{\text{max}25}$, the maximum rate of electron transport at 25 °C, varied across species by a factor of two (Table 2.4). It ranged between $47.0 \pm 1.6 \mu\text{mol m}^{-2} \text{s}^{-1}$ and $107.2 \pm 5.4 \mu\text{mol m}^{-2} \text{s}^{-1}$. The two species (*L. havilandii* and *V. arborea*) considered as sun crown had much higher $J_{\text{max}25}$ values of 107.2 and 90.6 $\mu\text{mol m}^{-2} \text{s}^{-1}$ respectively. The other three species (*C. buruana*, *G. dulcis* and *P. coccinea*) situated inside the forest canopy and considered as shade crown had lower $J_{\text{max}25}$ values of 61.2, 46.9 and 68.3 $\mu\text{mol m}^{-2} \text{s}^{-1}$ respectively. Note that all rates are expressed on a one-sided leaf area basis. The photosynthetic parameters V_{cmax} and J_{max} were considerably higher for sun crown leaves (Table 2.4), indicating that leaves exposed to higher irradiance have higher rates of carboxylation and electron transport capacity per unit area.

J_{max} values of the present study species had a very similar spread to that was reported by Meir et al. (2002) for Central Amazonian rain forest trees, where it ranged between about 30 ~ 120 $\mu\text{mol m}^{-2} \text{s}^{-1}$. In another retrospective analysis Wullschleger (1993) reviewed the parameter values in tropical forest species (n=22), and he quoted a mean value of 107 $\mu\text{mol m}^{-2} \text{s}^{-1}$ out of a range of 30-222 $\mu\text{mol m}^{-2} \text{s}^{-1}$. Values for J_{max} of our study (47-107 $\mu\text{mol m}^{-2} \text{s}^{-1}$) correspond closely and fall in about that centre of the reported range. But our mean value (74.9 $\mu\text{mol m}^{-2} \text{s}^{-1}$) is considerably lower than that reported by Wullschleger (1993), which can also be attributed to the low nitrogen (average, 1.49 g m⁻²) concentration in the leaves of this montane rain forest trees.

The rate of increase in J_{\max} against leaf temperature varied across species (Figure 2.8). Three species (*GD*, *LH* and *VA*) had similar activation energies (E_a) for J_{\max} ranging from 170.0 to 178.0 kJ mol⁻¹ with an average value of 173.2 kJ mol⁻¹. The two other species (*CB* and *PC*) had considerably lower (128.6 kJ mol⁻¹ and 155.5 kJ mol⁻¹ respectively) activation energies. On the other hand the energy of deactivation (E_d) for J_{\max} was found to be very similar among species. It ranged between 205.7 and 208.7 kJ mol⁻¹ among species with an average value of 207.4 kJ mol⁻¹. The variability in the temperature response of J_{\max} is illustrated in Figure 2.9, which shows the temperature responses normalized to 1 at 25 °C.

The average value of E_a for J_{\max} (161.0 kJ mol⁻¹) of the present study species was much higher compared to the values reported for European forest tree species (e.g. Dreyer et al. 2001; Medlyn et al. 2002; Leuning 2002). On the other hand E_d for J_{\max} of our sample species was very similar to the studies in European forests mentioned above. These values could not be compared with tropical values because of unavailability of data.

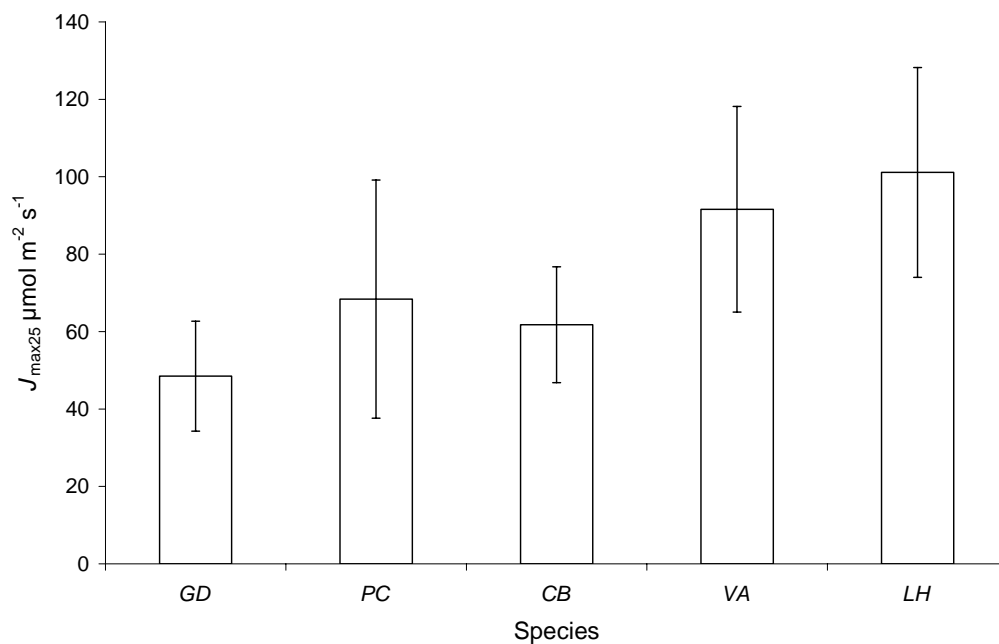


Figure 2.6. Species wise average values for the maximum rate of electron transport at 25 °C leaf temperature and their standard deviations.

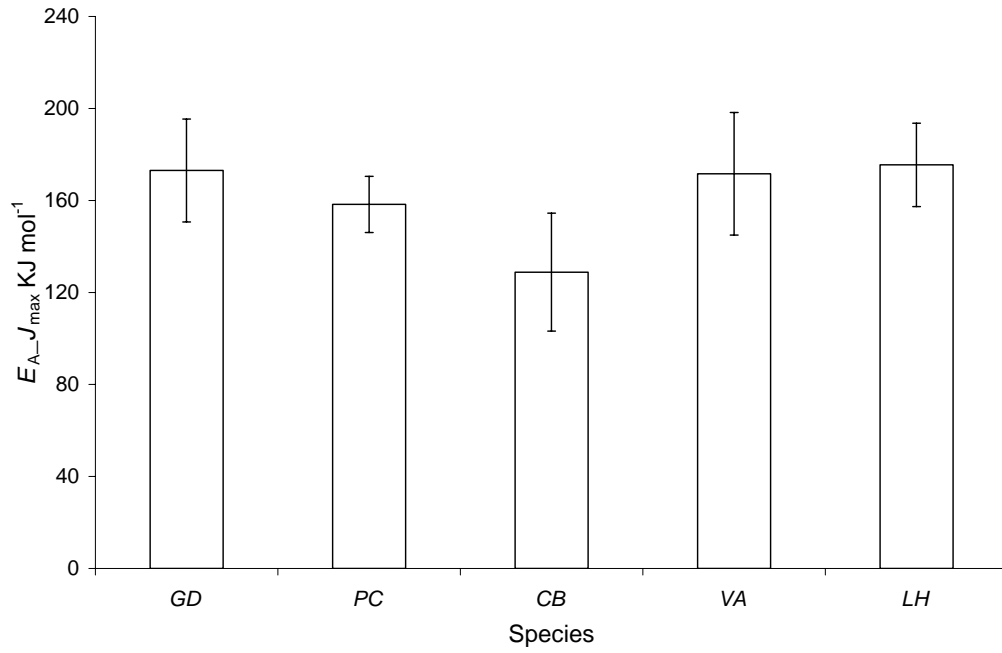


Figure 2.7. Species wise average values for activation energies of J_{max} and their standard deviations.

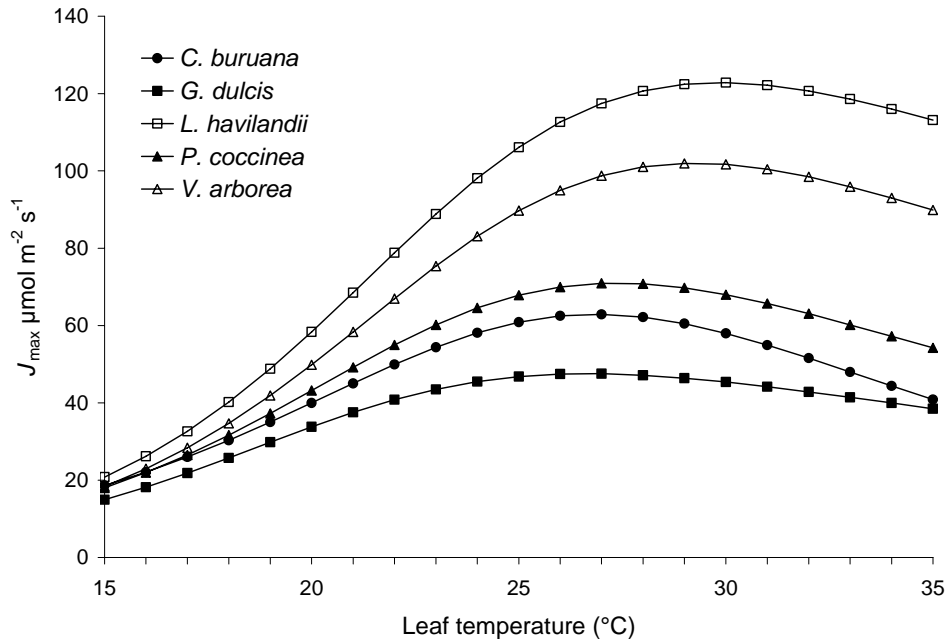


Figure 2.8. Relationships between simulated values for J_{max} and leaf temperature ($^{\circ}\text{C}$). Open symbols for sun crown and solid symbols for shade crown.

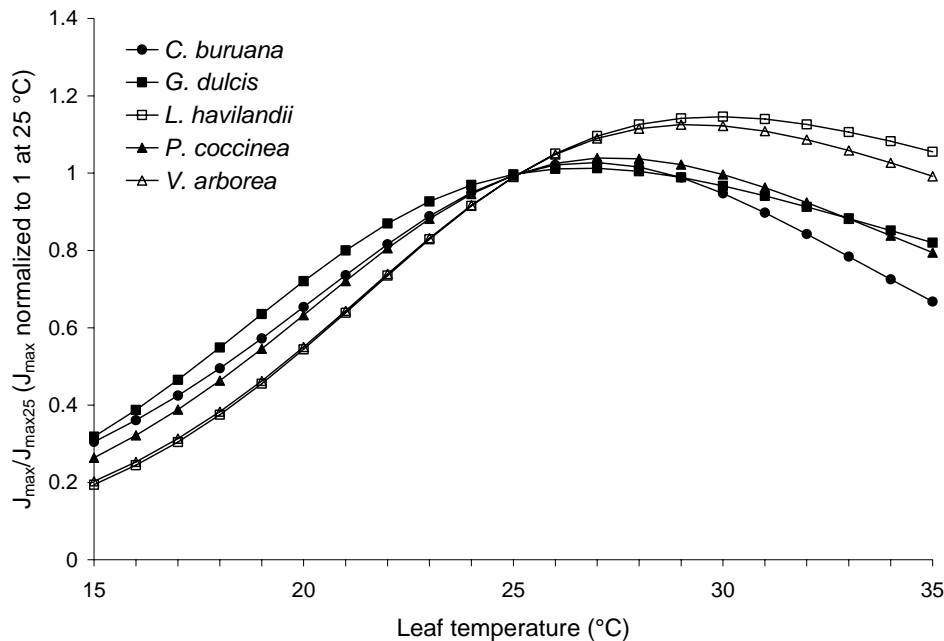


Figure 2.9. Responses of J_{max} to leaf temperatures. Simulated values are normalized to 1 at 25 °C.

2.4.4 Interrelationship between J_{max} and V_{cmax}

The ratio of the two most important photosynthetic parameters ($J_{max25} : V_{cmax25}$) ranged from 1.8 to 2.3 among species and averaged to 2.05. In general, sun crowns had lower (average, 1.85) ratios compared to the ratios of shade crowns (average, 2.1). A strong coupling effect was observed between J_{max} and V_{cmax} values of all species and for every leaf temperature level. When the predicted values of J_{max} and V_{cmax} at 25 °C leaf temperature for all species were plotted together (Figure 2.10) they had a very strong linear correlation (coefficient $R^2=0.88$). Besides, Figure 2.11 shows the relationship between actual values of J_{max} and V_{cmax} for all species and at every measured leaf temperatures. There it showed very strong coupling effect too and V_{cmax} described 87% of the values for J_{max} .

It is suggested that across a wide range of conditions, plants are able to optimize the allocation of resources, particularly nitrogen, in order to preserve a balance between enzymatic (i.e. Rubisco) and light-harvesting (i.e. chlorophyll) capabilities. Our tree species of the tropical montane rain forest differed to a considerable extent in their biochemical capacity to assimilate CO_2 from the atmosphere but they preserved

a close functional balance in the allocation of resources to these two component processes Figures 2.10 and 2.11. A similar observation was noted by Wullschleger (1993) and Thompson et al. (1992) who showed a tight coupling of V_{cmax} and J_{max} for leaves grown under different light and nutrient regimes in tropical rain forest trees.

For all five species, the maximum rate of rubisco carboxylation was less sensitive to increasing leaf temperature up to 25 °C than J_{max} was, resulting to an increase in the ratios of J_{max}/V_{cmax} . Whereas, beyond 25 °C leaf temperature the maximum rate of rubisco carboxylation was more sensitive to increasing leaf temperature than J_{max} was, resulting to a decrease in the ratios of J_{max}/V_{cmax} . A polynomial function was fitted ($R^2=0.76$) to this relationship between the $J_{max}:V_{cmax}$ ratios and leaf temperature (Figure 2.12) for data pooled from five species.

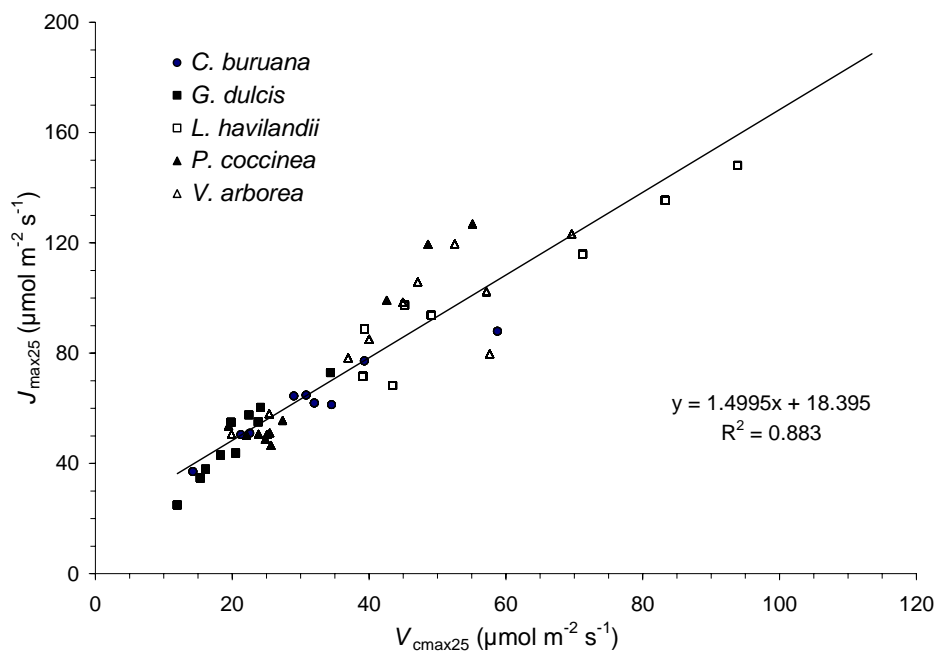


Figure 2.10. Relationship between J_{max} and V_{cmax} at 25 °C leaf temperature.

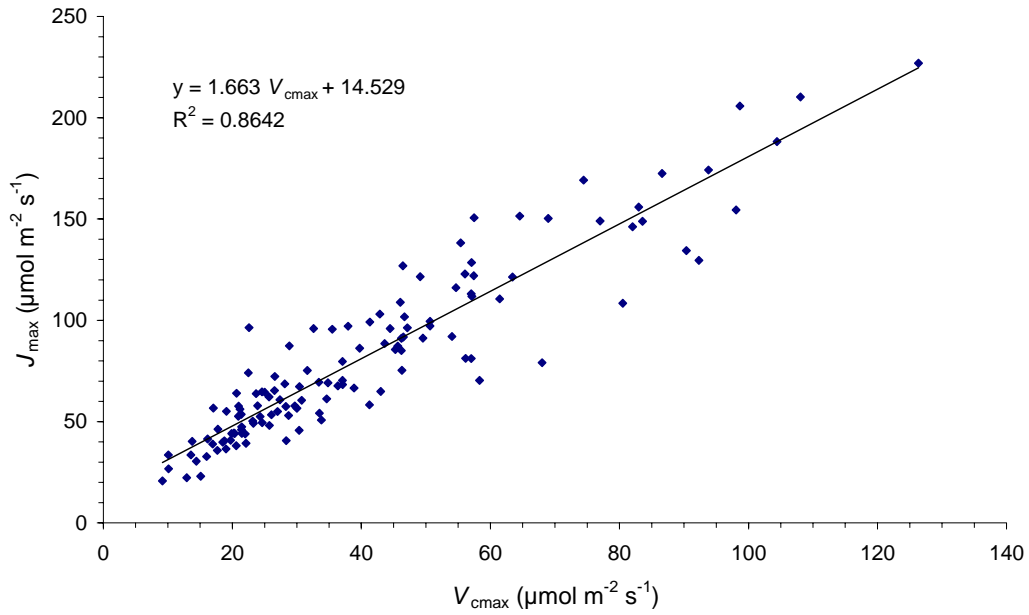


Figure 2.11. Relationship between V_{cmax} and J_{\max} (J_{\max} calculated from A/Q response curves) at different leaf temperatures ranging between 18 °C to 30 °C.

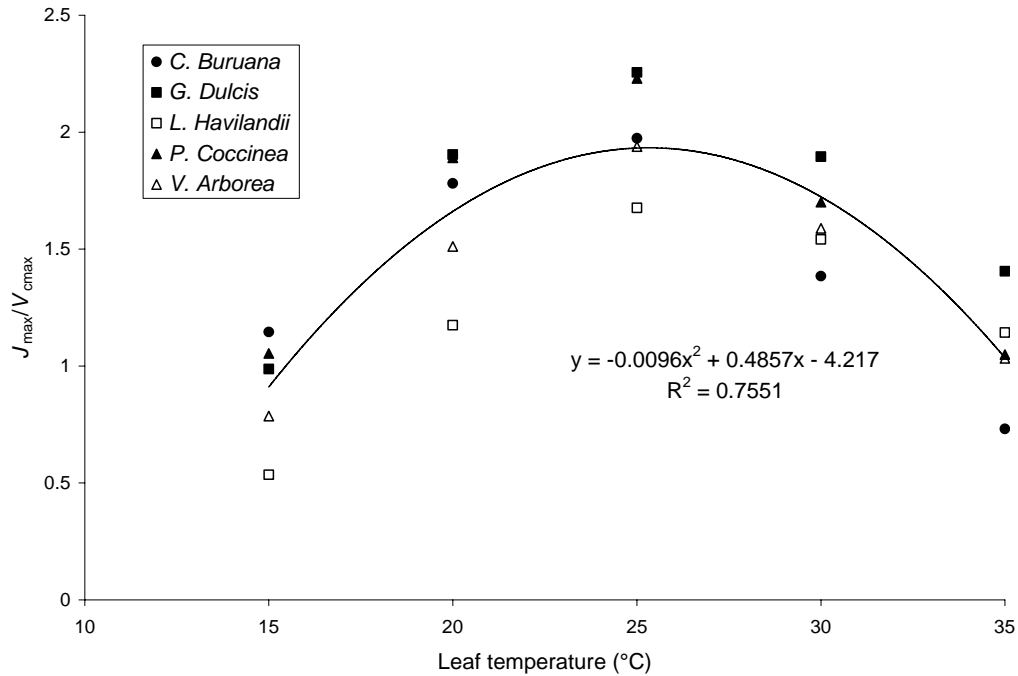


Figure 2.12. Relationship between leaf temperatures and the ratios of maximum rate of electron transport to maximum rate of rubisco carboxylation. The relationship among species looks very similar, so a single line was fitted to the pooled data.

2.4.5 Temperature dependence of R_d

Dark respiration (R_d) and its temperature response (Q_{10}) also varied among tree species. Variation in R_{d25} and variation in Q_{10} within and across species are presented in Figures 2.13 and 2.14 respectively. In general variation in Q_{10} within and among species was less than that of the variation in R_{d25} . At the reference temperature of 25 °C fitted R_{d25} values were similar among four species (Table 2.4) which ranged from 1.0 to 1.3 $\mu\text{mol m}^{-2} \text{s}^{-1}$ and had an average value of 1.1 $\mu\text{mol m}^{-2} \text{s}^{-1}$. *G. dulcis* had a much smaller value (0.77 $\mu\text{mol m}^{-2} \text{s}^{-1}$) compared to the average value of the other four species. This was shown in case of all three photosynthetic parameters that *G. dulcis* was always the lowest. This low value could be related to the very low nitrogen and phosphorus content that could be an intrinsic character of this species.

Dark respiration rate of the present study montane rain forest trees are considerably higher compared to Brazilian rain forest trees. Meir et al. (2001) reported much lower values (range 0.13 – 0.57, mean 0.34 $\mu\text{mol m}^{-2} \text{s}^{-1}$, excluding palm and climber species) for tropical rain forest species at Jaru Biological Reserve, Rondonia State, South-West Brazil, compared to ours (range 0.77 – 1.3, mean 1.05 $\mu\text{mol m}^{-2} \text{s}^{-1}$). R_d values of the present study were also higher compared to another study in tropical rain forest of Manaus in Central Amazonia, Brazil (Meir et al. 2002). But Reich et al. (1998) reported very similar values for a terra firme rain forest in Venezuela, where it ranged between 0.7 – 1.2 $\mu\text{mol m}^{-2} \text{s}^{-1}$ at 25 °C.

Dark respiration increased in every species with increasing leaf temperature (Figure 2.115). The relative increase in reaction rate at which R_d increased with increasing temperature of 10 °C (Q_{10}) was generally low and being the lowest (1.5) for species *G. dulcis*. For the other four species Q_{10} varied from 1.62 to 2.1 and averaged to 1.9. This value of Q_{10} for montane rain forest trees was much lower compared to rain forest species of Jaru Biological Reserve, Rondonia State, South-West Brazil, where it ranged between 1.5 – 4.1 and averaged to 2.3 $\mu\text{mol m}^{-2} \text{s}^{-1}$ (Meir et al., 2001). So it can be said that foliage respiration of this montane rainforest trees are less sensitive to temperature compared to lowland tropical rainforest. The variability in the temperature response of R_d is illustrated in Figure 2.16, which shows the temperature responses normalized to 1 at 25 °C.

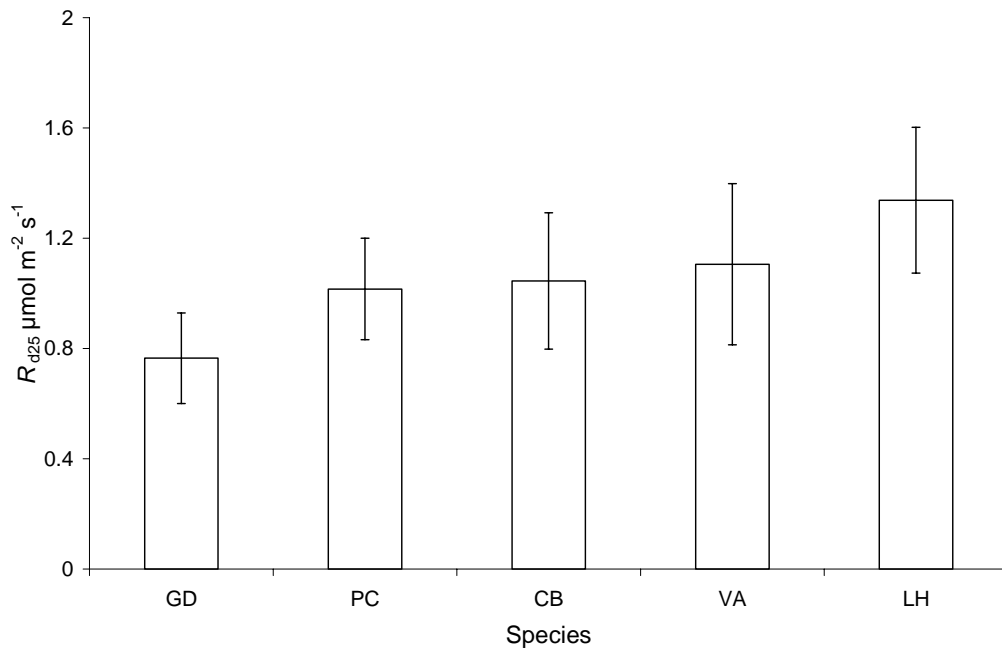


Figure 2.13. Species wise average values for the dark respiration at the reference leaf temperature of 25 °C and their standard deviations.

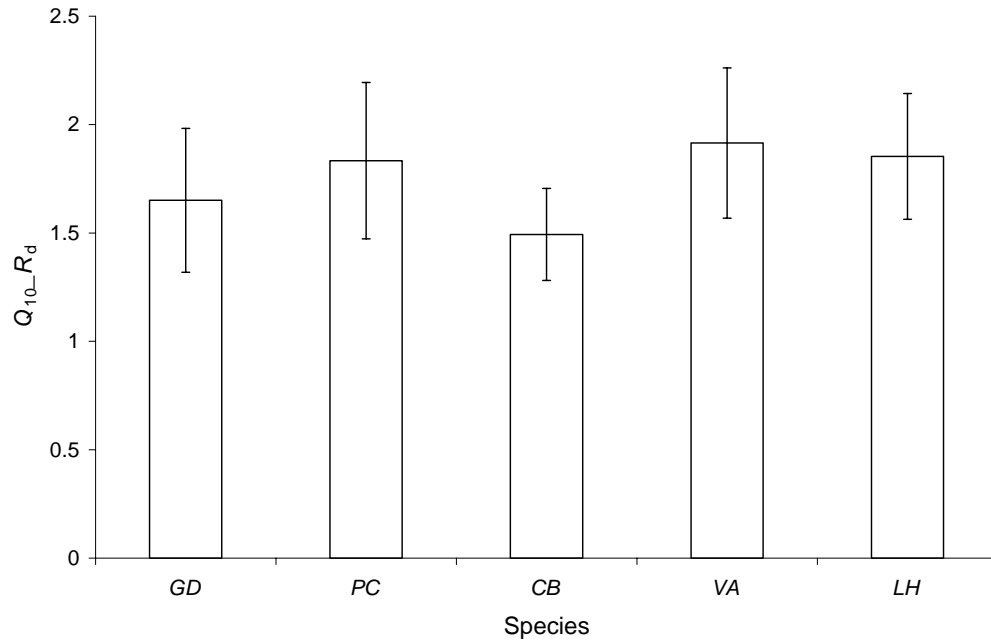


Figure 2.14. Species wise average values for the temperature of dark respiration (Q_{10}) and their standard deviations.

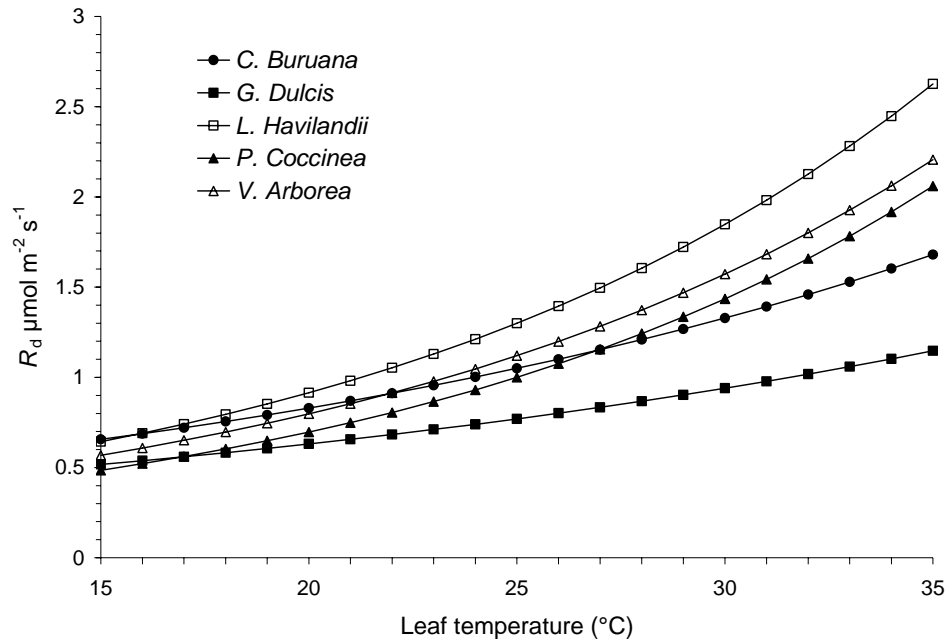


Figure 2.15. Relationships between simulated dark respirations and leaf temperatures.

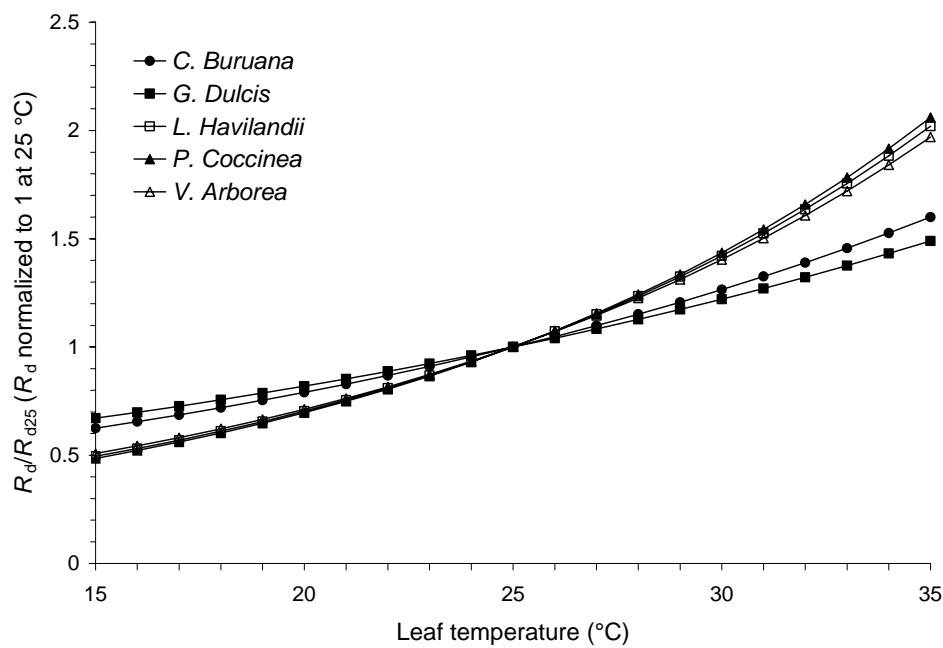


Figure 2.16. Responses of dark respiration to leaf temperatures. Simulated values are normalized to 1 at 25°C .

2.5 Conclusions

Though photosynthetic capacities and respiration rate varied among species but the physiological processes i.e. (E_a , E_d and Q_{10}) were more or less similar. Quantum yield of electron transport (α) of the five sampled species did not differ considerably and on an average α values are larger compared to other tropical forest trees. This large α value and on the other hand smaller theta (θ) value of curvature of light response are the indicators of high photosynthetic capacities of this montane rainforest trees. The low r^2 values of species wise model fittings for standardized V_{cmax} , J_{max} and R_d may be due to a narrow temperature range. Looking at the standard errors it seems that they are relatively low for the standardized parameters (V_{cmax25} , J_{max25} and R_{d25}) and much higher for their activations energies (E_a). These high standard errors for E_a could also be due to narrow observed temperature range. Larger activation energies of J_{max} compared with E_a of V_{cmax} could be due to the fact that $E_a_{V_{cmax}}$ was fitted with an original Arrhenius function. On the other hand incorporation of deactivation function into the original Arrhenius function in case of J_{max} fittings might influence $E_a_{J_{max}}$ by a counter balance force of deactivation. That could lead to a considerably higher $E_a_{J_{max}}$. From the results presented in this chapter it can be said that similar pattern in the photosynthetic capacities among species have emerged, though r^2 are very low. Next chapter investigates the residual variability of these parameter estimations.

2.6 Reference:

- Barker, M.G., Press, M.C. and Brown, N.D. (1997) Photosynthetic characteristics of dipterocarp seedlings in three tropical rain forest light environments: a basis for niche partitioning. *Oecologia* **112**, 453-463.
- Carswell, F.E., Meir, P., Wandelli, E.V., Bonates, L.C.M., Kruijt, B., Barbosa, E.M., Nobre, A.D., Grace, J. and Jarvis, P.G. (2000) Photosynthetic capacity in a central Amazonian rain forest. *Tree Physiology* **20**, 179-186.
- Dreyer, E., Roux, X.L., Montpied, P., Daudet, F.A. and Masson, F. (2001) Temperature response of leaf photosynthetic capacity in seedlings from seven temperate tree species. *Tree Physiology* **21**, 223-232.
- Dungan, R.J., Whitehead, D. and Duncan, R.P. (2003) Seasonal and temperature dependence of photosynthesis and respiration for two co-occurring broad-leaved tree species with contrasting leaf phenology. *Tree Physiology* **23**, 561-568.
- Falge, E., Graber, W., Siegwolf, R. and Tenhunen, J.D. (1996) A model of the gas exchange response of *Picea abies* to habitat conditions. *Trees* **10**, 277-287.
- Farquhar, G.D., Caemmerer, S. Von and Berry, J.A. (1980) A biochemical model of photosynthetic CO_2 assimilation in leaves of C_3 species. *Planta* **149**, 78-90

- Grant, R.F. and Nalder, I.A. (2000) Climate change effects on net carbon exchange of a boreal aspen-hazelnut forest: estimates from the ecosystems model ecosys. *Global Change Biology* **6**, 183-2000.
- Grassi, G., Vicinelli, E., Ponti, F., Cantoni, L. and Magnani, F. (2005) Seasonal and interannual variability of photosynthetic capacity in relation to leaf nitrogen in a deciduous plantation in northern Italy. *Tree Physiology* **25**, 349-360.
- Gunawan, D., Gravenhorst, G. and Jacob, D. (2003) Rainfall variability studies in South Sulawesi, using Regional Climate Model, REMO. *J. Met. Geo.* **4(5)**, 65-70.
- Gunderson, C.A., Norby, R.J. and Wullschleger, S.D. (2000) Acclimation of photosynthesis and respiration to simulated climatic warming in northern and southern populations of *Acer saccharum*: laboratory and field evidence. *Tree Physiology* **20**, 87-95.
- Harley, P.C. and Tenhunen, J.D. (1991) Modeling the photosynthetic response of C3 leaves to environmental factors. In: Modeling crop photosynthesis – From Biochemistry to Canopy. Vol. 19, American society of Agronomy and crop Science Society of America, Madison, WI, pp 17-39.
- Harley, P.C., Thomas, R.B., Reynolds, J.F. and Strain, B.R. (1992) Modelling photosynthesis of cotton grown in elevated CO₂. *Plant, Cell and Environment* **15**, 271-282.
- Ibrom, A., Oltchev, A., June, T., Ross, T., Kreilein, H., Falk, U., Merklein, J., Twele, A., Rakkibu, G., Grote, S., Rauf, A., and Gravenhorst, G. (2007) Effects of land-use change on matter and energy exchange between ecosystems in the rain forest margin and the atmosphere. In: Tschardtke, T., Leuschner, C., Zeller, M., Guhardja, E. and Bidin, A. (eds), *The stability of tropical rain forest margins, linking ecological, economic and social constraints of land use and conservation*, Springer Berlin 2007, pp 463-492.
- Ibrom, A., Jarvis, P.G., Clement, R., et al. (2006) A comparative analysis of simulated and observed photosynthetic CO₂ uptake in two coniferous forest canopies. *Tree Physiology* **26**, 845-864.
- June, T. (2005) The light gradients inside soybean leaves and their effect on the curvature factor on the light response curves of photosynthesis. *Biotropia* **25**, 29-49.
- Kellomäki, S. and Wang, K.Y. (1997) Effects of long term CO₂ and temperature elevation on crown nitrogen distribution and daily photosynthetic performance of Scots pine. *Forest Ecology and Management* **99**, 309-326.
- Leuning, R. (1997) Scaling to a common temperature improves the correlation between the photosynthesis parameters J_{amx} and V_{cmax} . *Journal of Experimental Botany* **48**, 345-347.
- Leuning, R. (2002) Temperature dependence of two parameters in a photosynthesis model. *Plant, Cell and Environment* **25**, 1205-1210.
- Leuning, R., Cromer, R.N. and Rance, S. (1991) Spatial distribution of foliar nitrogen and phosphorus in crowns of *Eucalyptus grandis*. *Oecologia* **88**, 504-510.
- Marengo, R.A. and Vieira, G. (2005) Specific leaf area and photosynthetic parameters of tree species in the forest understorey as a function of the microsite light environment in Central Amazonia. *Journal of tropical forest science* **17(2)**, 265-278.
- Medlyn, B.E., Dreyer, E. Ellsworth, D. et al. (2002) Temperature response of parameters of a biochemically based model of photosynthesis. II. A review of experimental data. *Plant, Cell and Environment* **25**, 1167-1179.

- Medlyn, B.E., Loustau, D. and Delzon, S. (2002) Temperature response of parameters of a biochemically based model of photosynthesis. I. Seasonal changes in mature maritime pine (*Pinus pinaster* Ait.). *Plant, Cell and Environment* **25**, 1155-1165
- Meir, P., Grace, J. and Miranda, A.C. (2001) Leaf respiration in two tropical rainforests: constraints on physiology by phosphorus, nitrogen and temperature. *Functional Ecology* **15**, 378-387.
- Meir, P., Kruijt, B., Broadmeadow, M., Barbosa, E., Kull, O., Carswell, F., Nobre, A. and Jarvis, P.G. (2002) Acclimation of photosynthetic capacity to irradiance in tree canopies in relation to leaf nitrogen concentration and leaf mass per unit area. *Plant, Cell and Environment* **25**, 343-357.
- Niinemets, Ü., Oja, V. and Kull, O. (1999a) Shape of leaf photosynthetic electron transport versus temperature response curve is not constant along canopy light gradients in temperate deciduous trees. *Plant, Cell and Environment* **22**, 1497-1531.
- Reich, P.B., Walters, M.B., Ellsworth, D.S., Vose, J.M., Volin, J.C., Gresham, C. and Bowman, W.D. (1998) Relationships of leaf dark respiration to leaf nitrogen, specific leaf area and leaf life-span: a test across biomes and functional groups. *Oecologia* **114**, 471 – 482.
- Singsaas, E.L., Ort, D.R. and DeLucia, E.H. (2001) Variation in measured values of photosynthetic quantum yield in ecophysiological studies. *Oecologia* **128**, 15-23.
- Thompson, W.A., Huang, L.K. and Kriedemann, P.E. (1992) Photosynthetic response to light and nutrients in sun-tolerant and shade-tolerant rainforest trees.II. Leaf gas exchange and component process of photosynthesis. *Australian Journal of Plant Physiology* **19**, 19-42.
- Tscharntke, T., Leuschner, C., Zeller, M., Guhardja, E. and Bidin, A. (eds) (2007) Stability of Tropical Rainforest Margins, linking ecological, economic and social constraints of land use and conservation, Springer Berlin 2007, pp 515.
- Walcroft, A.S. Whitehead, D., Silvester, W.B. and Kelliher, F.M. (1997) The response of photosynthetic model parameters to temperature and nitrogen concentration in *Pinus radiata* D.Don. *Plant, Cell and Environment* **20**, 1338-1348.
- Williams, M., Malhi, Y., Nobre, A.D., Rastetter, E.B., Grace, J. and Pereira, M.G.P., (1998) Seasonal variation in net carbon exchange and evapotranspiration in a Brazilian rain forest: a modeling analysis. *Plant Cell and Environment* **21**, 953-968.
- Wullschleger, S.D. (1993) Biochemical limitations to carbon assimilation in C₃ plants---a retrospective analysis of the A/C_i curves from 109 species. *Journal of Experimental Botany* **44**, 907-920.
- Zhang, L.M., Yu, G.R., Sun, X.M., Wen, X.F. et al. (2006) Seasonal variations of ecosystem apparent quantum yield (α) and maximum photosynthesis rate (P_{\max}) of different forest ecosystems in China. *Agricultural and Forest Meteorology* **137**, 176-187.

3 Chapter- III: Scaling of photosynthesis and respiration in a montane rainforest with leaf properties and temperature dependencies

3.1 Abstract

Photosynthetic capacities such as the maximum carboxylation rate of the enzyme RUBISCO (V_{cmax}), the maximum rate of electron transport (J_{max}) and the dark respiration (R_{d}) were linearly related to leaf traits. Variability in V_{cmax} , J_{max} and R_{d} within leaves of a tree and among species was well described by the leaf chemical properties such as nitrogen per unit area (N_{a}), phosphorus per unit area (P_{a}) and physical properties such as mass per unit area (M_{a}).

For V_{cmax} , leaf nitrogen per unit area (N_{a} , g m^{-2}) had in general stronger relationships compared to P_{a} and M_{a} . Leaf nitrogen described on an average about 61% of the variations in V_{cmax} at species level, whereas M_{a} and P_{a} described 42% and 52% respectively. Slopes of the linear regressions with N_{a} ranged between 6.0 and 48.0 $\mu\text{mol g}^{-1} \text{s}^{-1}$ among species and the overall slope for the data pooled from five species was 33.0 $\mu\text{mol g}^{-1} \text{s}^{-1}$.

For J_{max} , also N_{a} was in general the stronger predictor compared to P_{a} and M_{a} . Leaf nitrogen described on an average about 63% of the variations in J_{max} at species level, whereas M_{a} and P_{a} described 59% and 49% respectively. Slopes of the linear regressions with N_{a} ranged from 21.0 to 120.0 $\mu\text{mol g}^{-1} \text{s}^{-1}$ among species and the overall slope for the data pooled from five species was 41.0 $\mu\text{mol g}^{-1} \text{s}^{-1}$.

In case of R_{d} , leaf mass (M_{a}) and leaf phosphorus (P_{a}) had similar and stronger correlation than with N_{a} . On an average M_{a} and P_{a} described about 41% of the variations in R_{d} at species level, whereas N_{a} described 33%. Slopes of the linear regressions with N_{a} ranged from 0.17 to 0.41 $\mu\text{mol g}^{-1} \text{s}^{-1}$ among species and the overall slope for the data pooled from five species was 0.37 $\mu\text{mol g}^{-1} \text{s}^{-1}$. Incorporation of P_{a} in a combined model with N_{a} generally did not explain the variation better than that was explained by N_{a} alone.

3.2 Introduction

Among the most important components of global biogeo-chemical cycling are the processes that mediate the fluxes of carbon, water and energy between biosphere

and atmosphere. The need for a clear understanding of the role of the terrestrial biosphere in global climate change generates a requirement for assessments of processes such as photosynthesis and respiration at large scales. A major difficulty in improving our understanding of the functioning of the biosphere-atmosphere system lies in the problem of effectively scaling measurements of the key processes, such as photosynthesis, respiration and evapotranspiration, to generate regional estimates of these fluxes. Generally, the ability to make measurements of the various components of these coupled systems is strictly limited in some dimensions of space and time.

The photosynthetic capacities of leaves in canopies acclimate to the light environment in which the leaves are growing (Meir et al. 2002). Most canopy trees experience diverse light conditions during their lifetime, starting as seedlings on the poorly lit forest floor but gaining access to the well-lit canopy layer at maturity. Many tree species have different maximum photosynthetic capacities, i.e. photosynthesis rates at light saturation according to growth stage or light conditions, or both, as a result of differences in leaf morphological and biochemical properties (Larcher 2003). It is well known that sun leaves, i.e. leaves of the sun crown, have higher leaf nitrogen and leaf mass per unit area, corresponding to higher photosynthetic capacities, than shade leaves, i.e. leaves of the shade crown. Shade leaves have higher leaf chlorophyll content and are thinner and thus have a lower dark respiration rate and light compensation point than sun leaves (Lambers et al. 1998). To guide development of models of carbon dioxide fixation there is a need for a detailed understanding of the changes in the photosynthetic capacities and respiration with the leaf chemical and morphological characteristics.

The dark respiration of leaves plays a key role in the carbon economy of plants, but it is poorly understood in comparison to photosynthesis. Leaf respiration in forest canopies may consume 9-22% of gross primary production, and comprise 50-70% of above-ground (autotrophic) respiration (Malhi et al. 1999; Yoda 1983). A linear relationship between dark respiration and leaf chemical (nitrogen and phosphorus) and physical (leaf mass per unit area) properties of tropical rain forest trees has been shown in many studies (Meir et al. 2001).

Within canopy, profiles of leaf nitrogen (or photosynthetic capacity) have been shown to be significantly non-uniform in canopies of a diverse range of species (de Pury & Farquhar 1997). Profiles of leaf properties have led to the hypothesis that

leaves adapt or acclimate to their radiation environment such that a plant's nitrogen resources may be distributed to maximize daily canopy photosynthesis (Hirose & Werger 1987). An optimal distribution of leaf nitrogen exists when any re-allocation of nitrogen would decrease daily photosynthesis. It has been further hypothesized that the optimal distribution of nitrogen occurs when the nitrogen is distributed in proportion to the distribution of absorbed irradiance in the canopy, averaged over the previous several days to a week, the time over which leaves are able to adapt (de Pury & Farquhar 1997).

Photosynthetic capacity is closely linked to nitrogen content through the nitrogen-rich carbon-fixing enzyme Rubisco (Cao et al. 2007). A general relationship between leaf nitrogen and maximum assimilation often occurs across gradients in geography (Reich et al. 1997), functional types (Field and Mooney 1986), species within functional types (Harrington et al. 1989) and growth light environment (Niinemets and Tenhunen 1997). This discovery has been useful in confirming hypotheses about plant functioning and establishing relationships over broad gradients of leaf characteristics (Reich et al. 1997). A link to leaf nitrogen also provides the potential to estimate photosynthetic capacity at high temporal resolutions and large scales specially, if practical methods were developed to estimate nitrogen from remote sensing (Wessman 1990). However, the utility of these relationships in describing all sources of variability at a single site is less certain. There is evidence indicating important variations in the relationship between leaf nitrogen and photosynthesis. Linear correlations do not always occur within species and the regression coefficients are often strongly dependent on species or treatment effects (Wilson et al. 2000). Slopes between leaf nitrogen and maximum assimilation rates can vary by a factor of 10 among species (Evans 1989). Several researches have concluded that effects of leaf age can be described only by changes in leaf nitrogen (Field and Mooney 1983, Reich et al. 1991), but others have not. For example, there is evidence that nitrogen allocated to Rubisco and chlorophyll can vary with leaf age (Poorter and Evans 1998, Rey and Jarvis 1998).

Leaf photosynthetic capacity and respiration are dependent on leaf temperature. Incorporation of temperature response into models of photosynthesis for parameter up-scaling is thus important. Several examples of scaling up photosynthesis from leaf to canopy on temperate forest canopy have appeared in the last decade (Kull & Jarvis

1995) but none so far on tropical montane rain forest canopy despite its importance in global CO₂ and energy balance largely because they are variable, diverse in species and generally more difficult to study than other vegetation types. The aim of the study was (i) to examine the relationship between leaf level physiological model parameters and physico-chemical leaf properties (ii) to examine whether incorporation of temperature response in the model improves the model fit for parameter up-scaling and (ii) to determine physiological model parameters for forest canopy photosynthesis modeling.

3.3 Materials and methods

3.3.1 Models used

The rate of photosynthesis in a leaf is determined by the rates of carboxylation and regeneration of ribulose-1,5-bisphosphate (RuBP) catalyzed by the enzyme RUBISCO (Farquhar et al., 1980, von Caemmerer and Farquhar 1981). The rate of photosynthesis is limited by the smaller of these two rates. Parameters for the model describing this relationship are V_{cmax} , the maximum rate of RUBISCO-catalyzed RuBP carboxylation when CO₂ is at limiting concentrations; J_{max} , the rate of electron transport where irradiance (Q) is saturating (=RuBP is limiting); R_d , the rate of dark respiration (i.e., respiration due to processes other than photosynthesis). Photosynthetic capacities (V_{cmax} , J_{max}) and dark respiration (R_d) of investigated leaves were fitted with leaf chemical (N_a , P_a) and morphological (M_a) traits for linear regression according to the following equations:

Firstly, a simple linear model was fitted as

$$V_{cmax25} = a_v P_s + b_v \quad (3.1)$$

$$J_{max25} = a_j P_s + b_j \quad (3.2)$$

$$R_{d25} = a_R P_s + b_R \quad (3.3)$$

Where, P_s are the scaling parameters (N_a or M_a or P_a), a_v , a_j and a_R are proportionality coefficients (slopes) and b_v , b_j and b_R are intercepts of the regressions between V_{cmax25} , J_{max25} and R_{d25} and scaling parameters respectively.

In a second approach a multiple linear model was fitted as

$$V_{c\max25} = a_v N_a + b_v P_a + C_v \quad (3.4)$$

$$J_{\max25} = a_j N_a + b_j P_a + C_j \quad (3.5)$$

$$R_{d25} = a_R N_a + b_R P_a + C_R \quad (3.6)$$

Where N_a and P_a are combined scaling parameters. a_v , a_j , a_R are slopes for N_a and b_v , b_j , b_R are slopes for P_a and c_v , c_j , c_R are intercepts of the regressions between $V_{c\max25}$, $J_{\max25}$ and R_{d25} .

In a third approach, models of temperature dependencies given in equations 1.6, 1.7 and 1.8 in chapter- I was modified by replacing parameter values at 25 °C with the proportionality coefficients between parameters and leaf traits as follows:

$$V_{c\max}(T_{leaf}) = (a_v P_s + b_v) \exp\left[\frac{E_a(T_{leaf} - 25)}{298RT_k}\right] \quad (3.7)$$

$$J_{\max}(T_k) = (a_j P_s + b_j) \exp\left[\frac{E_a(T_k - 298)}{298RT_k}\right] \frac{1 + \exp\left(\frac{298\Delta S - E_d}{298R}\right)}{1 + \exp\left(\frac{T_k \Delta S - E_d}{T_k R}\right)} \quad (3.8)$$

$$R_d = (a_R P_s + b_R) Q_{10}^{\frac{T_{leaf} - 25^\circ C}{10^\circ C}} \quad (3.9)$$

Where, P_s are the scaling parameters (N_a or M_a or P_a), a_v , a_j and a_R are proportionality coefficients (slopes) and b_v , b_j and b_R are intercepts of the regressions between $V_{c\max}$, J_{\max} and R_d and scaling parameters respectively. E_a is the activation energy (describes the exponential rate of rise of the function), R is the universal gas constant ($8.314 \text{ J mol}^{-1}\text{K}^{-1}$), T_{leaf} is the leaf temperature in °C and T_k is leaf temperature in K, E_d is the deactivation energy (describes the rate of decrease of the function above the optimum) of J_{\max} and ΔS is known as an entropy term ($700 \text{ J mol}^{-1} \text{ K}^{-1}$). Q_{10} is the relative increase in reaction rate at which R_d increases with an increase in temperature of 10 °C.

3.3.2 Data analysis

Photosynthetic parameters were estimated by fitting the model equations of Farquhar et al. (1980) to the measurements of leaf gas exchange by nonlinear least square regressions. Scatter plots of photosynthetic capacities and dark respiration (i.e., V_{cmax} , J_{max} and R_{d}) with leaf chemical and morphological properties were analyzed by linear regression. Temperature response parameters were obtained by fitting equations 7, 8 and 9 to response curves of V_{cmax} , J_{max} and R_{d} respectively, to leaf temperature response data using SAS (SAS Institute Inc. 2004, Cary, NC, USA). A single factor ANOVA (Scheffe's test) of the residuals of the model fitting was used to assess the significance of the differences among species for V_{cmax} , J_{max} and R_{d} . Leaf properties among species were tested for significant differences.

3.4 Results and discussions

3.4.1 Species wise relationships between V_{cmax} and leaf biochemical and morphological properties

It was seen in the last chapter that there are some variations in the photosynthetic and respiration parameters within leaves and trees. But these variations in all these parameters were well linked to the leaf traits, the growth environment in which they are exposed. Relationships between the maximum carboxylation rate at 25 °C leaf temperature ($V_{\text{cmax}25}$, $\mu\text{mol m}^{-2} \text{s}^{-1}$) on one hand, and leaf nitrogen per unit area (N_{a} , g m^{-2}), leaf mass per unit area (M_{a} , g m^{-2}) and leaf phosphorus per unit area (P_{a} , mg m^{-2}) on the other hand are shown in the Figure 3.1 and Table 3.1. Generally there are strong positive correlations between V_{cmax} and leaf chemical and physical properties. Not all the five investigated tree species showed the same relationship with leaf trait. There are variations among species in the slopes (Figure 3.1) of the relationships. Except for the species *G. dulcis*, which was not significant, N_{a} has the most significant and similar relationships to V_{cmax} among species. The coefficients of determination (r^2) were generally higher for $V_{\text{cmax}}/N_{\text{a}}$ regressions (Table 3.1) than for $V_{\text{cmax}}/M_{\text{a}}$ and $V_{\text{cmax}}/P_{\text{a}}$, with N_{a} explaining between 37% and 88% of the variance in area based V_{cmax} which is a strong significant correlation. The average slope ($32.5 \mu\text{mol g}^{-1} \text{N s}^{-1}$) and correlation coefficient (0.61) of $V_{\text{cmax}}/N_{\text{a}}$ regressions were stronger compared to a study in central Amazonian rain forest trees where it was $11.4 \mu\text{mol g}^{-1}$

^{15}N s^{-1} and 0.40 respectively (Carswell et al. 2000), indicating higher nitrogen economy in the leaves of upland rain forest trees of Sulawesi.

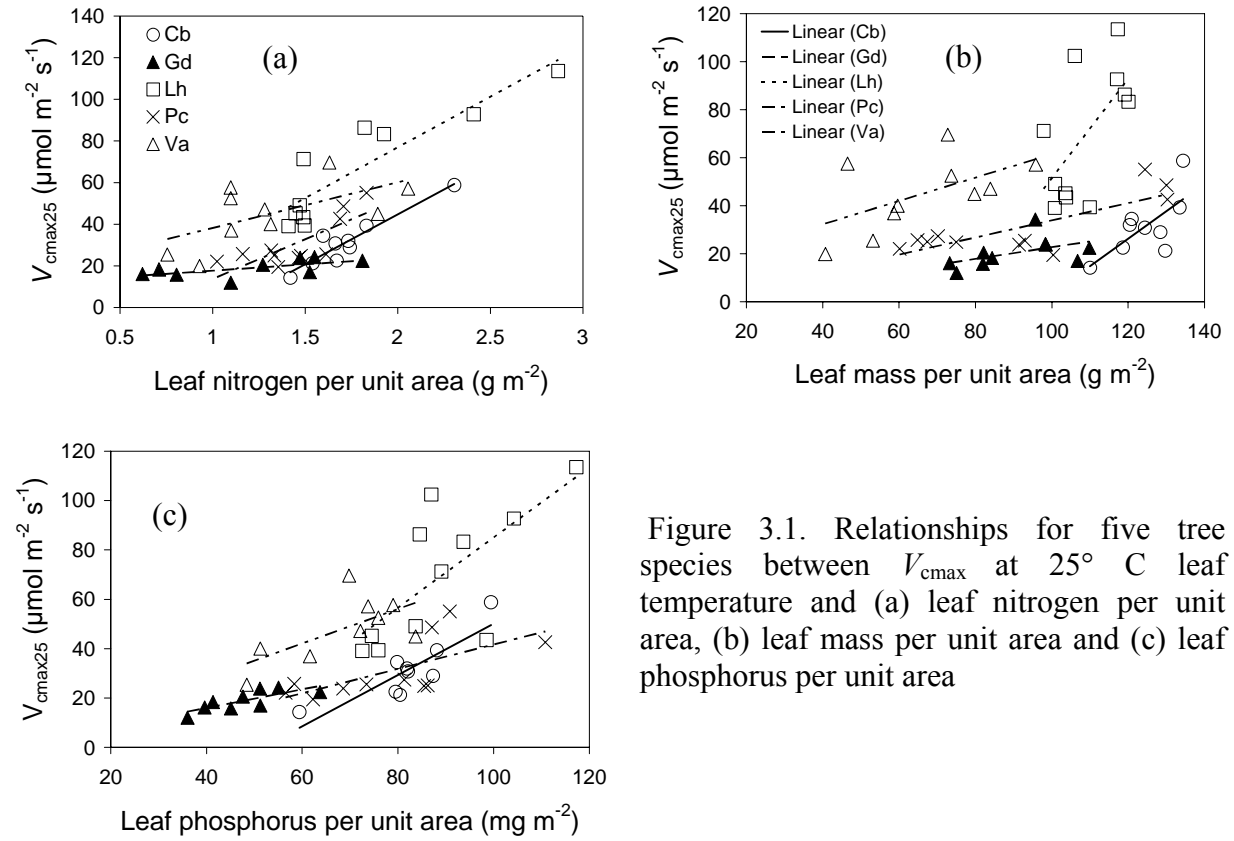


Figure 3.1. Relationships for five tree species between V_{cmax} at 25°C leaf temperature and (a) leaf nitrogen per unit area, (b) leaf mass per unit area and (c) leaf phosphorus per unit area

Table 3.1. Linear regression results for V_{cmax25} ($\mu\text{mol m}^{-2} \text{s}^{-1}$) versus N_a (g m^{-2}), M_a (g m^{-2}) and P_a (mg m^{-2}). Significance of the slopes and non-zero intercepts were $P < 0.05$ (*), $P < 0.01$ (**), and $P < 0.001$ (***). Abbreviations: Cb (*C. buruana*), Gd (*G. dulcis*), Lh (*L. havilandii*), Pc (*P. coccinea*) and Va (*V. arborea*).

Species	n	V_{cmax25} versus N_a			V_{cmax25} versus M_a			V_{cmax25} versus P_a		
		Intercept	Slope	R^2	Intercept	Slope	R^2	Intercept	Slope	R^2
Cb	9	-51.0**	47.9***	0.88	-111.2	1.15*	0.5	-54.1*	1.04**	0.75
Gd	10	11.5*	6.1	0.39	-1.6	0.24	0.26	-4.5	0.51*	0.48
Lh	10	-20.3	48.5***	0.81	-155.3	2.0*	0.39	-57.2	1.42*	0.5
Pc	11	-24.5	38.2**	0.61	-1.7	0.36**	0.64	-7.7	0.49*	0.45
Va	10	16.3	21.9*	0.37	12.8	0.49	0.32	0.22	0.7	0.42

As it was seen above that, though N_a described majority of the variation in V_{cmax} but still there were about 40% of the variation remained unexplained. To see whether the residual variation was related to P_a , a combined model was fitted as given in equation 3.4. The result of this combined model is presented in Table 3.2. Overall it can be said that the combined model did not give better results and slopes were almost insignificant. Only in case of *G. dulcis*, P_a described about 25% of the remaining variation. On the other hand r^2 was decreased by 20% in *L. havilandii* and remained almost unchanged in the other three species. Among the leaf traits, N_a was found to be the main source of variation in V_{cmax} .

Table 3.2. Multiple linear regression results for $V_{\text{cmax}25}$ ($\mu\text{mol m}^{-2} \text{s}^{-1}$) versus N_a (g m^{-2}) and P_a (mg m^{-2}) combined together. Significance of the slopes and non-zero intercepts were $P < 0.05$ (*), $P < 0.01$ (**) and $P < 0.001$ (***)

Species	n	N_a _slope	P_a _slope	Intercept	r^2
Cb	9	39.5*	225.4	-55.2**	0.88
Gd	10	-9.6	862.0*	-10.0	0.64
Lh	10	32.7	450.3	-28.2	0.58
Pc	11	30.3	159.8	-25.7	0.63
Va	10	8.4	542.1	-0.6	0.47

3.4.2 Species wise relationships between J_{max} and leaf biochemical and morphological properties

Relationships between the maximum electron transport rate at 25 °C leaf temperature ($J_{\text{max}25}$, $\mu\text{mol m}^{-2} \text{s}^{-1}$) on one hand, and N_a , M_a and P_a on the other hand are shown in the Figure 3.2 and Table 3.3. Maximum electron transport rate also showed positive linear relationships with leaf chemical and physical properties. There were some variations in the relationships among species (Figure 3.2) for all the three leaf traits. Leaf nitrogen per unit area (N_a) had more significant relationships to J_{max} compared to M_a and P_a (Table 3.3). The coefficients of determination (r^2) were generally higher for J_{max}/N_a regressions than for J_{max}/M_a and J_{max}/P_a , with N_a explaining between 46 and 81% of the variance in area based J_{max} . The average slope ($67.8 \mu\text{mol g}^{-1} \text{s}^{-1}$) and correlation coefficient (0.63) of J_{max}/N_a regressions were also

stronger compared to a study in central Amazonian rain forest trees where it was $32.85 \mu\text{mol g}^{-1} \text{s}^{-1}$ and 0.50 respectively (Carswell et al. 2000).

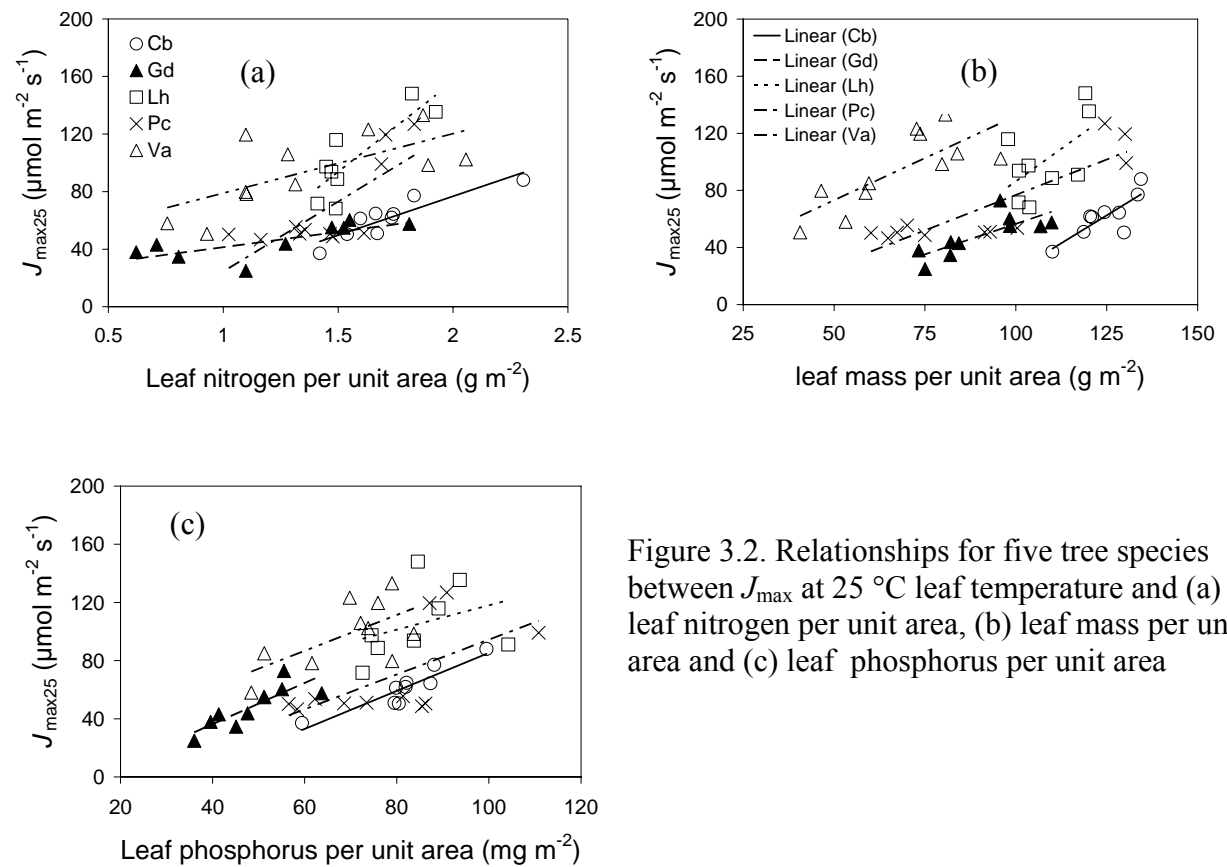


Figure 3.2. Relationships for five tree species between J_{\max} at 25°C leaf temperature and (a) leaf nitrogen per unit area, (b) leaf mass per unit area and (c) leaf phosphorus per unit area

Table 3.3. Linear regression results for $J_{\max 25}$ ($\mu\text{mol m}^{-2} \text{s}^{-1}$) versus N_a (g m^{-2}), M_a (g m^{-2}) and P_a (mg m^{-2}). Significance of the slopes and non-zero intercepts were $P < 0.05$ (*), $P < 0.01$ (**) and $P < 0.001$ (***). Abbreviations: Cb (*C. buruana*), Gd (*G. dulcis*), Lh (*L. havilandii*), Pc (*P. coccinea*) and Va (*V. arborea*).

Species	n	$J_{\max 25}$ versus N_a			$J_{\max 25}$ versus M_a			$J_{\max 25}$ versus P_a		
		Intercept	Slope	R^2	Intercept	Slope	R^2	Intercept	Slope	R^2
Cb	9	-31.2	54.0***	0.81	-132.4*	1.56**	0.67	-45.6*	1.3***	0.85
Gd	9	20.2	21.2*	0.55	-29.0	0.86**	0.6	-20.2	1.4**	0.7
Lh	9	-74.2	105.2**	0.7	-96.0	1.8	0.34	34.1	0.84	0.12
Pc	11	-72.7	97.2**	0.60	-22.5	1.0***	0.75	-25.3	1.2*	0.4
Va	11	37.5	41.4*	0.46	14.1	1.2**	0.6	12.8	1.2*	0.4

Apart from simple linear relation between N_a and J_{\max} , a combined model with P_a (equation 3.5) was fitted to see whether it can describe the variation better. Results of the fittings are presented in Table 3.4. The relationship of J_{\max} with N_a and P_a in the combined model became insignificant ($P > 0.05$). As in V_{cmax} , only in case of *G. dulcis*, P_a described about 20% of the remaining variation. On the other hand r^2 was decreased by 50% in *L. havilandii* and remained almost unchanged in the other three species. The remaining variation in J_{\max} could not be described by P_a .

Table 3.4. Multiple linear regression results for $J_{\max 25}$ ($\mu\text{mol m}^{-2} \text{s}^{-1}$) versus N_a (g m^{-2}) and P_a (mg m^{-2}) combined together. Significance of the slopes and non-zero intercepts were $P < 0.05$ (*), $P < 0.01$ (**) and $P < 0.001$ (***)

Species	n	N_a _slope	P_a _slope	Intercept	r^2
Cb	9	23.7	818.2	-46.2*	0.89
Gd	10	-12.1	1852.9**	-27.2	0.75
Lh	9	42.2	-661.7	87.9	0.15
Pc	11	83.6	277.8	-74.8	0.61
Va	11	15.7	738.0	22.6	0.42

3.4.3 Species wise relationships between R_d and leaf biochemical and morphological properties

Relationships between dark respiration (R_{d25} , $\mu\text{mol m}^{-2} \text{s}^{-1}$) on one hand, and N_a , M_a and P_a on the other hand are shown in the Figure 3.3 and Table 3.5. R_d also increased with the increase of all three leaf properties. Among species there was more similarity in the R_d/N_a relationships compared to the relationships of R_d/M_a and R_d/P_a .

The overall coefficients of determination (r^2) for R_d/M_a (42%) and R_d/P_a (42%) relationships were similar and little higher than that of R_d/N_a (34%) relationship. Similar strong dependence of R_d on P_a was found by Meir et al. (2001) in an undisturbed natural rain forest of Reserva Jaru, Brazil, where slopes of R_d/P_a and R_d/N_a relationships were $11.99 \mu\text{mol g}^{-1} \text{s}^{-1}$ and $0.18 \mu\text{mol g}^{-1} \text{s}^{-1}$ respectively. In the present study steeper slopes (averaged to $0.29 \mu\text{mol g}^{-1} \text{s}^{-1}$) of R_d/N_a relationships also indicates higher nitrogen economy in the montane rain forest trees of Central Sulawesi.

The present study in the montane rain forest with five species showed that photosynthetic physiological parameters (V_{cmax} , J_{max} and R_d) were more closely correlated with leaf nutrient concentrations (N_a and P_a) than leaf physical characteristics (M_a). It is well established that physiological parameters correlate with N concentrations (e.g. Meir et al. 2002; Reich et al. 1999) but in the present study the strong relationships between leaf P concentrations and physiological parameters are remarkable. Similar relationships have been reported by Hölcher et al. (2006) from a nearby forest at Wuasa, Central Sulawesi, having similar topographic and climatic conditions.

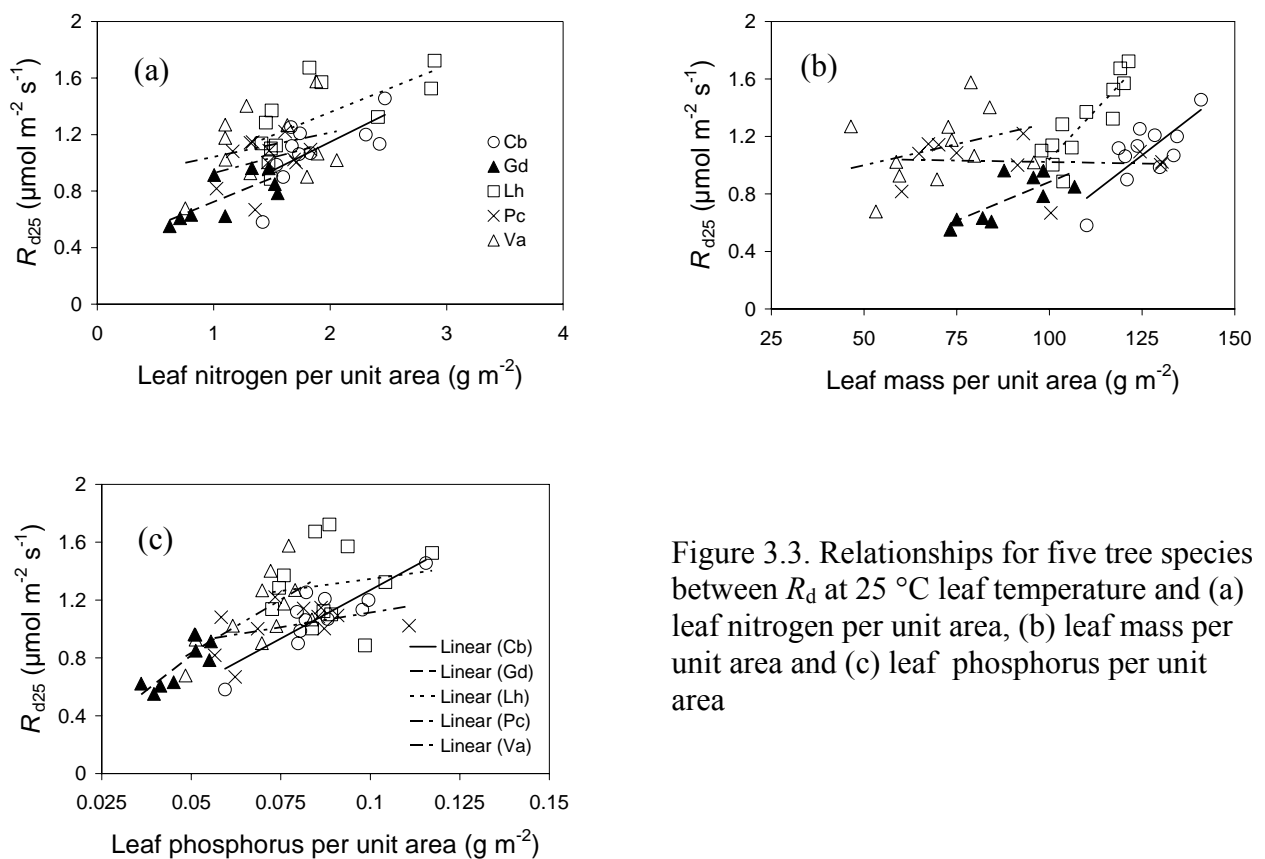


Figure 3.3. Relationships for five tree species between R_d at 25 °C leaf temperature and (a) leaf nitrogen per unit area, (b) leaf mass per unit area and (c) leaf phosphorus per unit area

Table 3.5. Linear regression results for R_{d25} ($\mu\text{mol m}^{-2} \text{s}^{-1}$) versus N_a (g m^{-2}), M_a (g m^{-2}) and P_a (g m^{-2}). Significance of the slopes and non-zero intercepts were $P < 0.05$ (*), $P < 0.01$ (**) and $P < 0.001$ (***). Abbreviations: Cb (*C. buruana*), Gd (*G. dulcis*), Lh (*L. havilandii*), Pc (*P. coccinea*) and Va (*V. arborea*).

Species	n	R_{d25} versus N_a			R_{d25} versus M_a			R_{d25} versus P_a		
		Intercept	Slope	R^2	Intercept	Slope	R^2	Intercept	Slope	R^2
Cb	11	0.33	0.41*	0.46	-1.42	0.02**	0.6	-0.07	13.0***	0.74
Gd	9	0.39*	0.34*	0.55	-0.2	0.01*	0.56	-0.15	19.0**	0.69
Lh	12	0.69**	0.33*	0.47	-1.7**	0.027***	0.78	1.01	3.3	0.03
Pc	11	0.71*	0.22	0.11	1.06***	-0.0004	0.005	0.7*	4.1	0.17
Va	11	0.87*	0.17	0.08	0.7	0.006	0.12	0.1	14.6*	0.43

3.4.4 Overall relationships between photosynthetic capacities and leaf biochemical and morphological properties within the crown.

Apart from species wise relationships, pooled data about photosynthetic capacities and respiration from all investigated species were fitted against leaf nitrogen concentration to represent relationships across the canopy. Data and regression models are shown in Figure 3.4. Though correlation coefficients of the relationships for pooled data are lower than those of species wise data, still leaf nitrogen holds the linear relationships between photosynthetic parameters across the canopy and explains 41%, 26% and 43% of variations in V_{cmax} , J_{max} and R_d respectively. The overall slope of $V_{\text{cmax}25}/N_a$ regression ($31.3 \mu\text{mol g}^{-1} \text{s}^{-1}$) was very similar ($28.01 \mu\text{mol g}^{-1} \text{s}^{-1}$) to a study in Bornean tropical rainforest (Kumagai et al. 2006). Combined models as in equations 3.4, 3.5 and 3.6 were fitted for pooled data sets. Incorporation of P_a in to the linear relationship of parameters with N_a did not improve the model fitting considerably (results not shown).

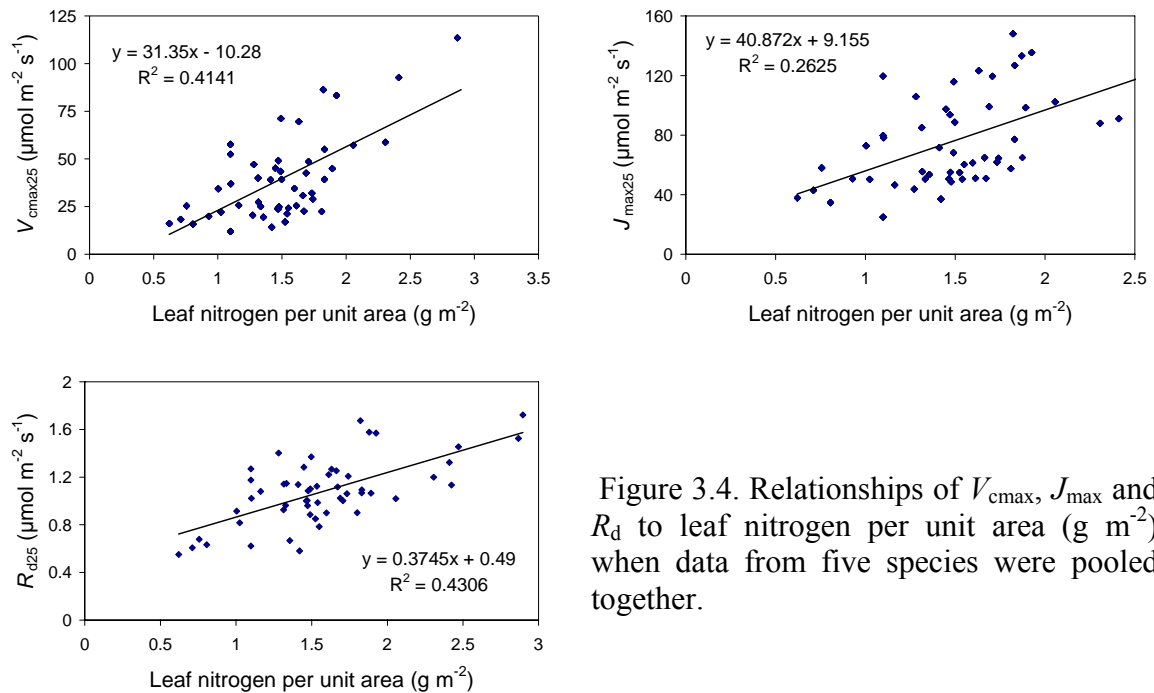


Figure 3.4. Relationships of V_{cmax} , J_{max} and R_d to leaf nitrogen per unit area (g m⁻²) when data from five species were pooled together.

3.4.5 Interrelationship among leaf chemical and physical properties

Species specific and overall average values for leaf traits are given in Table 3.6. In case of leaf nitrogen per unit area (N_a) there were similarity among species except the one species (*Garcinia dulcis*), which was significantly (Scheffe's tests, $P < 0.05$) different from the other four. On the other hand there were more significant differences among species in case of other leaf traits such as leaf phosphorus per unit area (P_a), leaf mass per unit area (M_a) and specific leaf area (A_m). Overall leaf nitrogen concentration (1.49 g m⁻²) of the present study sample trees was very similar (1.53 g m⁻²) to the tropical rainforest of San Carlos del Rio Negro, Venezuela in the northern Amazon basin but it was much lower compared to the values (2.66 g m⁻²) of central Amazonian rain forest (Reich et al. 1999 and Craswell et al. 2000 respectively).

Table 3.6. Species wise and over all mean values for leaf traits of sample trees.

Abbreviations: Cb (*C. buruana*), Gd (*G. dulcis*), Lh (*L. havilandii*), Pc (*P. coccinea*) and Va (*V. arborea*). N_a (nitrogen per unit area), P_a (phosphorus per unit area), M_a (mass per unit area) and A_m (area per unit mass).

Leaf traits	Cb	Gd	Lh	Pc	Va	Over all	
						Mean	SD
N_a (g m ⁻²)	1.72	1.19	1.76	1.45	1.32	1.49	0.42
P_a (g m ⁻²)	0.082	0.049	0.089	0.078	0.068	0.074	0.019
M_a (g m ⁻²)	124.52	90.58	108.76	91.55	66.43	95.96	24.89
A_m (cm ² g ⁻¹)	80.6	112.45	92.42	117.76	160.99	113.18	37.3

Leaf properties data from all five species have been pooled together and tested for the interrelationships among leaf characteristics. There were strong and significant relationships between leaf physical and chemical properties of the study forest site. Leaf nitrogen per unit area (N_a) had a strong ($r^2=0.57$) and significant ($P<0.0001$) relationship with leaf phosphorus per unit area (P_a) (Figure 3.5, a). N_a had also significant ($P<0.0001$) but little weaker ($r^2=0.46$) correlation with leaf mass per unit area (M_a) (Figure 3.5, b). There was a weak ($r^2=0.3$) but still a significant ($P<0.0001$) correlation between P_a and M_a (Figure 3.5, c).

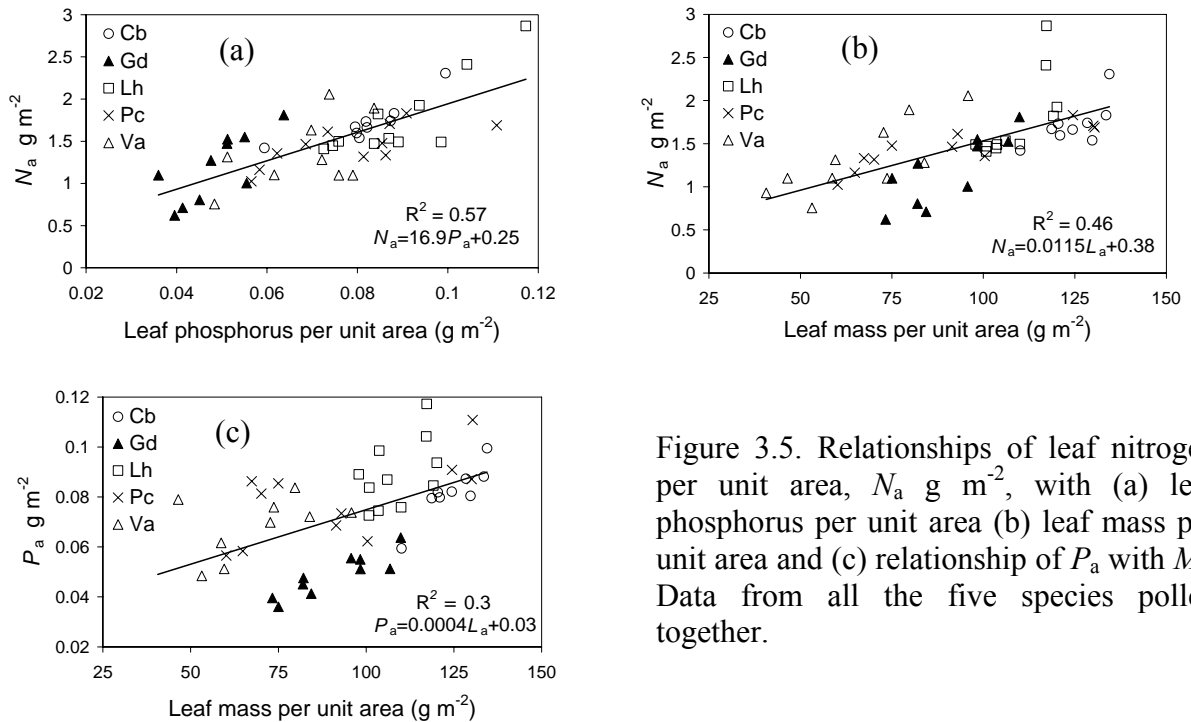


Figure 3.5. Relationships of leaf nitrogen per unit area, N_a g m^{-2} , with (a) leaf phosphorus per unit area (b) leaf mass per unit area and (c) relationship of P_a with M_a . Data from all the five species pooled together.

From the relationships between photosynthetic capacities and leaf properties discussed previously it can be seen that the physiological model parameters (V_{cmax} , J_{max} and R_d) of the five studied species had similar relationships either with N_a or with P_a . And it is also seen that N_a and P_a was strongly and significantly related among the leaves of sample tree species. So, either of these two chemical leaf properties can be considered as scaling parameter from leaf level to tree level and to canopy level for the photosynthetic model parameters of the investigated forest canopy.

3.4.6 Species wise photosynthetic model parameters and their temperature responses when scaled with leaf properties

Variability in photosynthetic and respiration parameters within and between trees was better described by leaf properties when temperature dependence was included in the present linear model. Species wise fitted model parameter values, their level of significance and correlation coefficients when scaled with leaf nitrogen per unit area (N_a), leaf mass per unit area (M_a) and leaf phosphorus per unit area (P_a) are given in Tables 3.7, 3.8 and 3.9 respectively. Overall, it can be seen that all the parameter values were highly significant ($P < 0.001$ or $P < 0.01$) and had strong correlation coefficients (r^2 ranged from 0.6 to 0.83) which was much higher r^2

compared to the results of fittings without temperature dependence, presented in the Tables 3.1, 3.3 and 3.5 respectively. Generally, incorporation of temperature response for the scaling of parameters improved the model predictions considerably. But still different leaf traits showed different amount of relationships with the three major model parameters (V_{cmax} , J_{max} and R_d).

In case of V_{cmax} , N_a happened to be the most significant and strongest scaling parameter (Table 3.7) except in one species (*G. dulcis*) where it had little weaker correlation coefficient ($r^2=0.6$) than that of when scaled with M_a and P_a (Tables 3.8 and 3.9 respectively). Present model (Equation 3.7), when scaled with N_a , described about 70% (average value from five species) of the variations in V_{cmax} which was higher compared to the other two leaf traits, where it was 63% and 64% for M_a and P_a respectively. Slopes of the relationships for every species were highly significant ($P<0.001$). Species wise activation energies (E_a) for V_{cmax} among the three scaling parameters were very similar and the variations in E_a among species ranged between 30.0 and 45.0 kJ mol^{-1} for N_a scaling, which was less compared to the variations of without scaling parameter values presented in chapter- II.

In case of J_{max} , N_a and M_a both happened to be highly significant ($P<0.001$) and strong ($r^2 = 0.49 \sim 0.7$ for N_a and $r^2 = 0.53 \sim 0.74$ for L_a) scaling parameters (Tables 3.7 and 3.8 respectively). Present model when scaled with both N_a and M_a it described about 62% (average value from five species) of the variations in J_{max} which was higher compared to P_a , where it was 53%. Slopes of the relationships for every species were also highly significant ($P<0.001$). Activation energies (E_a) for J_{max} among species were also very similar incase of scaling J_{max} with the three different scaling parameters. Variations in E_a among species ranged between 129.0 and 172.0 kJ mol^{-1} for N_a scaling which was also less compared to the variations of without scaling parameter values in chapter- II.

Leaf dark respiration (R_d) had also significant relationship with N_a for all five species whereas, in case of scaling with M_a and P_a , it was not significant for species *P. coccinea* and *L. havilandii* respectively (Tables 3.8 and 3.9). The average coefficients of determination of model fittings was little smaller when scaled with N_a (65%) compared to when scaled with M_a (70%) and P_a (71%). Species wise values for Q_{10} of

R_d were also very similar for all the three scaling parameters and Variations in Q_{10} among species ranged between 1.7 and 2.1 for N_a scaling which was also less compared to the variations of without scaling parameter values in chapter- II. From the results presented above it can be argued that N_a would be considered as the best scaling parameter for up-scaling photosynthesis and respiration parameters for canopy model for the investigated forest.

Table 3.7. Species wise photosynthetic parameter values as functions of leaf nitrogen per unit area (N_a , g m^{-2}) at the reference leaf temperature of 25 °C: a and b are proportionality coefficients (slope and intercept respectively) of regressions between V_{cmax} , J_{max} and R_d and the scaling parameter N_a , activation energy (E_a), deactivation energy (E_d) and temperature coefficient for dark respiration (Q_{10}). Significance of the Parameter values were $P < 0.05$ (*), $P < 0.01$ (**), $P < 0.001$ (***)

Scaled with N_a	<i>C. buruana</i>	<i>G. dulcis</i>	<i>L. havilandii</i>	<i>P. coccinea</i>	<i>V. arborea</i>
Values for V_{cmax}					
a ($\mu\text{mol m}^{-2} \text{s}^{-1}$)	46.0***	7.24***	44.76***	38.0***	25.7***
b ($\mu\text{mol m}^{-2} \text{s}^{-1}$)	-47.2***	10.7***	-12.6	-23.5**	11.4
E_a (kJ mol^{-1})	39.4±9.3***	30.1±8.2**	34.5±12.7*	40.9±10***	45.7±12.6**
r^2	0.83	0.6	0.71	0.74	0.62
Values for J_{max}					
a ($\mu\text{mol m}^{-2} \text{s}^{-1}$)	67.9***	19.3***	77.5***	96.4***	37.5***
b ($\mu\text{mol m}^{-2} \text{s}^{-1}$)	-55.5***	24.6***	-15.0	-70.7***	41.8***
E_a (kJ mol^{-1})	128.7±5.7***	172.2±5.3***	164.8±7.5***	155.7±8.6***	169.8±7.5***
E_d (kJ mol^{-1})	208.715	205.754	207.445	207.522	207.789
r^2	0.66	0.62	0.7	0.64	0.49
Values for R_d					
a ($\mu\text{mol m}^{-2} \text{s}^{-1}$)	0.32**	0.36***	0.295***	0.264*	0.34**
b ($\mu\text{mol m}^{-2} \text{s}^{-1}$)	0.466*	0.368***	0.786***	0.638**	0.635***
Q_{10}	1.7±0.18***	1.7±0.17***	1.9±0.2***	2.1±0.2***	1.9±0.25***
R^2	0.56	0.65	0.69	0.74	0.59

Table 3.8. Species wise photosynthetic parameter values as functions of leaf mass per unit area (M_a , g m^{-2}) at the reference leaf temperature of 25 °C: a and b are slope and intercept respectively of linear regressions, activation energy (E_a), deactivation energy (E_d) and temperature coefficient for dark respiration (Q_{10}).

Scaled with M_a	<i>C. buruana</i>	<i>G. dulcis</i>	<i>L. havilandii</i>	<i>P. coccinea</i>	<i>V. arborea</i>
Values for V_{cmax}					
a ($\mu\text{mol m}^{-2} \text{s}^{-1}$)	1.21***	0.265***	1.85***	0.343***	0.644**
b ($\mu\text{mol m}^{-2} \text{s}^{-1}$)	-117.7**	-4.3	-138.35*	0.48	2.15
E_a (kJ mol^{-1})	38.2±14.5*	28.9±7.0***	39.4±15.9*	41.1±10.7***	46.0±13.3**
r^2	0.62	0.7	0.56	0.7	0.58
Values for J_{max}					
a ($\mu\text{mol m}^{-2} \text{s}^{-1}$)	1.33***	0.664***	2.54***	0.98***	1.1***
b ($\mu\text{mol m}^{-2} \text{s}^{-1}$)	-103.6**	-13.0	-169.1***	-20.34*	18.54
E_a (kJ mol^{-1})	127.7±6.8***	172.6±5.1***	179.9±7.5***	155.2±7.2***	170.5±6.7***
E_d (kJ mol^{-1})	208.715	205.754	207.445	207.522	207.789
r^2	0.53	0.65	0.63	0.74	0.58
Values for R_d					
a ($\mu\text{mol m}^{-2} \text{s}^{-1}$)	0.019***	0.0126***	0.0225***	0.001	0.009**
b ($\mu\text{mol m}^{-2} \text{s}^{-1}$)	-1.78*	-0.355*	-1.15*	0.93***	0.484*
Q_{10}	1.77±0.16***	1.63±0.13***	1.93±0.16***	2.07±0.2***	1.94±0.25***
r^2	0.68	0.75	0.79	0.69	0.6

Table 3.9. Species wise photosynthetic parameter values as functions of leaf phosphorus per unit area (P_a , g m^{-2}) at the reference leaf temperature of 25 °C: a and b are slope and intercept respectively of linear regressions, activation energy (E_a), deactivation energy (E_d) and temperature coefficient for dark respiration (Q_{10}).

Scaled with P_a	<i>C. buruana</i>	<i>G. dulcis</i>	<i>L. havilandii</i>	<i>P. coccinea</i>	<i>V. arborea</i>
Values for V_{cmax}					
a ($\mu\text{mol m}^{-2} \text{s}^{-1}$)	1044.3***	464.6***	1176.2***	463.0***	755.0**
b ($\mu\text{mol m}^{-2} \text{s}^{-1}$)	-52.5***	-2.7	-41.4	-5.0	-1.8
E_a (kJ mol^{-1})	37.9±10.5**	30.6±5.8***	45.3±14.7**	37.3±13.6*	43.5±13.7**
r^2	0.79	0.8	0.59	0.51	0.53
Values for J_{max}					
a ($\mu\text{mol m}^{-2} \text{s}^{-1}$)	1271.3***	1125.0***	1804.6***	1169.1***	1039.5***
b ($\mu\text{mol m}^{-2} \text{s}^{-1}$)	-41.1**	-7.4	-43.7	-22.6	24.6
E_a (kJ mol^{-1})	127.0±5.7***	172.4±5.4***	179.4±8.4***	153.3±11***	165.4±7.9***
E_d (kJ mol^{-1})	208.715	205.754	207.445	207.522	207.789
r^2	0.67	0.6	0.56	0.4	0.42
Values for R_d					
a ($\mu\text{mol m}^{-2} \text{s}^{-1}$)	12.6***	20.0***	4.6	5.2**	16.9***
b ($\mu\text{mol m}^{-2} \text{s}^{-1}$)	-0.028	-0.183	0.89*	0.61***	-0.02
Q_{10}	1.78±0.15***	1.63±0.12***	2.0±0.24***	2.0±0.17***	1.82±0.2***
r^2	0.71	0.81	0.55	0.76	0.72

3.4.7 Canopy photosynthesis model parameters and their temperature responses when scaled with leaf properties

In order to get physiological parameters for the forest canopy photosynthesis model (MAESTRA), measurements from all the sample trees were pooled together and fitted for estimates. To see how far the sample trees can be considered as representative for the canopy, an analysis of variance of the residuals of the proc model (SAS Institute Inc. 2004, Cary, NC, USA) was done. According to the ANOVA results for V_{cmax} , J_{max} and R_{d} proc models residuals (Scheffe's test), two groups of species could be considered. One group consisted of species *L. havilandii* and *V. arborea*, which are considered as sun crown and the other group consisted of species *C. buruana*, *G. dulcis* and *P. coccinea*, which are considered shade crown. When a single model was fitted to all the species data there was little over estimation and under estimation for shade crown and sun crown trees respectively. As it was seen that photosynthetic and respiration parameters/ N_{a} relationships for every sample species was significant and also similar among sample species, pooled data was used to estimate parameters for canopy photosynthesis model (MAESTRA) with N_{a} as scaling parameter. Besides, two separate models for sun and shade crowns of the canopy are also presented for comparisons. Parameters for these models are given in Table 3.10. Parameter values for models when up-scaled with M_{a} and P_{a} are given in Tables 3.11 and 3.12 respectively.

The coefficients of regression between V_{cmax} and scaling parameters for canopy models were, slope = $30.6 \mu\text{mol g}^{-1} \text{s}^{-1}$ ($P < 0.001$) and intercept = -9.2 in case of N_{a} , slope = $0.24 \mu\text{mol g}^{-1} \text{s}^{-1}$ ($P < 0.01$) and intercept = 15.5 ($P < 0.05$) in case of M_{a} , and slope = $712.9 \mu\text{mol g}^{-1} \text{s}^{-1}$ ($P < 0.001$) and intercept = -12.8 ($P < 0.05$) in case of P_{a} . Activation energy (E_{a}) for V_{cmax} for canopy model was $42.7 \pm 9.0 \text{ kJ mol}^{-1}$ ($P < 0.001$) when scaled with N_{a} . On the other hand E_{a} was $46.2 \pm 11.7 \text{ kJ mol}^{-1}$ ($P < 0.001$) and $43.7 \pm 9.1 \text{ kJ mol}^{-1}$ ($P < 0.001$) when scaled with M_{a} and P_{a} respectively. The coefficient of determination was higher ($r^2 = 0.5$) for the present $V_{\text{cmax}}/N_{\text{a}}$ models than that of ($r^2 = 0.41$) the model without temperature response presented earlier.

The coefficients of regression between J_{max} and scaling parameters for canopy models were, slope = $41.0 \mu\text{mol g}^{-1} \text{s}^{-1}$ ($P < 0.001$) and intercept = 6.5 in case of N_{a} , slope = $0.34 \mu\text{mol g}^{-1} \text{s}^{-1}$ ($P < 0.001$) and intercept = 44.4 ($P < 0.001$) in case of M_{a} and slope = $1139.2 \mu\text{mol g}^{-1} \text{s}^{-1}$ ($P < 0.001$) and intercept = -5.6 ($P < 0.001$) in case of P_{a} . Activation energies (E_{a}) for J_{max} for canopy models were 161.8 ± 5.8 ($P < 0.001$),

167.0 ± 6.8 ($P < 0.001$) and 165.7 ± 5.7 ($P < 0.001$) kJ mol⁻¹ when scaled with N_a , M_a and P_a respectively. The coefficient of determination was higher ($r^2 = 0.37$) for the present J_{\max}/N_a models than that of ($r^2 = 0.26$) the model without temperature response presented earlier.

The coefficients of regression between R_d and scaling parameters for canopy models were, slope = 0.39 $\mu\text{mol g}^{-1} \text{s}^{-1}$ ($P < 0.001$) and intercept = 0.46 ($P < 0.001$) in case of N_a , slope = 10.0 $\mu\text{mol g}^{-1} \text{s}^{-1}$ ($P < 0.001$) and intercept = 0.32 ($P < 0.001$) in case of P_a , and slope = 0.0036 $\mu\text{mol g}^{-1} \text{s}^{-1}$ ($P < 0.001$) and intercept = 0.71 ($P < 0.001$) in case of M_a . Temperature coefficient (Q_{10}) for dark respiration for canopy models were 1.87 ± 0.1 ($P < 0.001$), 1.85 ± 0.1 ($P < 0.001$) and 1.93 ± 0.14 ($P < 0.001$) when up-scaled with N_a and P_a and M_a respectively. r^2 (0.63) for the present R_d/N_a models was higher than that of ($r^2 = 0.43$) the model without temperature response presented earlier.

Table 3.10. Canopy photosynthesis model parameters at 25 °C leaf temperature when scaled with N_a (g m^{-2}): a and b are slope and intercept, respectively of regressions between V_{cmax} , J_{max} and R_d and the scaling parameter, activation energy (E_a), deactivation energy (E_d) and temperature coefficient for dark respiration (Q_{10}). Significance of the parameter values were $P < 0.05$ (*), $P < 0.01$ (**), $P < 0.001$ (***). Canopy: (data from all five species), Sun Crown: (data from Lh and Va situated at the forest edge), Shade Crown: (data from Cb, Gd and Pc situated inside forest canopy).

Scaled with N_a	Canopy	Sun Crown	Shade Crown
Values for V_{cmax}			
a ($\mu\text{mol m}^{-2} \text{s}^{-1}$)	30.6***	36.0***	23.6***
b ($\mu\text{mol m}^{-2} \text{s}^{-1}$)	-9.2	-0.5	-6.0
E_a (kJ mol ⁻¹)	42.7±9.0***	39.9±9.0***	37.5±8.0***
r^2	0.5	0.68	0.62
Values for J_{max}			
a ($\mu\text{mol m}^{-2} \text{s}^{-1}$)	41.4***	38.0***	36.7***
b ($\mu\text{mol m}^{-2} \text{s}^{-1}$)	6.5	35.0***	5.8
E_a (kJ mol ⁻¹)	161.8±5.8***	170.0±5.6***	152.0±6.2***
E_d (kJ mol ⁻¹)	207.445	207.617	207.330
r^2	0.37	0.47	0.35
Values for R_d			
a ($\mu\text{mol m}^{-2} \text{s}^{-1}$)	0.392***	0.343***	0.35***
b ($\mu\text{mol m}^{-2} \text{s}^{-1}$)	0.469***	0.669***	0.4388***
Q_{10}	1.87±0.1***	1.88±0.15***	1.8±***
r^2	0.63	0.66	0.66

Table 3.11. Canopy photosynthesis model parameters at 25 °C leaf temperature when scaled with M_a (g m^{-2}): a and b are slope and intercept respectively of regressions between V_{cmax} , J_{max} and R_d and the scaling parameter, activation energy (E_a), deactivation energy (E_d) and temperature coefficient for dark respiration (Q_{10}).

Scaled with M_a	<i>Canopy</i>	<i>Sun Crown</i>	<i>Shade Crown</i>
Values for V_{cmax}			
a ($\mu\text{mol m}^{-2} \text{s}^{-1}$)	0.24**	0.51***	0.32***
b ($\mu\text{mol m}^{-2} \text{s}^{-1}$)	15.5*	8.8	-3.68
E_a (kJ mol^{-1})	46.2±11.7***	46.2±11.5***	36.4±9.5***
r^2	0.20	0.48	0.48
Values for J_{max}			
a ($\mu\text{mol m}^{-2} \text{s}^{-1}$)	0.34***	0.68***	0.56***
b ($\mu\text{mol m}^{-2} \text{s}^{-1}$)	44.4***	40.4***	4.0
E_a (kJ mol^{-1})	167.0±6.8***	177.1±6.0***	152.2±6.4***
E_d (kJ mol^{-1})	207.445	207.617	207.330
r^2	0.14	0.49	0.37
Values for R_d			
a ($\mu\text{mol m}^{-2} \text{s}^{-1}$)	0.0036***	0.0068***	0.0037***
b ($\mu\text{mol m}^{-2} \text{s}^{-1}$)	0.717***	0.598***	0.571***
Q_{10}	1.93±0.14***	1.97±0.16***	1.778±0.14***
r^2	0.44	0.64	0.49

Table 3.12. Canopy photosynthesis model parameters at 25 °C leaf temperature when scaled with P_a (g m^{-2}): a and b are slope and intercept respectively of regressions between V_{cmax} , J_{max} and R_d and the scaling parameter (P_a , g m^{-2}), activation energy (E_a), deactivation energy (E_d) and temperature coefficient for dark respiration (Q_{10}).

Scaled with P_a	<i>Canopy</i>	<i>Sun Crown</i>	<i>Shade Crown</i>
Values for V_{cmax}			
a ($\mu\text{mol m}^{-2} \text{s}^{-1}$)	712.9***	845.9***	481.6***
b ($\mu\text{mol m}^{-2} \text{s}^{-1}$)	-12.8*	-10.4	-5.5
E_a (kJ mol^{-1})	43.7±9.1***	44.9±10.2***	36.5±7.4***
r^2	0.48	0.57	0.67
Values for J_{max}			
a ($\mu\text{mol m}^{-2} \text{s}^{-1}$)	1139.2***	1070.6***	801.2***
b ($\mu\text{mol m}^{-2} \text{s}^{-1}$)	-5.58	19.13	3.93
E_a (kJ mol^{-1})	165.7±5.7***	173.5±5.9***	152.9±5.9***
E_d (kJ mol^{-1})	207.445	207.617	207.330
r^2	0.38	0.48	0.44
Values for R_d			
a ($\mu\text{mol m}^{-2} \text{s}^{-1}$)	10.0***	8.37***	8.8***
b ($\mu\text{mol m}^{-2} \text{s}^{-1}$)	0.32***	0.56**	0.33***
Q_{10}	1.85±0.1***	1.9±0.17***	1.76±0.09***
r^2	0.63	0.56	0.76

From the detailed results presented in this chapter, it is revealed that photosynthetic and respiration capacities in the leaves of the study forest canopy were controlled by both nitrogen and phosphorus. Again, in terms of level of significance in the scaling parameters and their coefficient of determinations N_a can be taken as better scaling parameter for photosynthetic capacities and dark respiration from leaves to canopy.

Predicted parameter values with the present model, scaled with N_a , are plotted against measured values in the figures 3.6, 3.7 and 3.8. In case of V_{cmax} (Figure 3.6), all three model predictions are very similar. Canopy model underestimates 1% (slope = 1.01), sun crown model underestimates 2% (slope = 1.02) and shade crown model estimates 100% (slope = 1.0). In case of J_{max} (Figure 3.7), there are more deviations among model predictions compared to V_{cmax} . Canopy and sun crown models overestimates by 1% and 4% (slopes = 0.99 and 0.96 respectively) and the shade crown model underestimates by 2% (slope = 1.02). In case of R_d (Figure 3.8), canopy and sun crown models estimate 100% (slopes = 1.0) and shade crown model underestimates by 1% (slope = 1.01).

Three particular leaves of *P. coccinea* had very high measured V_{cmax} and J_{max} values compared to their nitrogen concentrations. These data are seen in Figures 3.6 (a, c) and 3.7 (a, c) at their highest measured values, which seems to be outliers. But these data could not be excluded from fittings because during data quality control all the response curves from these leaves were found perfect. Leaf chamber conditions during their measurements were also perfect. To investigate possible reasons for these high measured values, residuals of the regression between measured and predicted value were fitted against leaf phosphorus concentration (P_a , g m⁻²). The residuals were only very poorly related to P_a . The coefficients of regressions (r^2) between residuals of V_{cmax} / P_a and residuals of J_{max} / P_a were 0.07 and 0.04 respectively. So it is unclear what could be the reasons for such high photosynthetic capacities of these leaves compared to their similar N_a with other leaves.

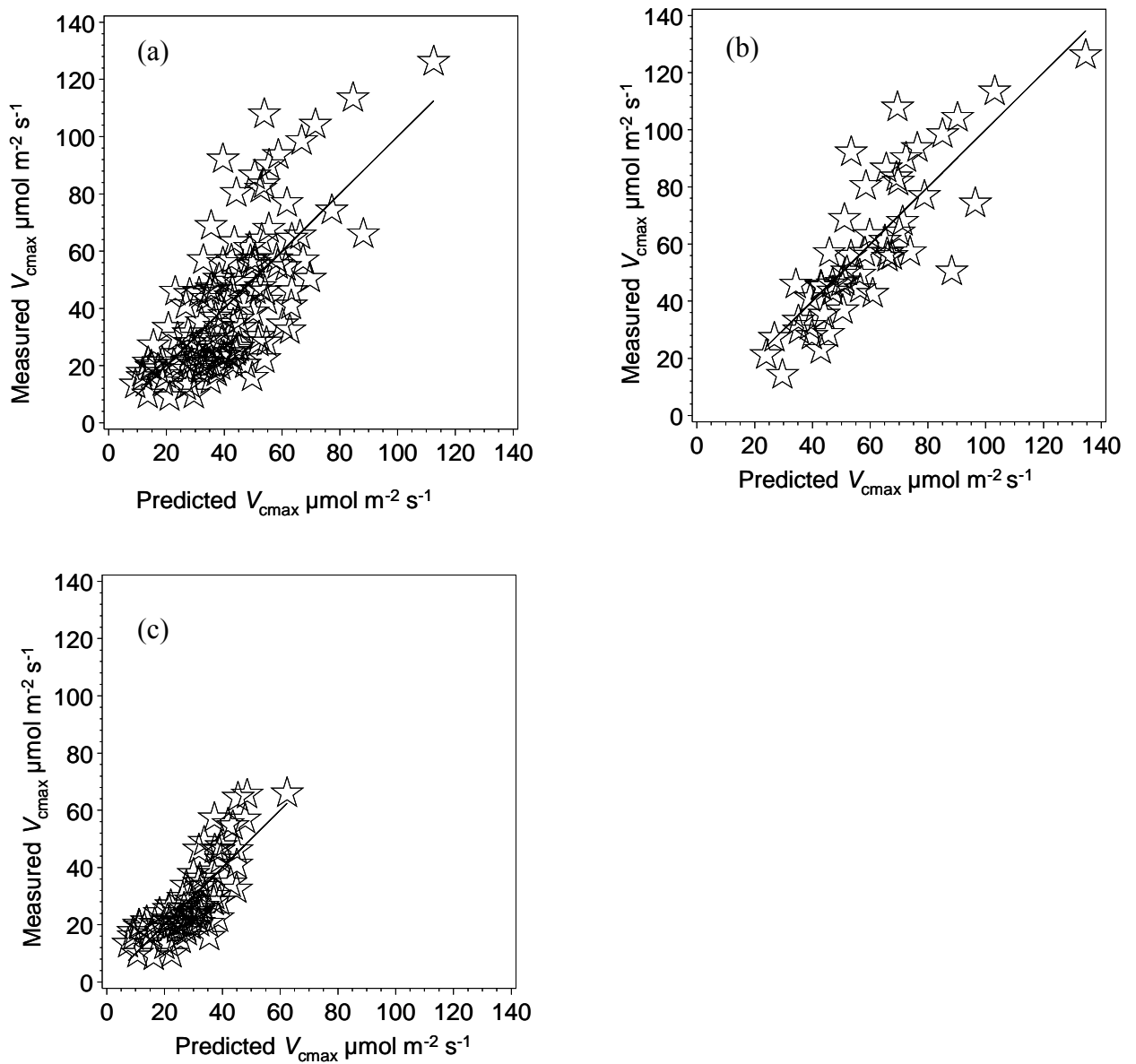


Figure 3.6. Plots of measured versus modeled V_{cmax} with N_a as scaling parameter. (a): Results of canopy model, Slope- 1.01, r^2 - 0.5 (b): Results of sun crown model, Slope- 1.02, r^2 - 0.68 (c): Results of shade crown model, Slope- 1.0, r^2 - 0.62

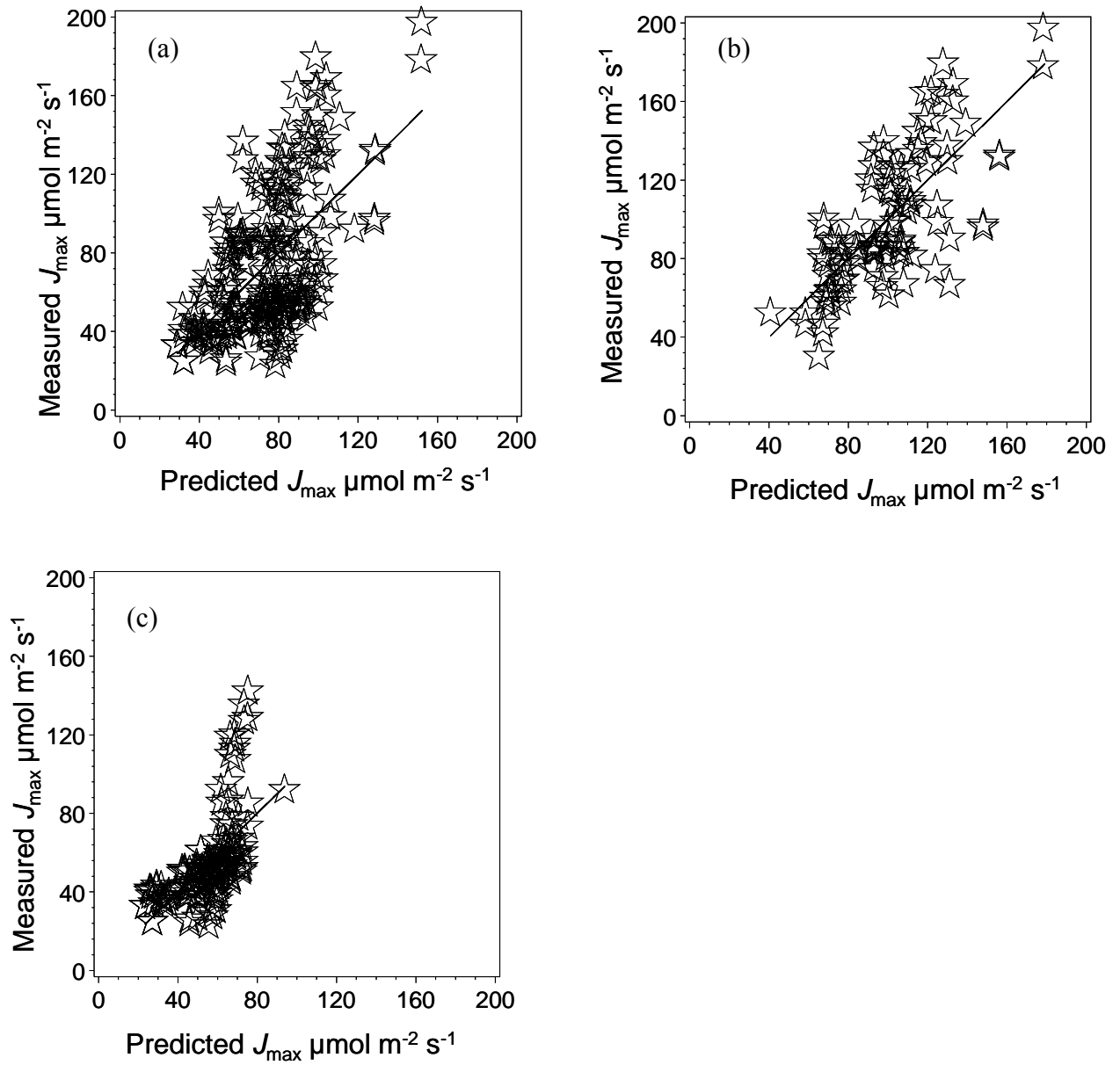


Figure 3.7. Plots of measured versus modeled J_{\max} with N_a as scaling parameter. (a): Results of canopy model, Slope- 0.99, r^2 - 0.34 (b): Results of sun crown model, Slope- 0.96, r^2 - 0.52 (c): Results of shade crown model, Slope- 1.02, r^2 - 0.37

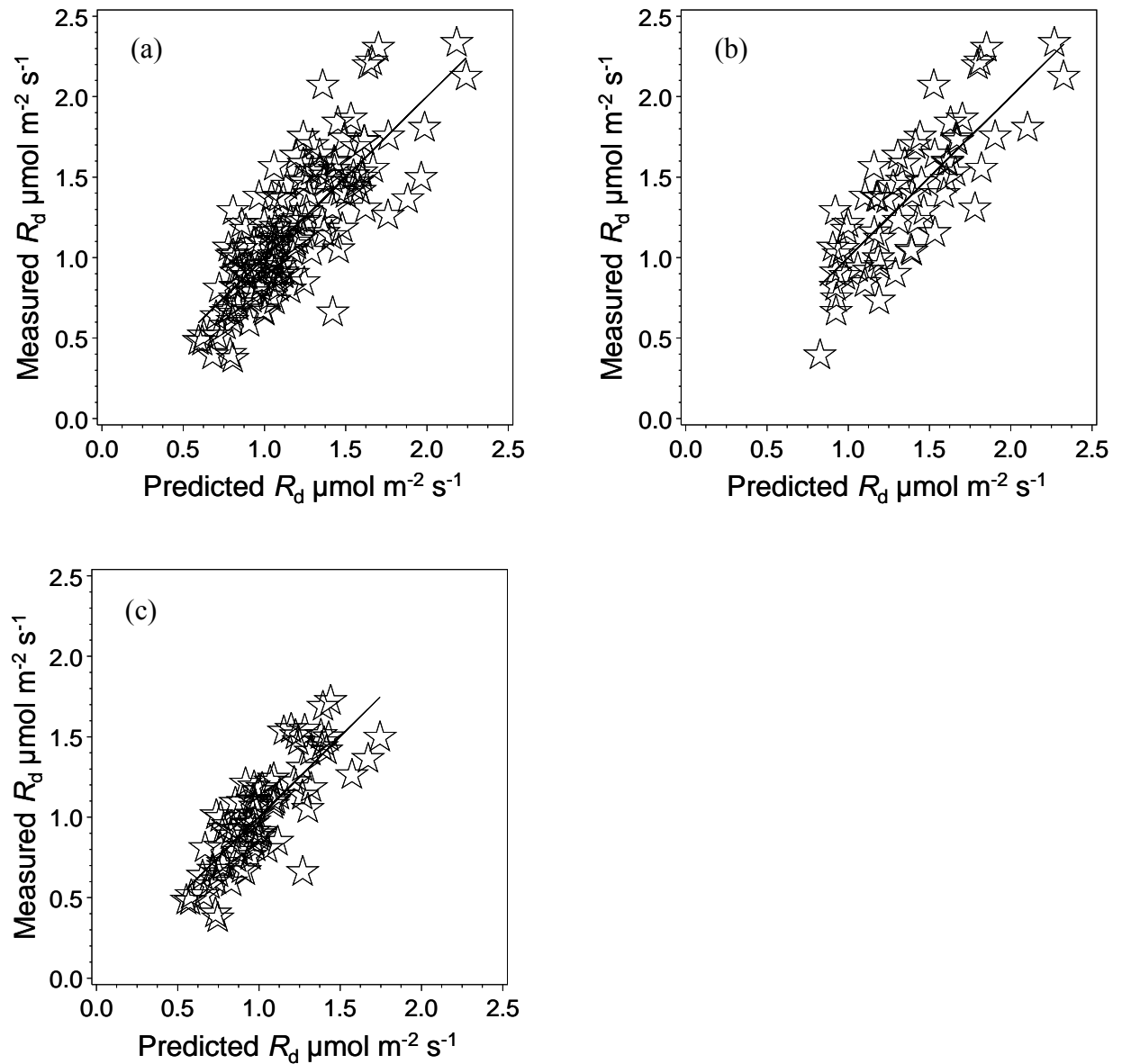


Figure 3.8. Plots of measured versus modeled R_d with N_a as scaling parameter. (a): Results of canopy model, Slope- 1.0, r^2 - 0.63 (b): Results of sun crown model, Slope- 1.0, r^2 - 0.66 (c): Results of shade crown model, Slope- 1.01, r^2 - 0.66

3.5 Conclusions

Quantifying the sources of variation in leaf-level photosynthetic and respiration parameters of the forest improves our understanding and ability to model forest carbon cycling. A considerable amount of the variability among leaves and species were described by leaf properties and the relationship between parameters and leaf

properties were strong and significant. Additionally temperature dependencies of these parameters were also important in describing the variations. When these relationships were incorporated in the fittings to estimate parameters, the model representation improved considerably, resulting much higher r^2 values compared to that in the previous chapter- II. Growth light environment of leaves (i.e. sun and shade conditions) influenced parameter values and their relationships with leaf properties. Accordingly two separate models for sun and shade crowns would have been better representative. A single canopy model also showed good results when model parameters were related to the foliage nitrogen content and temperature dependencies. Significant regressions of photosynthesis and respiration on foliage nitrogen content, particularly on area basis, indicates that such a model would be useful and accurate for the simulation of gross primary productivity of the investigated forest.

3.6 Reference:

- Cao, B., Dang, Q.L. and Zhang, S. (2007) Relationship between photosynthesis and leaf nitrogen concentration in ambient and elevated [CO₂] in white birch seedlings. *Tree Physiology* **27**, 891-899.
- Carswell, F.E., Meir, P., Wandelli, E.V., Bonates, L.C.M., Kruijt, B., Barbosa, E.M., Nobre, A.D., Grace, J. and Jarvis, P.G. (2000) Photosynthetic capacity in a central Amazonian rain forest. *Tree Physiology* **20**, 179-186.
- De Pury, D.G.G. and Farquhar, G.D. (1997) Simple scaling of photosynthesis from leaves to canopies without the errors of big-leaf models. *Plant Cell and Environment* **20**, 537-557.
- Evans, J.R. (1989) Photosynthesis and nitrogen relationships in leaves of C₃ plants. *Oecologia* **78**, 9-19.
- Farquhar, G.D., Caemmerer, S. Von and Berry, J.A. (1980) A biochemical model of photosynthetic CO₂ assimilation in leaves of C₃ species. *Planta* **149**, 78-90
- Field, C. and Mooney, H. (1986) The photosynthesis-nitrogen relationship in wild plants. *In* On the Economy of Plant Form and Function. Ed. T.J. Givnish. Cambridge Press, pp 25-55.
- Field, C. and Mooney, H.A. (1983) Leaf age and seasonal effects on light, water and nitrogen use efficiency in a California shrub. *Oecologia* **56**, 348-355.
- Grassi, G., Vicinelli, E., Ponti, F., Cantoni, L. and Magnani, F. (2005) Seasonal and interannual variability of photosynthetic capacity in relation to leaf nitrogen in a deciduous plantation in northern Italy. *Tree Physiology* **25**, 349-360.
- Harrington, R.A., Brown, B.J., Reich, P.B. and Fownes, J.H. (1989) Ecophysiology of exotic and native shrubs in southern Wisconsin. II. Annual growth and carbon gain. *Oecologia* **80**, 368-373.
- Hirose, T. and Werger, M.J.A. (1987) Maximising daily canopy photosynthesis with respect to leaf nitrogen allocation pattern in the canopy. *Oecologia* **72**, 520-526.

- Hölscher, D., Leuschner, C., Bohman, K., Hagemeyer, M., Jührbandt, J. and Tjitrosemito, S. (2006) Leaf gas exchange of trees in old-growth and young secondary forest stands in Sulawesi, Indonesia. *Trees* **20**, 278-285.
- Kenzo, T., Ichie, T., Watanabe, Y., Yoneda, R., Ninomiya, I. and Koike, T. (2006) Changes in photosynthetic and leaf characteristics with tree height in five dipterocarp species in a tropical rain forest. *Tree Physiology* **26**, 865-873.
- Kull, O. and Jarvis, P.G. (1995) The role of nitrogen in a simple scheme to scale up photosynthesis from leaf to canopy. *Plant, Cell and Environment* **18**, 1174-1182.
- Kumagai, T., Ichie, T., Yoshimura, M., et al. (2006) Modelling CO₂ exchange over a Bornean tropical rain forest using measured vertical and horizontal variations in leaf-level physiological parameters and leaf area densities. *Journal of Geophysical Research* **111**, D10107.
- Lambers, H., Chapin, F.S. III, and Pons, T.L. (1998) *Plant physiological ecology*. Springer-Verlag. New York, 540 p.
- Larcher, W. (2003) *Physiological plant ecology*. Fourth edition. Springer-Verlag. New York, 540p.
- Malhi, Y., Baldocchi, D.D. and Jarvis, P.G. (1999) The carbon balance of tropical, temperate and boreal forests. *Plant Cell and Environment* **22**, 715-740.
- Meir, P., Grace, J. and Miranda, A.C. (2001) Leaf respiration in two tropical rainforests: constraints on physiology by phosphorus, nitrogen and temperature. *Functional Ecology* **15**, 378-387.
- Meir, P., Kruijt, B., Broadmeadow, M., Barbosa, E., Kull, O., Carswell, F., Nobre, A. and Jarvis, P.G. (2002) Acclimation of photosynthetic capacity to irradiance in tree canopies in relation to leaf nitrogen concentration and leaf mass per unit area. *Plant, Cell and Environment* **25**, 343-357.
- Niinemets, U. and Tenhunen, J.D. (1997) A model separating leaf structural and physiological effects on carbon gain along light gradients for the shade tolerant species *Acer saccharum*. *Plant Cell Environment* **20**, 845-866.
- Poorter, H. and Evans J.R. (1998) Photosynthetic nitrogen-use efficiency of species that differ inherently in specific leaf area. *Oecologia* **116**, 26-37.
- Reich, P.B., Ellsworth, D.S., Walters, M.B., Vose, J.M., Gresham, C., Volin, J.C. and Bowman, W.D. (1999) Generality of leaf trait relationships: A test across six biomes. *Ecology* **80**, 1955-1969.
- Reich, P.B., Walters M.B. and Ellsworth, D.S. (1991) Leaf age and season influence the relationships between leaf nitrogen, leaf mass per area and photosynthesis in maple and oak trees. *Plant Cell Environment* **14**, 251-259.
- Reich, P.B., Walters, M.B. and Ellsworth, D.S. (1997) From tropics to tundra: global convergence in plant functioning. *Proc. Nat. Acad. Sci.* **94**, 13730-13734
- Rey, A. and Jarvis, P.G. (1998) Long-term photosynthetic acclimation to increased atmospheric CO₂ concentration in young birch (*Betula pendula*) trees. *Tree physiology* **18**, 441-450.
- Ryan, M.G. (1991) A simple method for estimating gross carbon budgets for vegetation in forest ecosystems. *Tree Physiology* **9**, 255-266.
- SAS Institute Inc. (2004) SAS 9.1.3 Help and Documentation, Cary, NC, USA
- Tscharntke, T., Leuschner, C., Zeller, M., Guhardja, E and Bidin, A. (eds) (2007) Stability of Tropical Rainforest Margins, linking ecological, economic and social constraints of land use and conservation, Springer Berlin 2007, pp 515.
- Wessman, C. (1990) Evaluation of canopy biochemistry. In Remote Sensing and Biosphere Functioning. Eds. R.J. Hobbs and H.A. Mooney. Springer-Verlag, New York, pp 135-154.

- Wilson, K.B., Baldocchi, D.D. and Hanson, P.J. (2000) Spatial and seasonal variability of photosynthetic parameters and their relationship to leaf nitrogen in a deciduous forest. *Tree Physiology* **20**, 565-578.
- Yoda, K. (1983) Community respiration in a lowland rainforest in Pasoh, Peninsular Malaysia. *Japanese Journal of Ecology* **33**, 183-197.

4 Chapter- IV: Simulation of CO₂ exchange of a tropical montane rain forest canopy of Central Sulawesi, Indonesia.

4.1 Abstract

Gross canopy photosynthesis (P_g) and foliage respiration (R_f) can be simulated with canopy photosynthesis models or retrieved from turbulent CO₂ flux measurements above the forest canopy. P_g and R_f of tropical montane rain forest of Central Sulawesi, Indonesia were simulated with the canopy model MAESTRA. Biophysical parameters for the model simulation were estimated from gas exchange measurements at leaf level. Meteorological data was taken from a measurement tower established in the forest. Model parameter acquisition and model sensitivity to selected parameters are described, and simulated results are compared with the measured values from turbulent flux data. Averaged daily modeled P_g and R_f was 7.15 g (C) m⁻² day⁻¹ and 3.18 g (C) m⁻² day⁻¹ respectively. Extrapolation of the average P_g to yearly value results 2608 g (C) m⁻² year⁻¹. Regression analysis revealed 3.9% smaller simulated P_g than observed P_g and 58% of the variation in observed P_g could be explained by the covariance with simulated P_g .

4.2 Introduction

It is recognized that the world's forests contribute significantly to the global carbon (C) balance, and that changes in forest C uptake may act as an important feedback to the current increase in atmospheric carbon dioxide (Malhi et al., 1999). The interannual and interdecadal variability in climate, and other changes in the environment, like rising atmospheric CO₂ concentration and large scale changes in land cover, have motivated several studies about the behaviour of ecosystems in a changing environment. Such studies lead to the development of several numerical models to understand the effects of these changes on the carbon, water and energy fluxes between the ecosystems and the atmosphere. Models of C, water and energy fluxes play an important role in the quantitative understanding of both the functioning of forests and their impacts on the atmospheric C cycle (Jarvis 1989, Sellers et al. 1997).

Southeast Asian tropical rain forests are among the world's most important biomes in terms of global carbon cycling; nevertheless, the impact of environmental factors on the ecosystem CO₂ flux remains poorly understood. Three-dimensional multilayer biosphere-atmosphere models such as MAESTRA (Wang and Jarvis 1990a, Medlyn 2004) are promising tools for understanding how interactions between environmental factors and leaf-level physiological parameters might impact canopy-level CO₂ exchange. In this study, a one dimensional multilayer canopy was modeled with MAESTRA to estimate the gross photosynthesis and foliar respiration for a tropical montane rain forest canopy. Sensitivity analysis was performed to determine the relative importance of variation in the main factors controlling carbon flux in the tropical montane rain forest.

4.3 Material and methods

4.3.1 Forest site topography, climate and vegetation

The study site is a tropical montane natural rain forest in Central Sulawesi, Indonesia. It lies in the Besoa region, in the eastern part (1° 39'S 120° 10'E) of the Lore Lindu National Park, at an altitude of 1427 m near the village Bariri. The study site is situated on a level plateau. The vegetation is uniform and the terrain is characterised by a smooth relief with a small slope < 5° within a distance of 1000 m. The study area has a humid tropical climate with almost no seasonal changes in temperature but with small seasonal changes in rainfall without a pronounced dry season. Mean annual precipitation and mean annual temperature at the study site was 1700 mm yr⁻¹ and 19.6°C respectively (Ibrom et al. 2007). However, at night it becomes considerably cooler and enhanced nocturnal cooling results in substantial amounts of dew fall and fog, particularly in the early morning hours. Seasonality is normally affected by the course of the Inter Tropical Convergence Zone. However the climate of Indonesia is also affected by occasionally occurring ENSO events, leading to strong anomalies in rainfall (Gunawan et al. 2003).

The forest canopy consists of many tree species (up to 90 species per ha) of different age and structure (Kessler et al. 2005). According to a recent inventory the dominant tree species with 12% of all individuals dbh ≥ 7 cm is *Castanopsis*

acuminatissima of the most abundant family Fagaceae (18%), which is followed in abundance by Myrtaceae (13%), Elaeocarpaceae (7%), and Monimiaceae (7%) Grote (2006). The forest is a closed stand with a stem density of 557 ha⁻¹ (dbh ≥ 10 cm). Additionally there were 10-fold large number of seedlings and saplings with dbh < 10 cm. Basal area per hectare was 53 m². Average height of trees with dbh ≥ 10 cm was 24 m with a range from 12 m to 40 m. Leaf area index (LAI) determined with hemispherical photography after correction for leaf clumping effects was estimated to 6.7. The forest shows no signs of major anthropogenic impact.

4.3.2 Parameterisation of the forest canopy model MAESTRA

MAESTRA (Medlyn 2004) is the latest version of the forest canopy model MAESTRO (Wang 1988, Wang and Jarvis 1990a). The main features of MAESTRA are the 3D descriptions of canopy structure and radiative transfer in the canopy, coupled to the physiological responses of leaves at different locations, representing the intra-tree variability. Following are the descriptions of inputs (climatic variables and parameter sets) used to drive the model.

4.3.3 Climate

Half-hourly meteorological data including incident photosynthetically active radiation (PAR), air temperature, wind speed, relative humidity and vapour pressure saturation deficit were obtained from the meteorological tower established by STORMA.

4.3.4 Tree dimensions and canopy structure

Necessary data about tree dimensions and tree locations to build the original stand (tree map) for the investigated site for MAESTRA simulation was not available. Instead a one dimensional uniform canopy of leaf columns was derived. In the canopy, individual box shaped (10*10 square meter area and 40 meter height) tree crowns are considered sitting side by side touching one another. And within the crowns, leaves are distributed according to the vertical beta distribution of leaf area density which was calculated from measured vertical leaf area distribution data (Figure 4.1) using the following function:

$$f(r,h) = a h^b (1-h)^c \quad (4.1)$$

where $f(r,h)$ is the normalized leaf area density at relative height h (0, crown base; 1, crown top) and relative radius r (0, next to trunk; 1, exterior of canopy). a , b and c are parameters of vertical beta distributions for leaf area density and the parameter “ a ” must be determined from the following constraint: the integral of $a h^b (1-h)^c$ from $h = 0$ to $h = 1$ must =1.

The estimated crown structure parameter (a , b and c) values used in the simulations are shown in Table 4.1. As a result of the tree dimensions and LAI of 6.7, each tree crown has a radius of 5.0 meters along both X and Y coordinates and consists of 670 m² of leaf area that is distributed vertically according to beta distribution function. MAESTRA uses the method of Norman and Welles (1983) to calculate PAR at grid points within the crown taking into account the spatial distribution of foliage within the target crown and in adjacent tree crowns. The canopy was stratified into ten vertical layers, which was found to be optimum, to allow MAESTRA to calculate absorbed PAR, key physiological parameters (V_{cmax} , J_{max}) and productivity at ten vertical grid points in the canopy. Target tree for simulation is selected at the centre of the plot and to further avoid the edge effects plot size is kept considerably larger having crowns of adjacent trees up to 125 meters along both the coordinates.

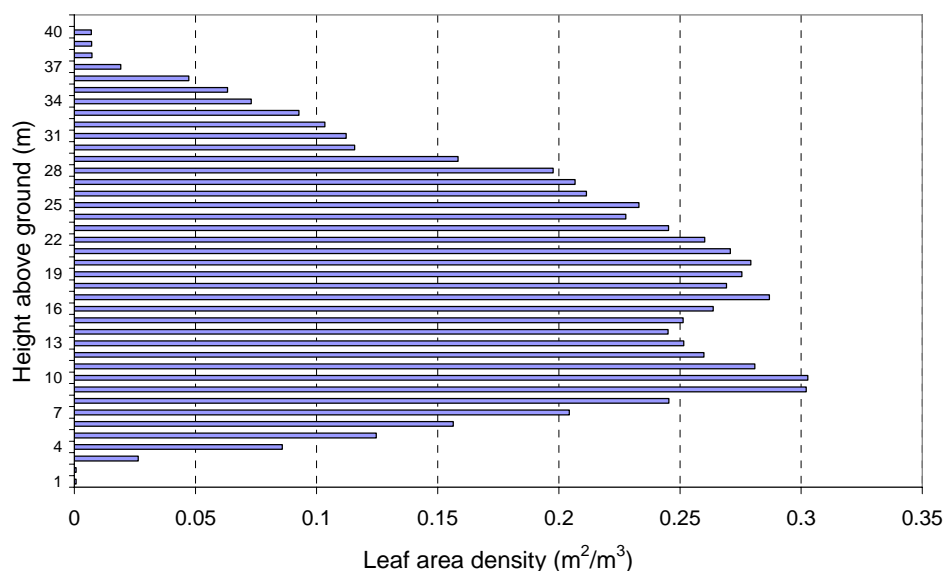


Figure 4.1. Vertical distribution of leaf area density of the investigated forest canopy. The integral of leaf area density equals to leaf area index (6.7) of the forest canopy.

Source: Grote (2006)

4.3.5 Photosynthetic responses to PAR and temperature

In MAESTRA leaves are considered to be individually distributed in space, i.e., they are not attached to a shoot and shading occurs according to the cumulative leaf areas along the paths of beams of PAR to a simulated point in the crown of a target tree. Absorption of PAR and photosynthesis are calculated from incident diffuse and beam radiation at one point considering leaf clumping and several leaf inclination angle classes (Ibrom et al. 2006).

Photosynthetic rates were estimated according to the model of Farquhar et al. (1980), for which the key parameters are the maximum rate of Rubisco activity (V_{cmax}), the maximum rate of electron transport (J_{max}), the initial slope (α) and curvature (θ) of the light response of electron transport and the dark respiration (R_d) and the temperature dependences of V_{cmax} , J_{max} and R_d . These parameters were calculated from gas exchange data of field measurements by nonlinear regression analysis using statistical procedures in release 9.1 of the statistical analysis system SAS. Details of these calculations are given in chapter - I.

In the field measurements, relationships between these key biochemical parameters and leaf traits, such as leaf nitrogen concentration, leaf phosphorus concentration and leaf mass per area, were investigated with the intention of using these relationships for up-scaling leaf-level measurements to canopy level. Among the three leaf properties investigated, leaf nitrogen per unit area (N_a) was found most significantly and strongly correlated with physiological parameters. Therefore, these parameters/ N_a relationships (shown in Chapter- III) were used as inputs in the simulation instead of estimated parameter values, which are presented in the previous chapter - II. Reference physiological and bio-physiological parameter values used in the MAESTRA simulations are listed in Table 4. 2.

4.3.6 Stomatal conductance

Stomatal conductance (g_s) was taken by Jarvis model of stomatal conductance (Jarvis 1976), which is given by:

$$g_s = \text{GSREF} * f(T) * f(\text{VPD}) * f(\text{CO}_2) * F(\text{PAR}) + \text{GSMIN} \quad (4.2)$$

where, GSREF and GSMIN are the maximum and minimum stomatal conductance to CO_2 ($\text{mol m}^{-2} \text{s}^{-1}$) respectively and the f 's are functions of environmental variables

which relate g_s to leaf temperature (T), vapour pressure saturation deficit (VPD), ambient carbon dioxide (CO_2) concentration and incident PAR. Values of the parameters for this model are given in Table 4.2.

4.3.7 Simulations

Simulation was done on a 260 x 260 m² plot which contained 676 identical box shaped tree crowns of 10 x 10 x 40 m³ in size each with a leaf area of 670 m². The grid size was chosen to maintain a tree density lower than the maximum limit allowed in MAESTRA simulation. A tree in the centre of the plot was selected as the target tree for simulation to avoid the edge effects. As the virtual trees and their environment were identical, the target tree was representative for the whole cohort. The structure of every individual crown was described by the general 1D (vertical) β -function calculated from the field measurement data. The simulation results at the tree scale were then used to calculate simulated stand gross photosynthesis, with stand LAI as a scaling factor.

4.3.8 Sensitivity analysis

Sensitivity analyses were performed to determine the relative importance of variation in the main factors in the MAESTRA controlling carbon dioxide exchange. Sensitivity analyses were performed by changing major parameters from its reference value to upward and downward in several steps.

Table 4.1. Parameter values of normalized β -functions of vertical leaf area density distributions used in the simulation. (Calculated from Grote 2006)

Namelist	Parameter	Reference values
LADD	A	14.044
	B	1.238
	C	1.861

Table 4.2. Physiological and biophysical parameter values used in the simulation.

Namelist ¹	Parameter (names ¹) and units	Reference values		
		PAR	NIR	IR
ABSORB	Soil reflectance (RHOSOL)	0.01 ^A	0.30 ^A	0.05 ^A
	Leaf transitivity (ATAU)	0.03 ^E	0.30 ^A	0.05 ^A
	Leaf reflectance (ARHO)	0.10 ²	0.35 ²	0.05 ²
JARGS	Cuticular conductance to CO ₂ (GSMIN) mol m ⁻² s ⁻¹	0.01 ^A		
	Maximum stomatal conductance for CO ₂ (GSREF) mol m ⁻² s ⁻¹	0.22 ³		
	Minimum temperature (T0) °C	5 ^A		
	Optimum temperature (TREF) °C	25 ^A		
	Maximum temperature (TMAX) °C	40 ^A		
	<i>D</i> threshold at 50% reduction of stomatal conductance (D0) Pa	3000 ⁴		
	Sensitivity of stomatal conductance to external [CO ₂] (GSJA) mol μmol ⁻¹	0.0109 ⁴		
	NSIDES	1		
	Leaf width (WLEAF)	0.055 ^E		
	Parameter of the hyperbolic response to <i>Q</i> (PAR0) μmol m ⁻² s ⁻¹	40 ⁴		
NFOL	Foliar nitrogen concentrations at ten layers g m ⁻²	1.75; 1.65; 1.55; 1.4; 1.3; 1.15; 1.0; 0.85; 0.75; 0.6 ^E		
JMAXN	Slope of the linear <i>J</i> _{max} response to leaf nitrogen content (JMAXA) μmol g ⁻¹ s ⁻¹	41.0 ^E		
	Offset of the linear <i>J</i> _{max} response to leaf nitrogen content (JMAXB) μmol m ⁻² s ⁻¹	6.5 ^E		
	Slope of the linear <i>V</i> _{cmax} response to leaf nitrogen content (VCMAXA) μmol g ⁻¹ s ⁻¹	30.6 ^E		
	Offset of the linear <i>V</i> _{cmax} response to leaf nitrogen content (VCMAXB) μmol m ⁻² s ⁻¹	-9.2 ^E		
JMAXPARS	Convexity parameter of the <i>Q</i> response of <i>J</i> (THETA) dimensionless	0.7 ^E		
	Activation energy temperature response of <i>J</i> _{max} (EAVJ) J mol ⁻¹	161000 ^E		
	deactivation energy temperature response of <i>J</i> _{max} (EDVJ) J mol ⁻¹	207445 ^E		
	Entropy term in temperature response of <i>J</i> _{max} (DELSJ) J K ⁻¹ mol ⁻¹	700 ⁵		
	Quantum yield of electron transport (AJQ) mol e ⁻ mol ⁻¹ absorbed PAR	0.29 ^E		

Namelist ¹	Parameter (names ¹) and units	Reference values
VCMAXPARS	Activation energy temperature response of V_{cmax} (EAVC) J mol^{-1}	42700 ^E
RDN	Slope of the linear dark respiration response to leaf nitrogen content (RDA) $\mu\text{mol m}^{-2} \text{s}^{-1}$	0.392 ^E
	Offset of the linear dark respiration response to leaf nitrogen content (RDB) $\mu\text{mol m}^{-2} \text{s}^{-1}$	0.46 ^E
RDPARS	Reference temperature for respiration response to temperature to temperature (RTEMP) $^{\circ}\text{C}$	25 ^A
	Scaling constant in the exponential respiration response function to temperature (Q10F) $^{\circ}\text{C}^{-1}$	0.062594 ^E
	Fraction by which dark respiration reduced in light (DAYRESP)	0.5 ⁴

^E Estimated from field measurements of this study

^A Assumed

¹ Names for parameters and their parameter groups used in the MAESTRA documentation.

² Souza and Valio (2003)

³ Motzer et al. (2005)

⁴ Ibrom, unpublished data

⁵ Fixed parameter

4.4 Results and discussions

4.4.1 Crown structure of the simulated forest

Vertical leaf area distribution (LAD) functions of the investigated forest were calculated from biometric field data (Grote 2006). The LAD distributions of all the virtual tree crowns were similar throughout the plot. Leaf area was $670 \text{ m}^2 \text{ tree}^{-1}$ and the majority of the leaf area was concentrated in the lower and middle part of the crown (Figure 4.2). The horizontal leaf area distribution data was not available and hence considered to be uniform.

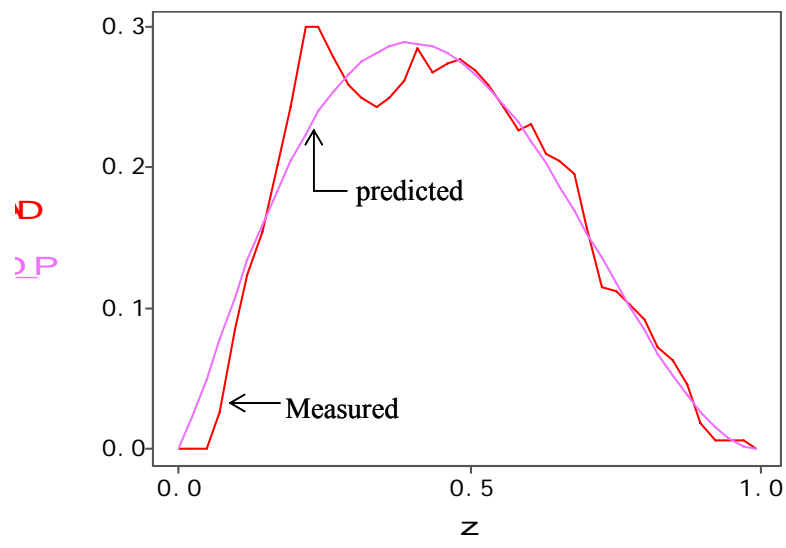


Figure 4.2. Measured (curved line) and predicted (smooth line) leaf area density with the calculated beta distribution coefficients.

4.4.2 Sensitivity analyses

4.4.2.1 *Gross canopy photosynthesis and PAR absorption to leaf area distribution*

The effects of leaf area distributions (LAD) within the tree crowns, uniform distribution (UD) and one dimension vertical distribution (1D LAD), on the simulated PAR absorption (Q_a) and gross primary productivity (P_g) were investigated. In the two simulations all values except those determining the LAD distributions were kept constant; i.e., the simulations differed only in the way the leaf area inside the tree crowns was more or less clumped. In a solitary tree, clumping of leaf area increases from uniform for 1D LAD distribution and is maximal at 2D LAD distribution; however, the situation at the stand scale is more complex because crowns may overlap and shade one another (Ibrom et al. 2006). But in the present simulation tree crowns were put side by side and touching one another without having overlapped, and the structure of the stand could be resembled to the structure of a tree.

Simulated Q_a and P_g were sensitive to leaf area density distributions. The relative effects of LAD distributions are shown in Table 4.3. With the uniform LAD distribution Q_a and P_g were considerably larger than those of with 1D LAD. Similar response of LAD was observed by Ibrom et al. (2006) in a German Norway spruce forest. The type of LAD distribution affected the simulation of Q_a and P_g in the range

of few percents up to 20%. The effect of parameterization of LAD distribution takes in the simulation depends on canopy traits like tree density, crown dimensions and relative absorptance (Ibrom et al. 2006). Simplified parameterizations, that neglect heterogeneity in LAD distribution, introduced artefacts in the description of the canopy structure, to which simulation was sensitive, indicating the need to use the 2D LAD distributions for simulations of dense forest canopies like tropical rain forest.

Table 4.3. Sensitivity of gross photosynthesis rates (P_g) and photosynthetically active radiation absorption rates (Q_{abs}) to two different leaf area distributions in the simulation. Abbreviations: UD stands for uniform; and 1D for one dimensional vertical leaf area density distribution.

Relative effect	Ratio
$Q_a(\text{UD})/ Q_a(\text{1D})$	1.20
$P_g(\text{UD})/ P_g(\text{1D})$	1.24

4.4.2.2 Sensitivity of gross primary productivity to the physiological parameters related to light and temperature responses

A range of parameter values, varying from the reference value, were used in simulations to see the relative sensitivity of gross primary productivity (P_g) to curvature of light response curve (THETA), quantum yield of light response (AJQ), activation energy of electron transport rate (EAVJ), deactivation energy of electron transport rate (EDVJ) and activation energy of Rubisco carboxylation rate (EAVC). Sensitivity results are shown in Figure 4.3. Among these parameters AJQ showed the highest influence on P_g . If quantum yield values of 0.246 and 0.333 were used, which are 15% lower and higher respectively than the estimated reference value (0.29 mol e⁻ mol⁻¹ absorbed PAR), simulated P_g would be 6.5% lower and 5.8% higher respectively than from the reference simulation. The parameter EAVC had almost no influence on P_g . EAVC values of 23485 and 61915, which are 45% lower and higher respectively than the estimated reference value (42700 J mol⁻¹), produced only 0.56% lower and 0.65% higher P_g respectively. The parameter EAVJ, for which estimated reference value (161000 J mol⁻¹) is apparently high compared to literature values, had only little influence on simulated P_g . This apparent high EAVJ value could have

arisen from small temperature range of the measurements. If values of 88550 or 64400 J mol⁻¹ were used, which are closer to literature values and 45% and 60% lower than the reference respectively, simulated P_g would be 3.1% and 3.08% higher than for the reference simulation. P_g was little positively correlated to the parameter EDVJ within 15% of both sides of the reference value (207445 J mol⁻¹). Values of 195000 and 176328 J mol⁻¹ that are 6% and 15% lower than reference value produced 4.4% and 3.9% higher P_g respectively. Further decrease in parameter also decreased P_g gradually. On the other hand values of 220000 and 238561 J mol⁻¹ that are 6% and 15% higher than the reference value produced 7.7% and 7.9% lower P_g respectively. Beyond that further increase in the parameter the model was insensitive.

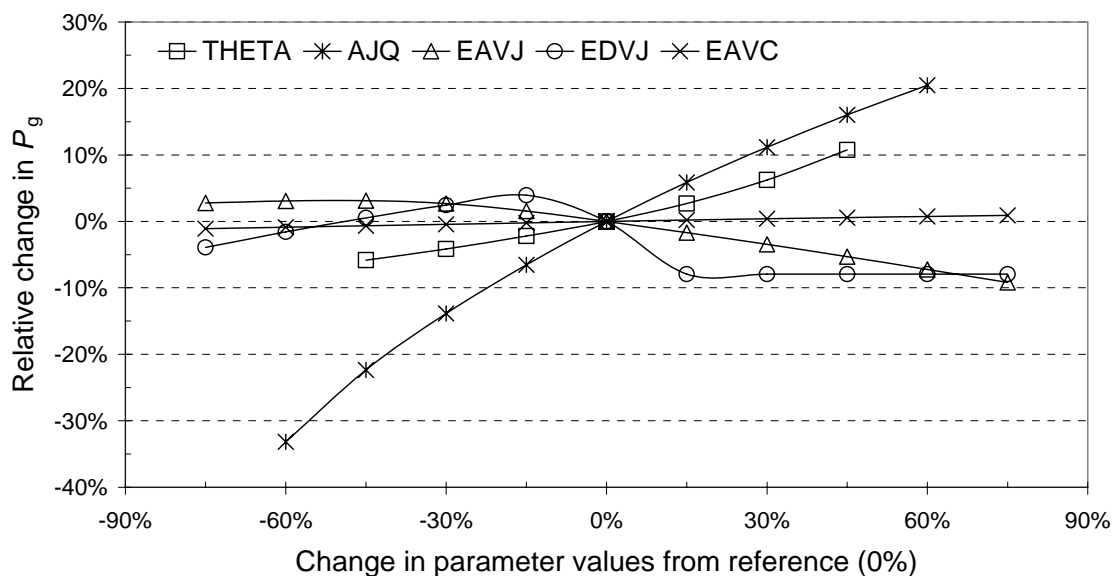


Figure 4.3. Relative sensitivity of gross primary productivity (P_g) to the physiological parameters related to light and temperature responses. Parameter values have been changed from the estimated reference (0%) to higher and lower values in steps of 15%.

4.4.2.3 Sensitivity of gross primary productivity to the parameters related to leaf nitrogen content

Sensitivity of gross primary productivity to the slopes (A) of V_{cmax} and J_{max} to nitrogen dependence has been shown in Figure 4.4. P_g was highly sensitive to the slopes of V_{cmax} and J_{max} as can be seen in the lower values from the estimated reference values of 30.6 and 41.0 $\mu\text{mol g}^{-1} \text{s}^{-1}$ for VCMAXA and JMAXA respectively. In this range increase in either VCMAXA or JMAXA separately increases P_g . But in the upper part of reference values, increase in only one parameter

e.g. VCMAXA did not increase P_g because the upper values might be already limited by the other e.g. JMAXA. This is because photosynthesis is limited by the minimum of any of these two as shown in equation 1, chapter-I. So increase in both of the parameters might increase P_g in the right branch of the graph as well. This is shown when leaf nitrogen concentration (NFOL) of the ten crown layers were changed in a similar way, P_g continues to increase as both VCMAXA and JMAXA would be higher with more nitrogen in the leaves. As these two parameters have large effects on P_g , any small error in estimating leaf nitrogen content would have contributed considerable variation in simulated output.

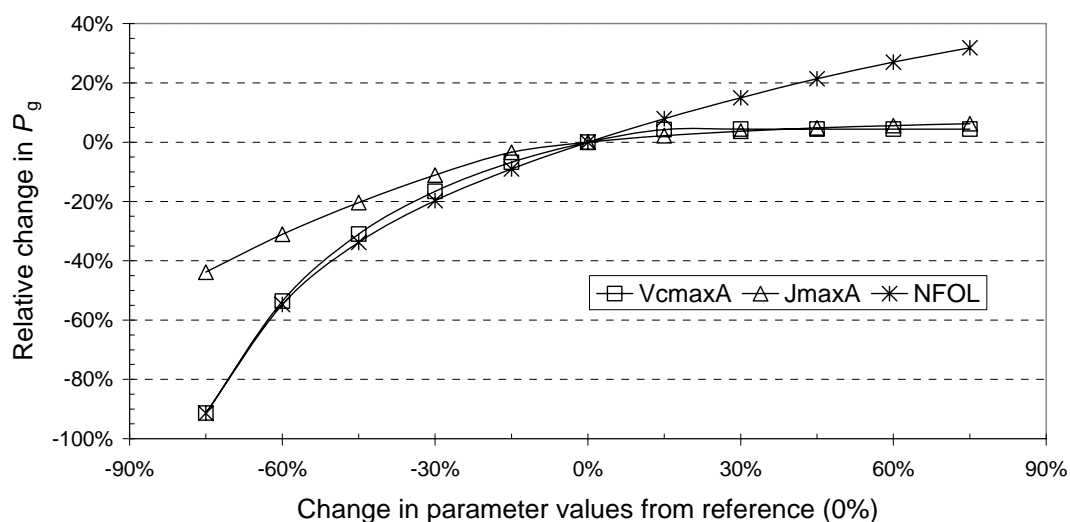


Figure 4.4. Relative sensitivity of gross primary productivity (P_g) to the physiological parameters related to leaf nitrogen content. Parameter values have been changed from the estimated reference (0%) to higher and lower values in steps of 15%.

4.4.2.4 Sensitivity of gross primary productivity to the parameters related to leaf stomatal conductance

Sensitivity of gross primary productivity (P_g) to maximum stomatal conductance (GSREF), cuticular conductance (GSMIN), vapour pressure deficit threshold at 50% reduction of stomatal conductance (D0), sensitivity of stomatal conductance to external CO_2 (GSJA), parameter of the hyperbolic response to Q (PAR0) are shown in Figure 4.5. Among these parameters P_g was relatively more sensitive to GSREF and D0. Other parameters had almost no sensitivity for P_g . The reference value for GSREF ($0.22 \text{ mol m}^{-2} \text{ s}^{-1}$) turned out to be the optimum for the sample canopy. Higher values from reference increased the productivity only a little and the rate of increase decreased gradually. Higher value of 0.253 (+15% from

reference) increased the total productivity by less than one percent. Values lower than the reference decreased the output considerably at an increasing rate. P_g was almost not sensitive to D0 at the higher values than the reference (3000 Pa) and only little sensitive at the lower values up to 1200 Pa. Lower values of 2550 and 2100 (-15% and -30% from reference) decreased the simulated productivity by 0.4% and 0.9% respectively.

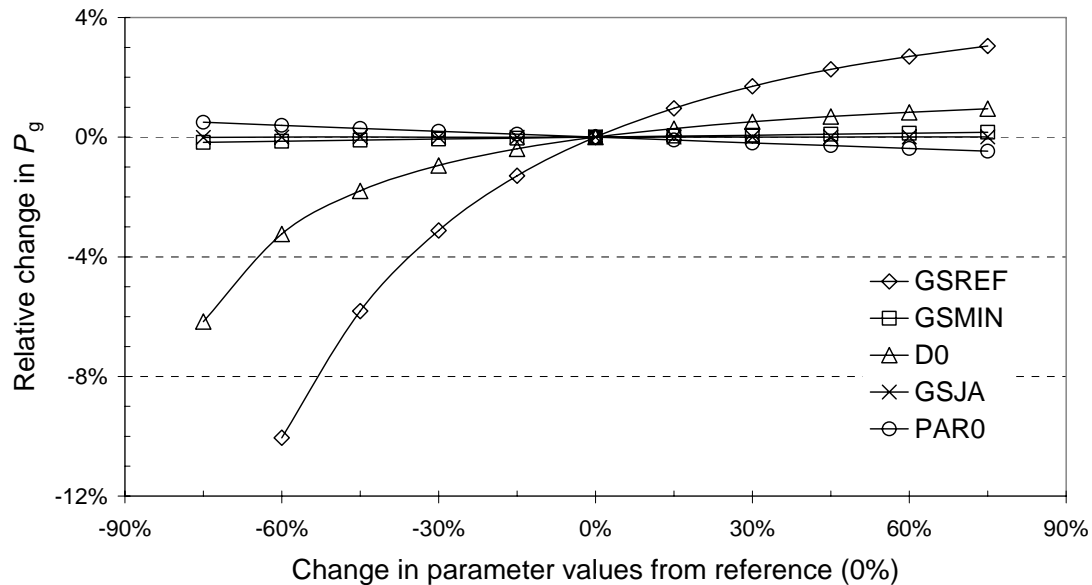


Figure 4.5. Relative sensitivity of gross primary productivity (P_g) to the physiological parameters related to leaf stomatal conductance. Parameter values have been changed from the estimated reference (0%) to higher and lower values in steps of 15%.

4.4.2.5 Influence of number of vertical layers in the canopy on simulated outputs

Optimum numbers of vertical stratifications in the forest crown for which leaf nitrogen are to be specified, to calculate layer specific photosynthetic capacities for total canopy productivity, were taken from a sensitivity analysis. Influence of number of layers on photosynthetic photon flux absorption (APAR) and gross primary productivity (P_g) was tested in three simulations with five, ten and twenty layers in each. Leaf nitrogen content in layers for these three simulations was distributed keeping highest and lowest values fixed for top and bottom layers. Changes in APAR among three simulations were very small. Total absorption was 75.5%, 74.6% and 73.6% for crowns with 5, 10 and 20 layers respectively. On the other hand P_g for crowns with 10 and 20 layers were almost the same but it was 5% less for the crown

with 5 layers compared to the other two. Considering these results 10 vertical layers in the crown was justified for final simulations.

4.5 Simulated versus observed CO₂ uptake

4.5.1 Comparisons of gross primary productivity

A comparative study of gross primary productivity (P_g) was done between outputs from MAESTRA simulations and observed P_g from turbulent fluxes to determine whether MAESTRA was able to simulate the different biophysical behaviour of the investigated forest. Instead of the net ecosystem uptake (F_b) of CO₂, observed gross primary productivity (P_g) can be compared with the results of MAESTRA. For the comparison F_b has to be converted to P_g by adding ecosystem respiration (R_E). As it was known that there was seasonality in R_E , of the studied forest ecosystem (Andreas Ibrom, unpublished) we compare only three months (May, June and July) data where there was no pronounced variation. Average ecosystem R_E was determined from night time F_b for the period of comparison and was taken as constant. Results of the comparisons are shown in Figures 4.6a and 4.6b. It is seen that 58 % of the variation in observed P_g could be explained by covariance in simulated P_g and the regression analysis revealed a slightly smaller (3.9 %) simulated P_g than observed P_g . The regression line differed by about 4 % from the one-to-one line (Figure 4.6a). The slopes of monthly regressions between simulated and observed P_g varied moderately with values of 1.02 ± 0.04 , 1.01 ± 0.03 and 1.09 ± 0.03 for May, June and July. The observed and simulated estimates of P_g were completely independent of one other. During daytime the residual scatter was more or less homogeneously distributed around the regression line with a standard deviation of $5.5 \mu\text{mol m}^{-2} \text{s}^{-1}$. The source of the scatter may be attributed to the real flux variability and to errors both in the model and in the turbulent flux measurements. Additional bias in the observed P_g might have been caused by errors in the night time R_E measurements and its extrapolation over day time. However, the simulated results may be erroneous because of uncertainty in parameterization or use of oversimplifying assumptions in the model structure. Assuming that, bias in the meteorological input data was low, it can be expected that errors associated with the model will tend to be of a more systematic than random nature, because both model

structure and parameters were constant over the simulations. Thus, the scatter in the comparisons was most likely introduced by the turbulent flux data and not by the model output (Ibrom et al. 2006).

Average diurnal course and simulated and observed mean P_g were used for further comparisons. The simulated mean diurnal course of P_g followed closely its corresponding observed course (Figure 4.6b) and the daily means over the period of comparison differed by only 2.8 % with $14.17 \mu\text{mol m}^{-2} \text{s}^{-1}$ and $13.78 \mu\text{mol m}^{-2} \text{s}^{-1}$ for observed and simulated P_g respectively. The systematic differences between simulated and observed P_g in the early afternoon and before noon could be related to vapour pressure deficit (D). The small apparent overestimation by the model during the early afternoon (11:75 am to 15:25 pm) coincided with the time of largest $D > 930$ Pa, i.e., the time of the day when atmospheric demand for transpiration was the highest (Figure 4.7). Before noon time (10:75 am) until D was smaller than 760 Pa, model estimation was smaller. But in contrast in the early morning (6:75 to 7:75 am) model estimation was higher compared to observed. This was exactly the time when D started to increase sharply from a decreasing trend during night (Figure 4.7). A possible explanation for the systematic differences between observed and simulated P_g might be stomatal limitation of P_g that was not adequately represented by the model (Ibrom et al. 2006).

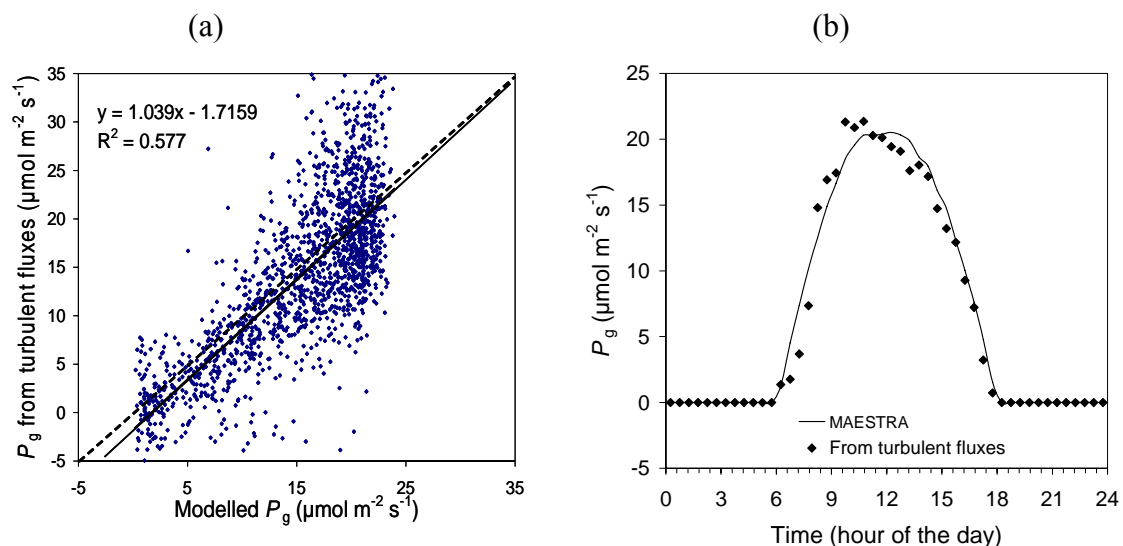


Figure 4.6. Relationships between simulated and observed gross photosynthetic rates (P_g) of the investigated forest. (a) scatter diagram of observed versus simulated P_g , regression line and parameter (solid) and 1:1 line (dashed). (b) Diurnal course of simulated P_g (solid line) and observed P_g (dots) averaged over the period of May, June and July 2004.

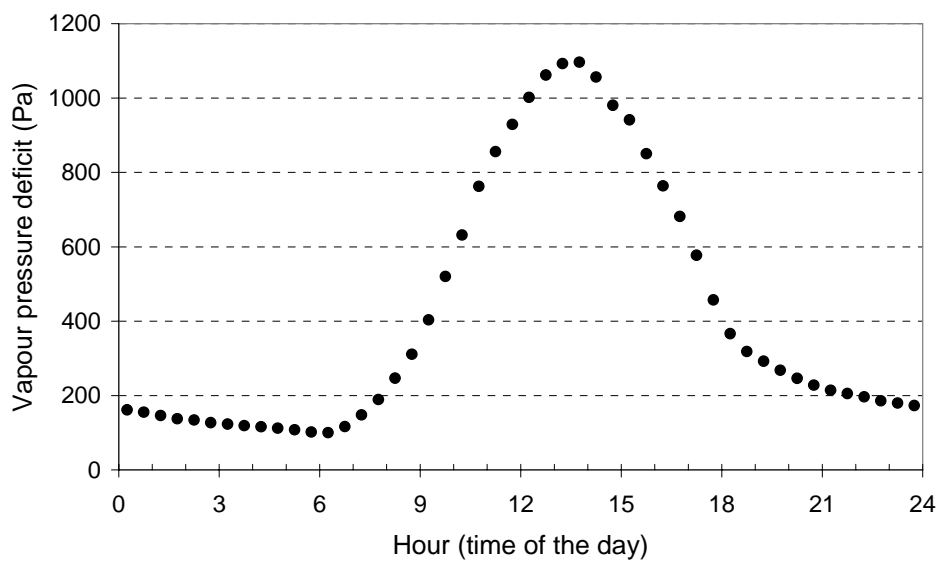


Figure 4.7. Half hourly average of air vapour pressure saturation deficit (D) for the month of May, June and July 2004.

4.5.2 Simulated budget of gross primary productivity and foliage respiration

The sensitivity analysis discussed above reveals that, model outputs of gross primary productivity (P_g) and foliage respiration (R_f) can vary considerably depending on the values of parameters. In the present simulation most of the important and influential parameters, such as physiological parameters and their nitrogen and temperature dependencies were derived from field measurements but others were taken from literature and a few were assumed. However, the parameter set (Tables 4.1 and 4.2) that has been used in the simulation has produced encouraging results. Table 4.4 shows rates of simulated outputs of P_g and R_f . Daily average P_g among the months of May, June and July was very similar, and varied only by 4%. The average daily P_g from this three months data was $7.15 \text{ g (C) m}^{-2} \text{ day}^{-1}$, and its extrapolation to a yearly value results in $2608 \text{ g (C) m}^{-2} \text{ year}^{-1}$, which is only 4% lower than the measured P_g of $2730 \text{ g (C) m}^{-2} \text{ year}^{-1}$ from turbulent fluxes (Ibrom et al., unpublished). According to Ibrom et al. (unpublished) weather conditions at the study site that cause seasonal variation in the fluxes are related to precipitation, for which two periods can be distinguished, a wet period from January to July and a drier period from August to December. Though P_g did not vary considerably between the two phases, the net ecosystem uptake (F_b) was higher during wet periods and lower during drier period,

because ecosystem respiration (R_E) was lower during wet periods and higher during drier periods. So the simulated daily and annual P_g can be representative for the whole year. F_b could not be simulated as we did not have soil respiration data and vegetation respiration data other than foliage. But generally, if considered 2/3 of P_g is respired then F_b would be $-869 \text{ g (C) m}^{-2} \text{ year}^{-1}$, which is a very high uptake compared to published values (Falge et al., 2002).

Table 4.4. Simulated daily average gross photosynthesis (P_g) and foliage respiration (R_f) from monthly and periodic data and extrapolation to yearly values from the averages. Values in the parentheses are standard deviations.

	P_g , $\text{g (C) m}^{-2} \text{ day}^{-1}$	P_g , $\text{g (C) m}^{-2} \text{ year}^{-1}$	R_f , $\text{g (C) m}^{-2} \text{ day}^{-1}$	R_f , $\text{g (C) m}^{-2} \text{ year}^{-1}$
May	7.17 (0.71)	2617	3.29 (0.15)	1201
June	7.28 (0.59)	2656	3.17 (0.10)	1158
July	7.0 (0.80)	2554	3.08 (0.10)	1124
overall	7.15 (0.71)	2608	3.18 (0.15)	1161

4.5.3 Comparisons of canopy photosynthetic light response

Responses of simulated and observed P_g to variation in Q are shown in Figure 4.8. MAESTRA was able to simulate the general established distribution pattern of P_g - Q relationship. At low Q values simulated photosynthetic response was almost a straight line, indicating that Q was the major limiting factor for P_g up to a Q value of about $200 \mu\text{mol m}^{-2} \text{ s}^{-1}$. Beyond this Q value, P_g became increasingly variable. P_g showed a tight relationship and was defined by Q up to $400 \mu\text{mol m}^{-2} \text{ s}^{-1}$, but became disrupted and variable with further increase in Q and seems to have been influenced by other factors. The arrow in Figure 4.8 indicates the Q value (about $1250 \mu\text{mol m}^{-2} \text{ s}^{-1}$), above which simulated P_g was saturated.

The initial slope (α , apparent quantum yield) of the simulated canopy response function was $0.039 \text{ (mol CO}_2 \text{ mol}^{-1} \text{ photons for } Q < 60 \mu\text{mol m}^{-2} \text{ s}^{-1})$. Simulated PAR absorptance of the investigated canopy revealed quite a low, with absorption of only 75% of the incoming Q . If simulated P_g is related to absorbed PAR (Q_{abs}), the initial slope of the $P_g(Q_{\text{abs}})$ function, called true quantum yield, is $0.052 \text{ mol CO}_2 \text{ mol}^{-1}$

absorbed PAR. This canopy true quantum yield was less steep and 83% compared to the average measured value at leaf scale ($0.063 \text{ mol CO}_2 \text{ mol}^{-1}$ absorbed PAR) that was used in the simulations.

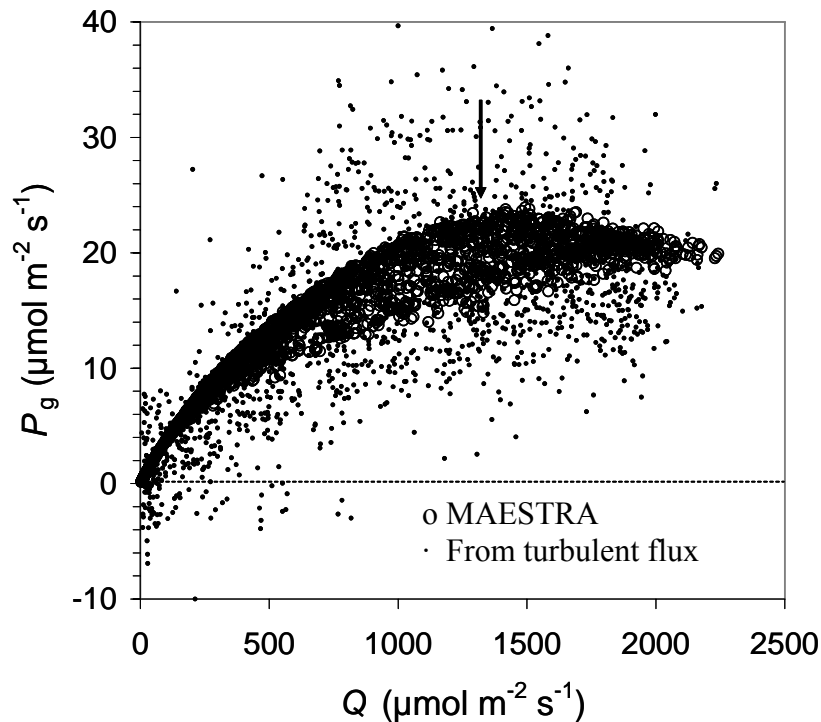


Figure 4.8. Responses of canopy photosynthesis (P_g) to photosynthetically active radiation (PAR). The arrow indicates saturation of simulated P_g . Open circles are simulated values and small dots are measured values from turbulent flux. Abbreviation: Q = PAR photon flux.

4.6 Conclusion

Simulated gross primary productivity (P_g) of the investigated forest ($2608 \text{ g (C) m}^{-2} \text{ year}^{-1}$) was very close to the measured value ($2730 \text{ g (C) m}^{-2} \text{ year}^{-1}$) by Ibrom et.al. (unpublished data). Net biotic flux could not be simulated because we did not have soil respiration data and above ground respiration data other than foliage respiration. Simulated P_g was able to describe 57% of the variations in measured P_g and the daily course of P_g was very well depicted in the simulated data. Model outputs were relatively more sensitive to physiological parameters and forest structural parameters than to other input parameters. So any error in the estimation of parameters would propagate error into the simulated results.

4.7 References

- Falge, E., Baldocchi, D., Tenhunen, J., et al. (2002) Seasonality of ecosystem respiration and gross primary production as derived from FLUXNET measurements, *Agricultural and Forest Meteorology*, **113**, 53-74.
- Farquhar, G.D., Caemmerer, S. Von and Berry, J.A. (1980) A biochemical model of photosynthetic CO₂ assimilation in leaves of C₃ species. *Planta* **149**, 78-90
- Grote, S. (2006) Struktur eines submontanen tropischen natürlichen Regenwaldes bei Bariri auf der indonesischen Insel Sulawesi. Masterarbeit, Institut für Bioklimatologie, Georg August Universität Göttingen.
- Ibrom, A., Jarvis, P.G., Clement, R., et al. (2006) A comparative analysis of simulated and observed photosynthetic CO₂ uptake in two coniferous forest canopies. *Tree physiology* **26**, 845-864.
- Jarvis, P.G. (1976) The interpretation of the variations in leaf water potential and stomatal conductance found in canopies in the field. *Philos. Trans. R. Soc. Lond. B* **273**:593-610.
- Jarvis, P.G. (1989) Atmospheric carbon dioxide and forests. *Philos. Trans. R. Soc. Lond. B* **324**, 369-392.
- Malhi, Y., Baldocchi, D. and Jarvis, P.G. (1999) The carbon balance of tropical, temperate and boreal forests. *Plant Cell Environment* **22**, 715-740.
- Marengo, R.A. and Vieira, G. (2005) Specific leaf area and photosynthetic parameters of tree species in the forest understorey as a function of the microsite light environment in Central Amazonia. *Journal of tropical forest science* **17(2)**, 265-278.
- Medlyn, B.E. (2004) A MAESTRO retrospective. *In* Forests at the land-Atmosphere Interface. Eds. M. Mencuccini, J. Moncrieff, K.G. McNaughton and J. Grace. CABI Publishing, Wallingford, U.K., pp 105-121.
- Motzer, T., Nunz, N., Koppers, M., Schmitt, D., and Anhuf, D. (2005) Stomatal conductance, transpiration and sap flow of tropical montane rain forest trees in the southern Equadorian Andes. *Tree Physiology* **25**, 1283-1293.
- Norman, J.M. and Welles, J.M. (1983) Radiative transfer in an array of canopies. *Agron. J.* **75**, 481-488
- SAS Institute Inc. (2004) SAS 9.1.3 Help and Documentation, Cary, NC, USA
- Souza, R.P. and Valio, I.F.M. (2003) Leaf optical properties as affected by shade in saplings of six tropical tree species differing in successional status. *Brazilian Journal of Plant Physiology* **15(1)**, 49-54.
- Sellers, P.J., Dickinson, R.E., Randall, D.A., et al. (1997) Modeling the exchanges of energy, water and carbon between continents and the atmosphere. *Science* **275**, 502-509.
- Wang, Y.P. (1998) Crown structure, radiation absorption, photosynthesis and transpiration. *In* IERM. University of Edinburg, Edinburg, 188p.
- Wang, Y.P. and Jarvis, P.G. (1990a) Description and validation of an array model – MAESTRO. *Agricultural and forest meteorology* **51**, 257-280.

5 Chapter- V: Photosynthetic light use efficiency of a tropical montane rain forest canopy of Central Sulawesi, Indonesia

5.1 Abstract

The use efficiency (E) of Photosynthetically active radiation (PAR) is an important parameter to derive carbon fluxes between forest canopies and the atmosphere. A common approach is to assume gross primary productivity (P_g) is proportional to PAR absorbed by vegetation (Q_{abs}) by defining the proportionality constant E_{GPP} . Simulated P_g and simulated (Q_{abs}) from a canopy photosynthesis model MAESTRA and meteorological data set of the investigated montane rain forest were used to derive values of E_{GPP} and to investigate the relationship between P_g and Q_{abs} . The half hourly P_g data showed a markedly clear saturation with Q_{abs} . P_g saturation was still evident when shifting from half hourly to daily and monthly time scales, indicating that P_g was insensitive to changes in Q_{abs} for a considerable time of the photo periods. Values of E_{GPP} were not constant and varied among both daily and monthly averages. In both cases E_{GPP} values were sensitive to Q_{abs} . These findings suggest that P_g of the investigated forest is not proportional to Q_{abs} and current linear E -approach is not suitable for the investigated tropical rain forest site. Simulated results showed a reasonably good agreement with measurements.

5.2 Introduction

Predicting the gross primary productivity (P_g) of the terrestrial ecosystems has been a major challenge in quantifying the global carbon cycle. Among all the predictive methods, the light use efficiency model may have the most potential to adequately address the spatial and temporal dynamics of P_g because of its theoretical basis and practicality (Running et al., 2000). A relatively simple and often used approach for the estimation of carbon accumulation by terrestrial vegetation was initially suggested by Monteith (1977). It assumes the rate of P_g is proportional to the rate of solar radiation intercepted by vegetation (Q_{abs}), with the proportionality factor of photosynthetically active radiation (PAR) use efficiency (E), such that

$$P_g = E_{GPP}Q_{abs}. \quad (5.1)$$

Where Q_{abs} stands for the amount of PAR that is absorbed by vegetation and E_{GPP} is the PAR-use efficiency.

The linear PAR-use efficiency approaches (*E*-approach) are currently used in regional and global studies based on remotely sensed vegetation structure data and regional meteorological ground data (e.g., Running et al., 2004, Xiao et al. 2004). The fraction of incident PAR that is absorbed by the vegetation can be estimated using adequately parameterized (one or three dimensional) radiation transfer models (Wang and Jarvis 1990, Gravenhorst et al. 1999, Ibrom et al. 2006). Xiao et al. (2004) suggests that only the fraction of Q_{abs} that is being absorbed by photosynthetically active vegetation (e.g. green leaves) be used for P_g calculation, and thus PAR-absorption by non assimilating structures, e.g., senescent or dry foliage, stems and branches, be ignored. Values of E_{GPP} vary significantly both between different geographical regions and across different vegetation types of the same natural zone as reported in several publications (Still et al. 2004, Ito and Oikawa 2004). Information on the spatial and temporal variability of E_{GPP} in tropical forests is relatively scarce compared to other vegetation types. In this study the relationships between simulated P_g and Q_{abs} in a mountainous tropical rain forest from South East Asia is investigated and related to current *E*-approaches. Objective of the study is to see, whether the canopy photosynthesis model MAESTRA used for simulations can be validated with estimated results (Ibrom et al. 2008) from turbulent flux measurements. Specifically, whether the major assumption of the *E*-approach i.e. the proposed linear relationship between P_g and Q_{abs} which does not exist at the investigated forest canopy, can be seen in the simulations.

5.3 Materials and methods

5.3.1 Simulation of gross primary productivity (P_g) of the investigated canopy

The detailed methodology for the derivation of simulated P_g is described in the previous Chapter-IV.

5.3.2 Simulation of PAR absorption by the canopy

Photosynthetically active radiation (PAR) absorption of the canopy (Q_{abs}) was calculated using the canopy photosynthesis model MAESTRA (Medlyn 2004), that is

described in the previous chapter- IV. For that the canopy was subdivided into ten vertical layers to get optimum Q_{abs} . The main input for the simulation is incident PAR, that was measured at the study site in a meteorological measurement tower.

5.3.3 PAR response of gross canopy photosynthesis

The empirical relationship between simulated half-hourly P_g and Q_{abs} was described with the non-rectangular hyperbola,

$$P_g = \frac{\alpha Q_{\text{abs}} + P_{\text{max}} - \sqrt{(\alpha Q_{\text{abs}} + P_{\text{max}})^2 - 4\theta\alpha Q_{\text{abs}} P_{\text{max}}}}{2\theta} \quad (5.2)$$

using the parameters quantum use efficiency (α), the maximum gross photosynthesis rate (P_{max}) and the curvature parameter (θ).

In a second approach P_{max} was allowed to depend on vapour pressure saturation deficit (D) as

$$P_{\text{max}} = \left(1 - e^{-\frac{a-b}{D^2}}\right) P_{\text{max}_0}, \quad (5.3)$$

with the empirical parameters a and b . P_{max_0} is P_{max} at $D \rightarrow 0$ Pa.

Rearranging Equation 5.1, E_{GPP} was calculated from P_g and Q_{abs} . To characterize the processes at different time scales, the data are analysed as half hourly data, day-time averages and monthly averages.

5.4 Results and discussions

5.4.1 PAR response of gross canopy photosynthesis

The general relationship between simulated gross primary productivity (P_g) and simulated absorbed PAR (Q_{abs}) at a half hourly timescale shows a hyperbolic increase of P_g with increasing Q_{abs} (Figure 5.1a) that is similar to results from CO₂ flux studies (Pilegaard et al. 2001, Ibrom et al. 2006). A linear dependence of P_g on Q_{abs} could only be seen up to a Q_{abs} value of about 250 $\mu\text{mol m}^{-2} \text{s}^{-1}$. Beyond this, P_g increased but at a decreasing rate and started saturating at Q_{abs} values of about 750 $\mu\text{mol m}^{-2} \text{s}^{-1}$. Form a Blackman response function (Blackman 1905), i.e. constraining the hyperbolic response function (Equation 5.2) to a theta value of 1, P_g saturated at $Q_{\text{abs}} = 648 \mu\text{mol m}^{-2} \text{s}^{-1}$, which can be computed as,

$$Q_{sat} = \frac{P_{\max, \theta=1}}{\alpha_{\theta=1}} \quad (5.4)$$

The relationship between simulated P_g and Q_{abs} is characterized by a very strong correlation ($R^2=0.98$). Inclusion of the sensitivity of the parameter P_{\max} to D , using Equation 5.3, changed the parameter values, but the correlation coefficient remains the same (Table 5.1). From regression parameters listed in Table 5.1, it can be seen that D had only a moderate influence on simulated P_g . The lower curve in the figure 5.1(a) shows the effect of extreme D (2000 Pa) and indicates a moderate sensitivity of P_g to weather conditions with high D . The dependence of $P_{g\max}$ on D is shown in Figure 5.1b using the combined regression model, i.e., Equation 5.2 and 5.3. The simulated results show a decrease of P_g when D exceeds about 750 Pa. The dependency of Q_{sat} on D was calculated using the combined model with a Blackman type of P_g - Q_{abs} response (Figure 5.1c). According to this simulation the maximum Q_{sat} is reached at about $670 \mu\text{mol m}^{-2} \text{s}^{-1}$, which is lower as compared to the estimated value of $900 \mu\text{mol m}^{-2} \text{s}^{-1}$ by Ibrom et al. (2008). Moreover the decrease of Q_{sat} with the increase of D was considerably smaller for simulations ($\sim 20\%$ compared to the estimated value) while there it decreased by $2/3$ of the measured value ($900 \mu\text{mol m}^{-2} \text{s}^{-1}$) over the range of observed D .

This smaller influence of D on simulated P_g and Q_{sat} could be the results of MAESTRA formulation, as in MAESTRA simulations P_g can only be influenced by D through stomatal conductance. Thus, if the maximum stomatal conductance to CO_2 (GSREF) in the simulations is kept high enough, which is the case, the observed range of D can not have expected influence on P_g that was seen in the measurements. In nature it is expected, that with the increase of D , stomatal conductance (g_s) and consequently C_i decreases, causing a decrease in P_g and Q_{sat} , too. A sensitivity test was conducted to investigate this possible reason and to get an impression of a lower GSREF value at which simulated P_g can be more sensitive to D , as was in observed data. Figure 5.2 shows the increased sensitivity of P_g with the decrease of GSREF. In Figure 5.2 D_0 in Pa (D threshold at 50% reduction of stomatal conductance) was kept 3000 Pa as of reference value used in the simulations that was used from personal communication (Ibrom, A.). Lower GSREF values of 0.1 and 0.05 showed higher sensitivity of P_g to D . It is understood that to get higher influence of D related

conditions on P_g , similar influence as observed, value of GSREF should be much lower around $0.1 \text{ mol m}^{-2} \text{ s}^{-1}$.

Though the dependence of P_g on D and saturation of P_g with Q_{abs} differed in magnitude from that of measurements, simulated results show similar effects and trends. The difference between measurements and simulations could arise from the errors in model parameter values, as apart from measured physiological model parameters, some simulation parameters were taken from literature and some were also assumed. It can be considered that, if all the parameters for canopy photosynthesis model MAESTRA could have been estimated from direct field measurements, simulations would yield more consistent results with measurements.

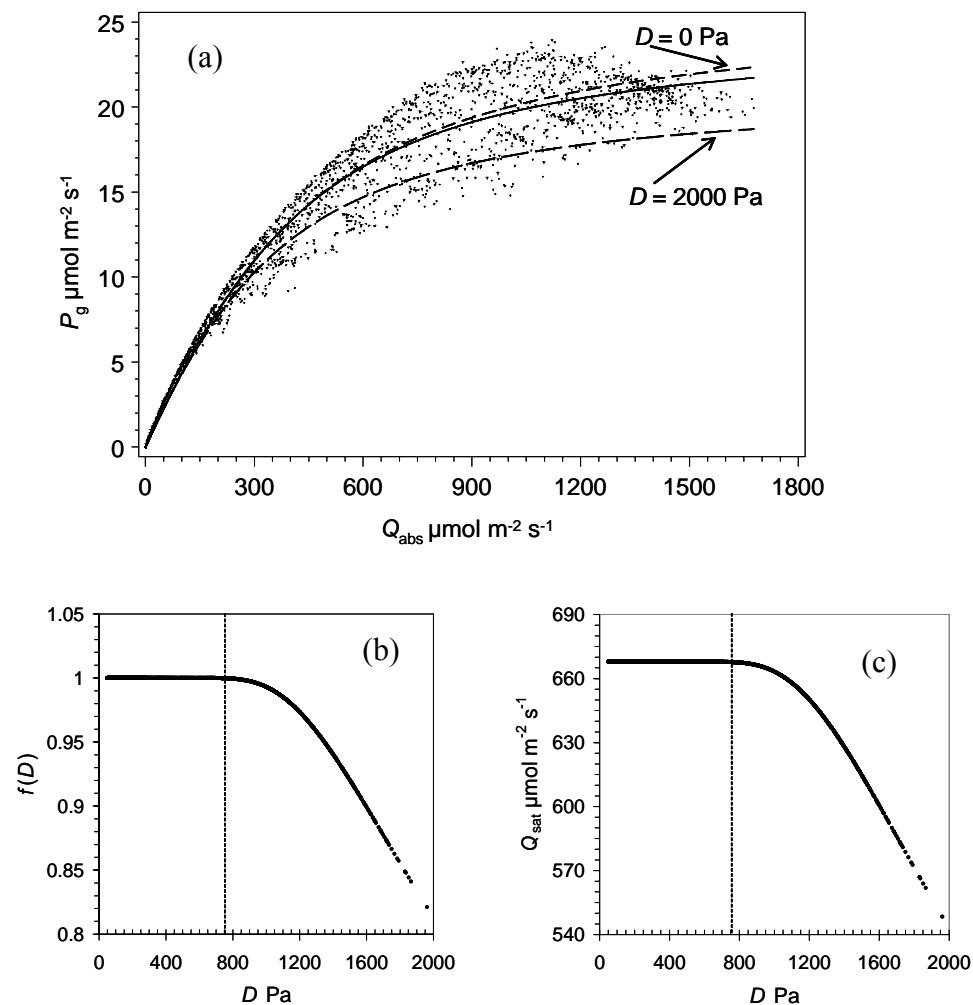


Figure 5.1. (a) Simulated half-hourly canopy gross primary production rates (P_g) versus simulated Q_{abs} for the period of May to July 2004. Broken curves are predicted P_g at a vapour pressure saturation deficit (D) = 0 Pa (upper curve) and D = 2000 Pa (lower curve). The solid line shows predicted P_g without any D dependency. 5.1. (b) shows the reducing effect of increasing D on saturated P_g (according to Equation 5.3) and 5.1. (c) shows the effect of increasing D on saturating Q_{abs} (Q_{sat}) according to Equation 5.4. The parameter values of the regression models are listed in Table 5.1.

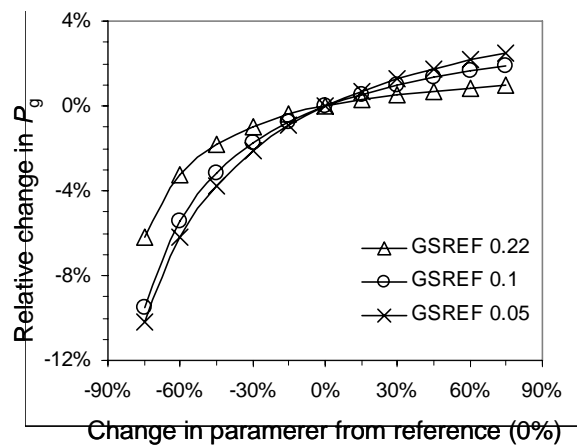


Figure 5.2. Sensitivity of P_g to $D0$ at three different values of maximum stomatal conductance.

At the daily time scale the dependence of P_g on Q_{abs} was to some extent similar to the relationships obtained for half-hourly data. Daily average Q_{abs} during the study period ranged from 3.1 to 8.7 MJ m⁻² day⁻¹ with the corresponding P_g range of 5.2 to 8.1 g (C) m⁻² day⁻¹ (Figure 5.3a). Low Q_{abs} was related to cloudy and rainy weather conditions. For days with sunny weather, when Q_{abs} was larger than 6.0 MJ m⁻² day⁻¹, P_g started saturating and became independent from Q_{abs} . Above the Q_{abs} value of 6.0 MJ m⁻² day⁻¹, saturation led to a more or less constant P_g value of 7.7 g (C) m⁻² day⁻¹ with a standard deviation of 0.34 g (C) m⁻² day⁻¹. The mean monthly day-time P_g and Q_{abs} varied only little during the investigated four months period, with Q_{abs} ranging between 5.7 and 7.0 MJ m⁻² day⁻¹ and P_g ranging between 7.0 and 7.8 g (C) m⁻² day⁻¹. Unlike the daily data, monthly results did not show considerable dependence of P_g on Q_{abs} (Figure 5.3c).

The averaged diurnal course of P_g , Q_{abs} and vapour pressure saturation deficit (D) are depicted in Figure 5.4. The value of P_g and Q_{abs} started to increase at the same time of the day and followed almost the same course throughout the day. P_g increased at a decreasing rate and reached to a maximum value at 10:45 am. Whereas Q_{abs} increased at an increasing rate until 9:45 am, afterward it increased at a decreasing rate and reached its maximum at about 12:45 pm. From 10:45 am to 12:45 pm P_g was almost constant, whereas Q_{abs} increased from 1070 to 1092 $\mu\text{mol m}^{-2} \text{s}^{-1}$ during that time, indicating a saturation period of about two hours around noon when Q_{abs} was in its highest range. D started to increase half an hour later than Q_{abs} from the night time level, but reached its maximum about one and a half hours after Q_{abs} did. At a D value

of about 750 Pa, P_g started saturating under high light conditions. This is the D value when half hourly P_g seems to be affected by D according to the combined regression model (Figure 5.1b). A small depression of P_g in the early afternoon coincided with the highest D values between 12:45 pm and 14:15 pm. The broken line in the upper panel of Figure 5.4 indicates the average diurnal course of Q_{sat} as calculated from Equation 5.4. These simulated results show a reasonable agreement with the measurements done by Ibrom et al. (2008).

Table 5.1. Regression results between simulated canopy gross photosynthesis (P_g) and absorbed PAR (Q_{abs}). The parameters α , θ and P_{max} are the initial slope, a curvature parameter and the saturated photosynthesis rate respectively. Index ‘c’ stands for combined Q -response model. Parameters a and b are empirical parameters for the vapour pressure saturation deficit (D) dependency of P_{max_0} , i.e. the Q saturated canopy photosynthesis rate at $D = 0$ Pa. R^2 is the relative proportion of the variability of simulated P_g rates that can be explained by model predictions.

Parameter and unit	Value	Standard Error
Equation 2		
α mol CO ₂ (mol photon) ⁻¹	0.046 (P< 0.0001)	0.000619
θ	0.66 (P< 0.0001)	0.0213
P_{max} $\mu\text{mol m}^{-2} \text{s}^{-1}$	24.55 (P< 0.0001)	0.2073
R^2	0.98	
Number of observations	4416	
Equation 2 and 3 combined		
α_c mol CO ₂ (mol photon) ⁻¹	0.047378 (P< 0.0001)	0.000638
θ_c	0.598363 (P< 0.0001)	0.0254
a	-0.57838 (P< 0.0046)	0.2122
b Pa ²	4392853 (P< 0.0001)	527964
P_{max_0} $\mu\text{mol m}^{-2} \text{s}^{-1}$	25.83978 (P< 0.0001)	0.2709
R^2	0.98	
Number of observations	4416	

5.4.2 PAR use efficiency of gross canopy photosynthesis (E_{GPP})

The simulated PAR responses of gross primary productivity (P_g) at different time scales do not suggest that E_{GPP} is a constant entity that describes the physiological capacity of transforming absorbed quanta into assimilated CO₂ of the investigated forest canopy. The traditional E -approach, that considers P_g as directly

proportional to Q_{abs} , that type of PAR-response of P_g can be accurately described by a Blackman response curve as long as $Q_{\text{abs}} < Q_{\text{sat}}$. Above this level E_{GPP} depends hyperbolically on Q_{abs} and to a certain degree on other factors like D (Ibrom et al. 2008). Simulated results show, that this key relationship was still valid when turning from half hourly to daily or monthly averages (Figures 5.3b and 5.3d). In both cases E_{GPP} values decreased with increasing Q_{abs} . Given saturation of P_g and definition of E_{GPP} , the daily E_{GPP} followed a hyperbolic relationship (Figure 5.3b) and ranged between 0.96 and 1.7 g (C) MJ⁻¹. E_{GPP} showed a parabolic diurnal course (lower panel of Figure 5.4). During the early morning and late afternoon hours E_{GPP} was the highest, 0.055 mol CO₂ (mol photon)⁻¹, during noon time being very low, and the lowest value of 0.021 mol CO₂ (mol photon)⁻¹ coincided with the averaged highest Q_{abs} of the diurnal course.

The simulated data showed clear saturation of P_g with increasing Q_{abs} and thus indicates that the current E -approaches can not be used to accurately predict half-hourly P_g values from Q_{abs} for the investigated forest with a single and constant E_{GPP} . The analysis here shows that P_g saturation occurs at the daily time scales and also indicated at monthly timescale. The E -approaches assume that the effect of saturation becomes negligible when averaging the data over longer intervals. Larger temporal averaging can, however, only mitigate the unfavourable effects of saturation, if conditions with P_g saturation are rare compared to unsaturated conditions (Ibrom et al. 2008). The averaged monthly value of E_{GPP} , for the period of May to August 2004, was 1.21 g (C) MJ⁻¹ which ranged between 1.12 and 1.28 g (C) MJ⁻¹. These simulated values are about 20% higher compared to the estimations of Ibrom et al (2008). The reason is probably that Ibrom et al (2008) used another model where it calculated 94% Q absorption (~ 20% larger than in the present study). Higher simulated E_{GPP} values in this study would have yielded from lower simulated Q_{abs} by MAESTRA. The lower simulated Q_{abs} could be related to forest structural parameters that were not measured by us and had to use reference values from Grote (2006). The variability in simulated averaged daily and monthly E_{GPP} and their relationships with Q_{abs} resembles to the measurements presented in Ibrom et al. (2008) for the investigated forest canopy.

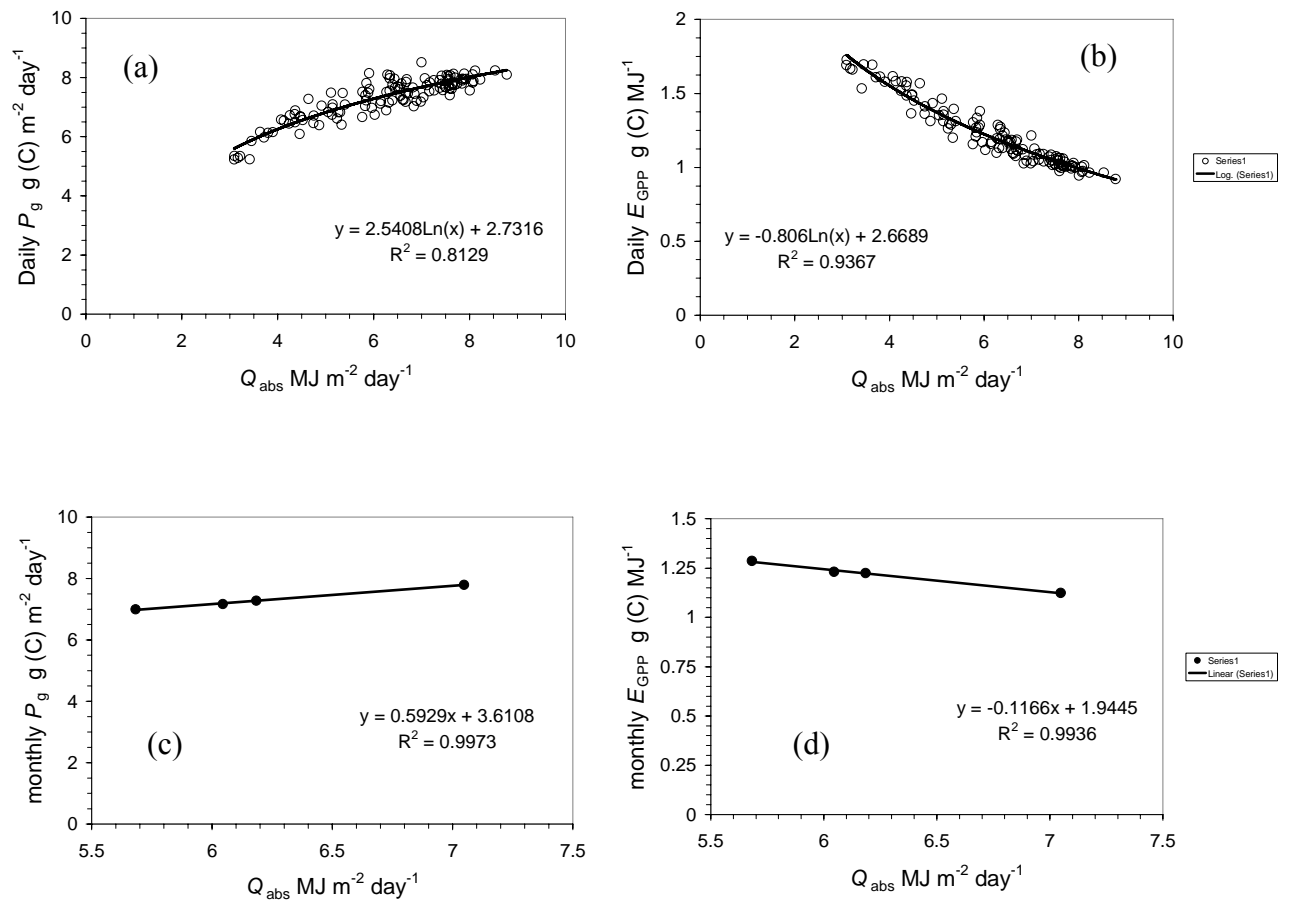


Figure 5.3. Simulated daily (a) and monthly (c) averaged daily gross primary productivity (P_g) versus simulated daily absorbed PAR (Q_{abs}) and the respective PAR-use efficiencies for P_g (E_{GPP}) (2 b and 2 d).

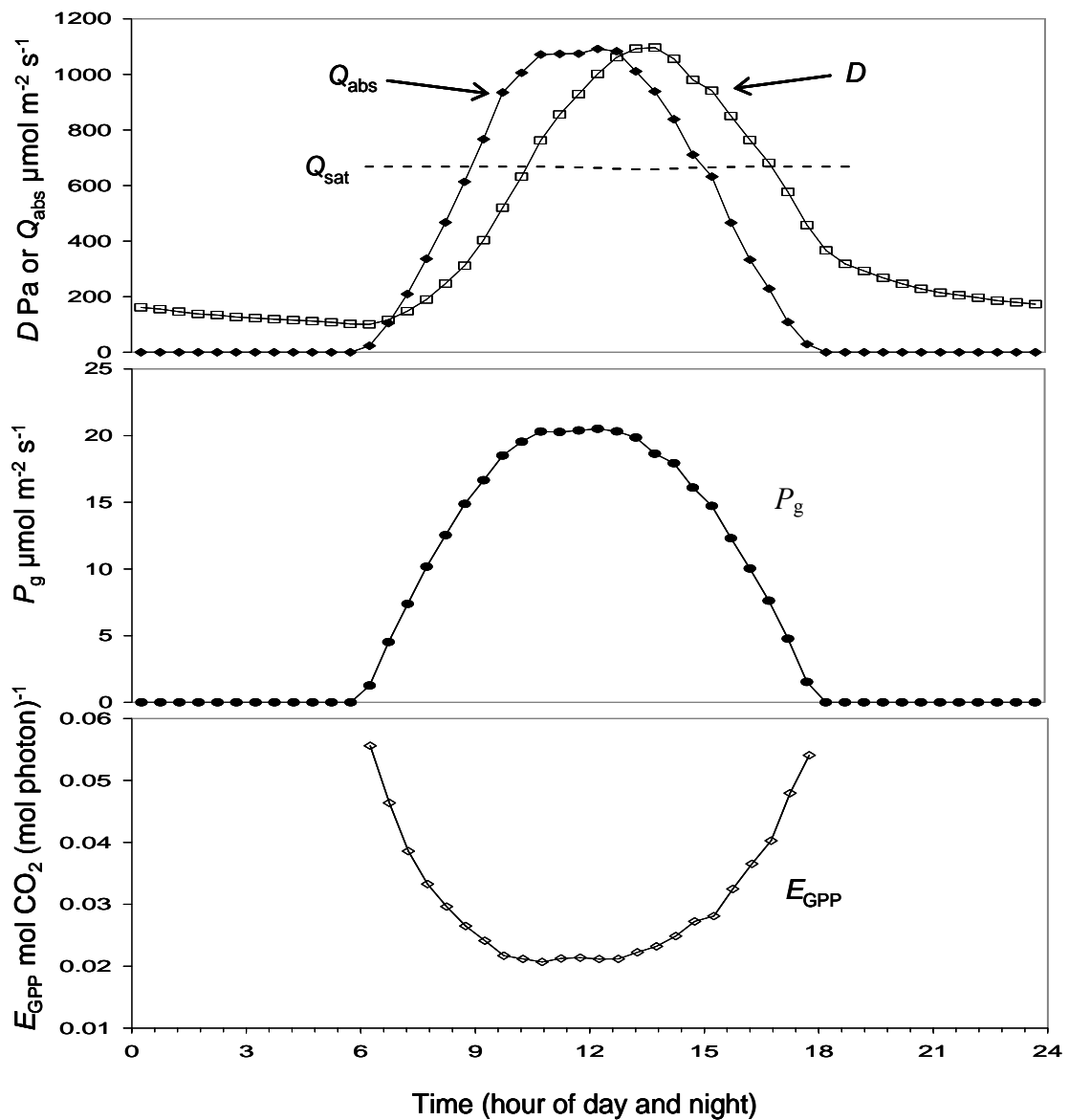


Figure 5.4. Average diurnal courses of absorbed PAR (Q_{abs}), water vapour pressure saturation deficits (D), gross primary production rates (P_g) and PAR use efficiencies of P_g (E_{GPP}).

5.5 Conclusion

The simulated light use efficiency results showed that P_g of the studied forest is proportional to Q_{abs} as long as Q_{abs} is smaller than Q_{sat} . So the current E -approach is not applicable straightway to this tropical rainforest. P_g saturations occurred at high Q_{abs} values. Q_{sat} (Q_{abs} values at which P_g saturated) values decreased under high vapour pressure saturation deficit (D) indicating influence of D on P_g . Though D has no direct influence on the MAESTRA simulations of P_g but its influence may be

explained with weather conditions that are related to D . At high D , it is assumed that the sky would be clear and the fraction of direct radiation (beam fraction) is more compared to diffused and vice versa with cloudy condition. These conditions might affect P_g , as we know that plants are capable of utilizing diffused radiation more efficiently than direct radiation.

5.6 Reference

- Gravenhorst, G., Knyazikhin, Y., Kranigk, J., Miessen, G., Panfyorov, O. and Schnitzler, K.G. (1999) Is forest albedo measured correctly? *Meteorologische Zeitschrift*, 107-114.
- Grote, S. (2006) Struktur eines submontanen tropischen natürlichen Regenwaldes bei Bariri auf der indonesischen Insel Sulawesi. Masterarbeit, Institut für Bioklimatologie, Georg August Universität Göttingen.
- Ibrom, A., Jarvis, P.G., Clement, R., et al. (2006) A comparative analysis of simulated and observed photosynthetic CO₂ uptake in two coniferous forest canopies. *Tree physiology* **26**, 845-864.
- Ibrom, A., Oltchev, A., June, T., Kreilein, H., Rakkibu, G., Ross, T., Panferov, O. and Gravenhorst, G. (2008) Variation in photosynthetic light-use efficiency in a mountainous tropical rain forest in Indonesia. *Tree Physiology* **28**, 499-508.
- Ito, A. and Oikawa, T. (2004) Global mapping of terrestrial primary productivity and light-use efficiency with a process based model. In *Global environmental change in the ocean and on land* Ed. M. Shiyomi. Terrapub, Tokyo, pp. 343-358.
- Medlyn, B.E. (2004) A MAESTRO retrospective. In *Forests at the land-Atmosphere Interface*. Eds. M. Mencuccini, J. Moncrieff, K.G. McNaughton and J. Grace. CABI Publishing, Wallingford, U.K., pp 105-121.
- Pilegaard, K., Hummelshøj, P., Jensen, N.O., and Chen, Z. (2001) Two years of continuous CO₂ eddy-flux measurements over a Danish beech forest. *Agric. For. Meteorol.* **107**:29-41.
- Running, S.W., Nemani, R.R., Heinsch, F.A., Zhao, M.S., Reeves, M. and Hashimoto, H. (2004) A continuous satellite-derived measures of global terrestrial primary production. *Bioscience* **54**, 547-560.
- Running, S.W., Thornton, P.E., Nemani, R. and Glassy, J.M. (2000) Global terrestrial gross and net primary productivity from the earth observing system. In: Sala, O.E., Jackson, R.B., Mooney, H.A. (Eds.), *Methods in Ecosystem Science*. Springer-Verlag, New York, pp. 44-47.
- Still, C.J., Randerson, J.T. and Fung, I.Y. (2004) Large-scale plant light-use efficiency inferred from the seasonal cycle of atmospheric CO₂. *Global Change Biology*, **10**:1240-1252.
- Wang, Y.P. and Jarvis, P.G. (1990) Description and validation of an array model – MAESTRO. *Agricultural and Forest Meteorology*, **51**, 257-280.
- Xiao, X., Hollinger, D., Aber, J., Goltz, M., Davidson, E., Zhang, Q. and Moore, B. (2004) Satellite based modelling of gross primary production in an evergreen needleleaf forest. *Remote sensing environment*. **89**, 519-534.

Acknowledgements

I wish to thank the following persons and institutions for direct and indirect contributions to this thesis:

Prof. Dr. Gode Gravenhorst, I thank him very much for accepting me as a PhD student and willing to become supervisor. Without his generosity I could not have started this work. I also thank him for encouragement and inspiring discussions which were vital for the success of this endeavor.

Prof. Dr. Andreas Ibrom, I thank him for his continuous and relentless efforts in guiding and advising me technically and academically throughout the entire period of this work both in the field and in the modeling. Without his supervision and support this work would have been unthinkable.

Heiner Kreilein, I thank him for his administrative support and technical assistance both in the field and in the institute.

Prof. Dr. Oleg Panferov, I thank him for his continuous assistance, advice and consultation during the data analysis, modeling and writing. He also helped me a lot in computing techniques. I appreciate very much his support and cooperation besides academic affairs that was indispensable for my stay and work.

Dr. Karl Radler, I thank him for his assistance in handling data in SAS and important discussions and consultations in understanding many subject matters related to this work. I appreciate his inspiration and cooperation in many ways besides academic things too.

Frau Baumann and all other colleagues in the Institute of Bioclimate, who have been very cordial and helpful

Research assistance of B1 Team in Indonesia, I am very thankful to them for their assistance and friendly company in Palu and Bariiri.

The STORMA coordination office in Palu, for providing all kinds of logistics needed in the field and laboratory work

the German Science foundation (DFG) which funded the project '*Stability of Rainforest Margins in Indonesia*' (STORMA) as its SFB 552. This research was conducted within the subproject B1 of the second phase.

Khulna University authority of Bangladesh for granting study leave for this work

My whole family, for supporting and encouraging higher study. My parent's, who are no more in this world, vision for education and their sacrifice lead me up to now. I am very grateful to my wife and little daughter, without their patience, moral support and loving care this work would have been very difficult.

Declaration of Honor

I hereby declare in accordance with § 6, para. 2 f) of the Dissertation regulation set forth by the Faculty of Forest Sciences and Forest Ecology on March 09, 2005, that I authored the submitted thesis on my own and did not use any other references and resources than cited and that I have not submitted it ever within any other dissertation procedure.

Eidesstattliche Erklärung

Hiermit versichere ich gemäß § 6 Abs. 2 f) der Prüfungsordnung zum Promotionsstudiengang, Forstwissenschaften und Waldökologie' vom 09.03.2005 an Eides statt, dass ich die vorliegende Arbeit selbständig verfasst und keine anderen als die angegebenen Quellen und Hilfsmittel benutzt habe sowie, dass ich die vorliegende Arbeit nicht bereits in einem anderen Prüfungsverfahren vorgelegt habe.

Göttingen, den .03.2008

Md. Golam Rakkibu

Curriculum vitae

Personal

Name : Md. Golam Rakkibu
 Date of birth : 29th January 1969
 Place of birth : Natore, Bangladesh
 Nationality : Bangladeshi
 Gender : Male
 Civil status : Married, one daughter
 Contact address : Forestry and Wood Technology Discipline, Khulna University,
 Khulna 9208, Bangladesh. Email:- golamrakkibu@yahoo.co.uk

Education

1987 – 1992 : Bachelor of Science (Honours) in Forestry, Chittagong University
 Bangladesh.
 1997 – 1998 : Master of Science (MSc) in Agroforestry, University of Wales,
 Bangor, UK.
 Sept.2004 –
 June 2008 : PhD study, Institute for Bioclimatology, Georg-August-University,
 Göttingen, Germany.

Profession

April1993 –
 March1995 : Forest establishment and management, Assistant Conservator of
 Forests, Bangladesh Forest Department.
 Since
 April 1995 : Teaching and research, Faculty, Forestry and Wood Technology
 Discipline, Khulna University, Khulna 9208, Bangladesh.